MEMBRANE CHANGES AND LIPID PEROXIDATION DURING AGEING IN SEEDS OF Lactuca sativa L.

by

Michael Trevor Smith

VOLUME 2

ULTRASTRUCTURAL STUDIES

figures for

CHAPTERS 3, 4 and 5

Submitted in partial fulfilment of the
requirement for the degree of
Doctor of Philosophy,
in the
Department of Biology,
University of Natal,
Durban
1986

CHAPTER 3 : ULTRASTRUCTURAL STUDIES - ANHYDROUS FIXATION

Figure 1 : Illustrates the poor quality of section obtained after combined formaldehyde and osmium tetroxide vapour fixation. A densely-staining wall (w), numerous lipid droplets (L) and a protein body (PB) may be seen. Membrane details are somewhat obscured by the thickness of the section but nevertheless appear laminar (arrowhead). Lead citrate staining. X 44 800.

Figure 2 : Illustrates membrane-like components (black arrowheads) which surround lipid bodies (L) and "cytoplasmic islands" which were seen to contain membrane profiles in negative relief (white arrow). These latter details have been lost in the excessive contrast. The irregular outline of the lipid droplets is clearly evident. Tissue preparation as for Figure 1. X 50 400.

Figure 3 : Low-power micrograph of cotyledonary tissue fixed by formalin and acrolein vapour. Numerous electron-dense protein bodies (PB) are evident as well as smaller, paler staining lipid droplets (L). Nuclei (N) appear compact and electron dense. Wall detail (W) appears to have been lost. Wall material (W) has been lost in many places (asterisk) possible as a result of the section staining routine. Limiting membrane-like elements clearly evident around lipid bodies (double arrowheads). Lanthanum nitrate staining. X 9 200.

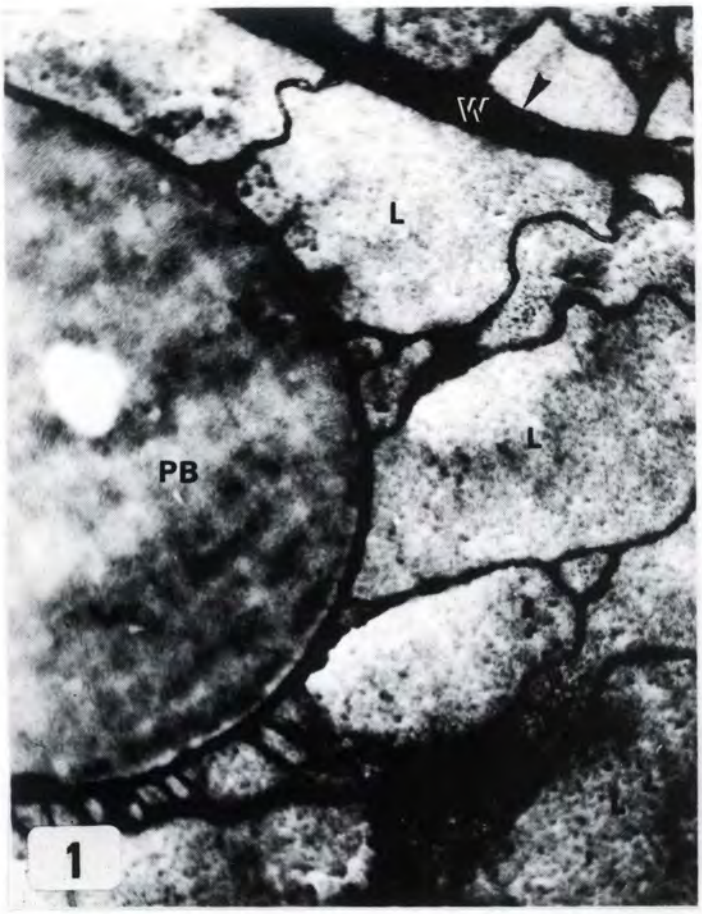
W
L
L
PB
1

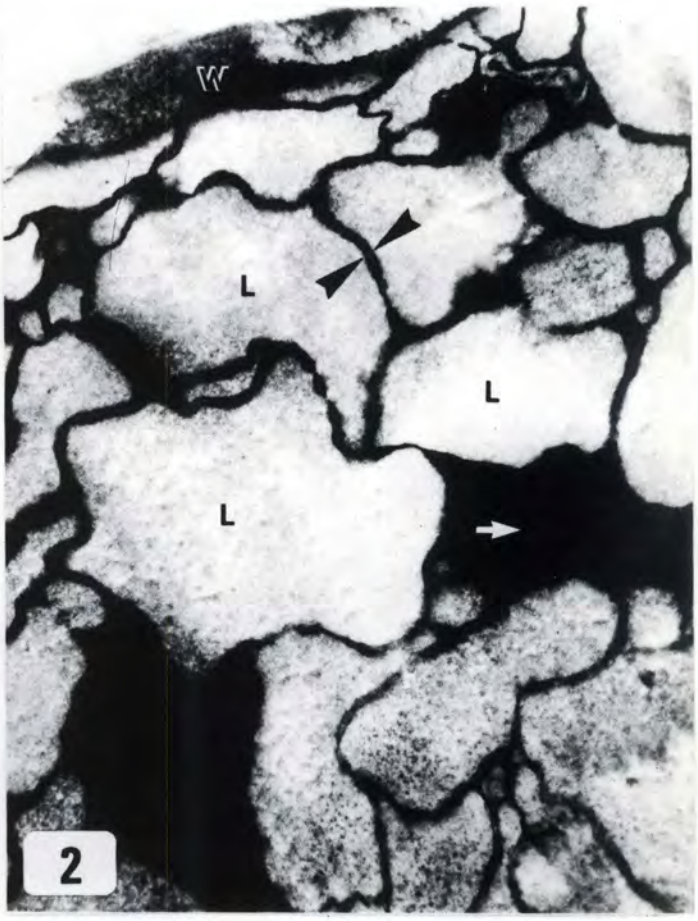
W
L
L
L
2

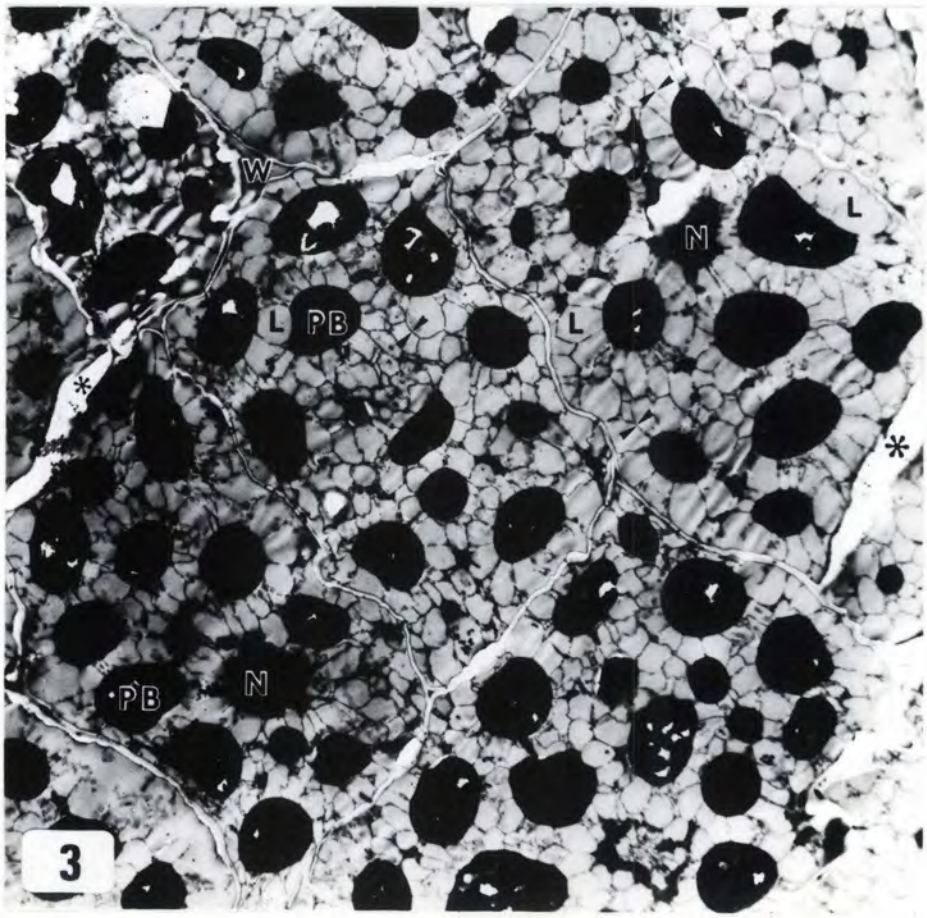
W
L
L
N
L
PB
L
*
*
PB
N
3

Figure 4 : Illustrates the appearance of a nucleus (N) in cotyledonary cell after formaldehyde-acrolein vapour vapour fixation and lanthanum nitrate staining. The profile of the nuclear envelope is highly irregular, lamellar, and negatively stained. Many membrane profiles are evident in close proximity to the nucleus but are not readily identifiable. A possible mitochondrion (M) is indicated. X 44 800.

Figures 5 & 7: Show the appearance of cell walls (W) after formaldehyde-acrolein vapour fixation and lanthanum nitrate staining. No clear fibrillar structure is evident and resin granularity predominates. Bilayer-like membranes appear contiguous with the wall, except where obliquely sectioned. X 108 640.

Figure 6 : Illustrates appearance of cotyledonary cells after formaldehyde-acrolein vapour fixation and lanthanum nitrate staining. Plasmodesmata (circles) may be seen in the obliquely-sectioned wall (W), and ribosome-like particles (squares) are evident in the cytoplasm. Lipid droplets (L) poorly stained, and numerous E.R.-like profiles may be seen in negative relief. A possible amyloplast with plastoglobuli and a starch grain (S) are indicated.

The limiting membrane (curved arrows) of the protein bodies (PB), appear bilayer-like because of densely staining regions on either side of the putative membrane which appears in negative relief. X 56 000.

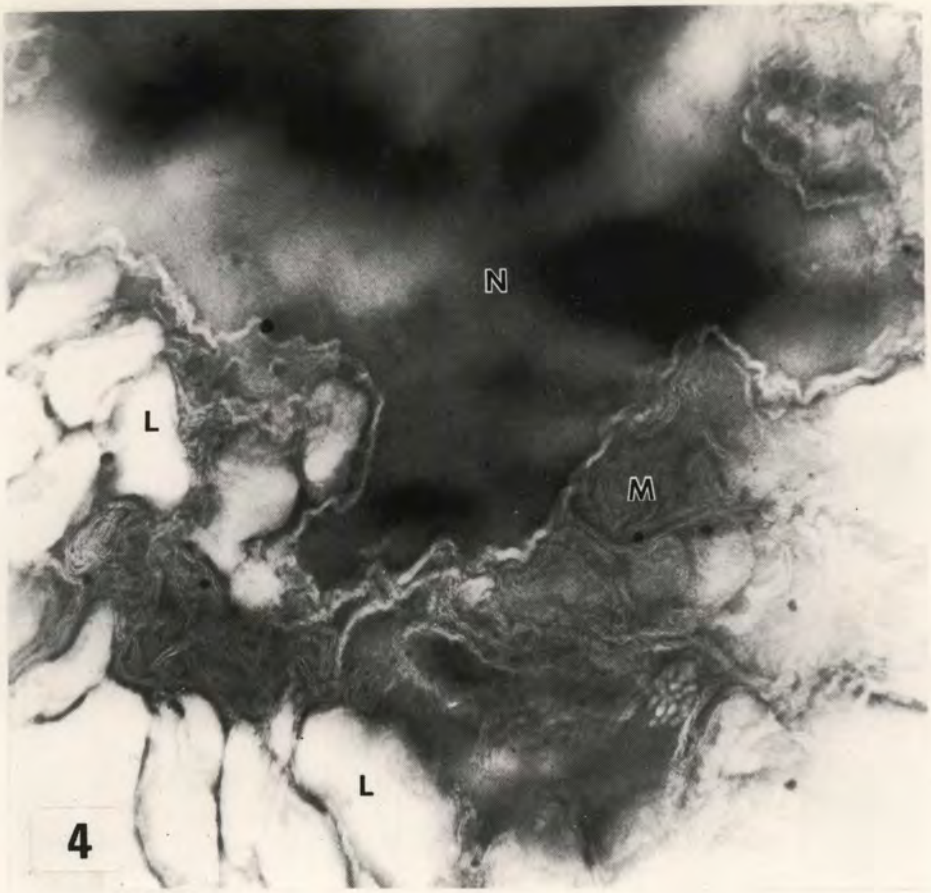

4

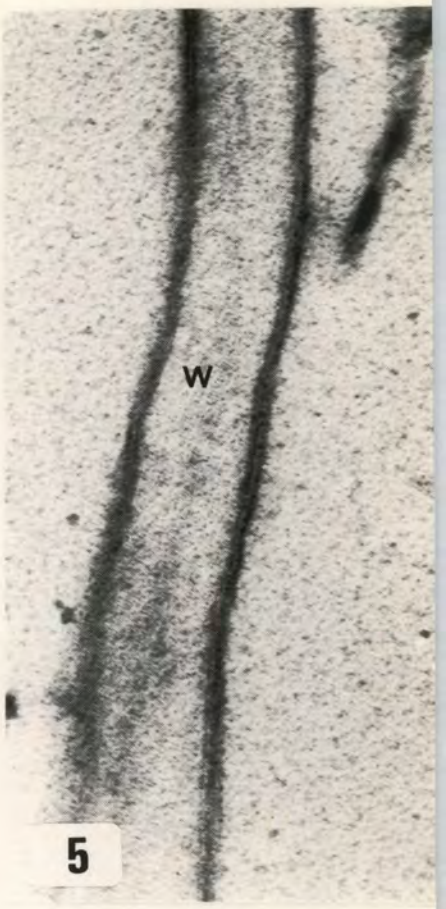

5

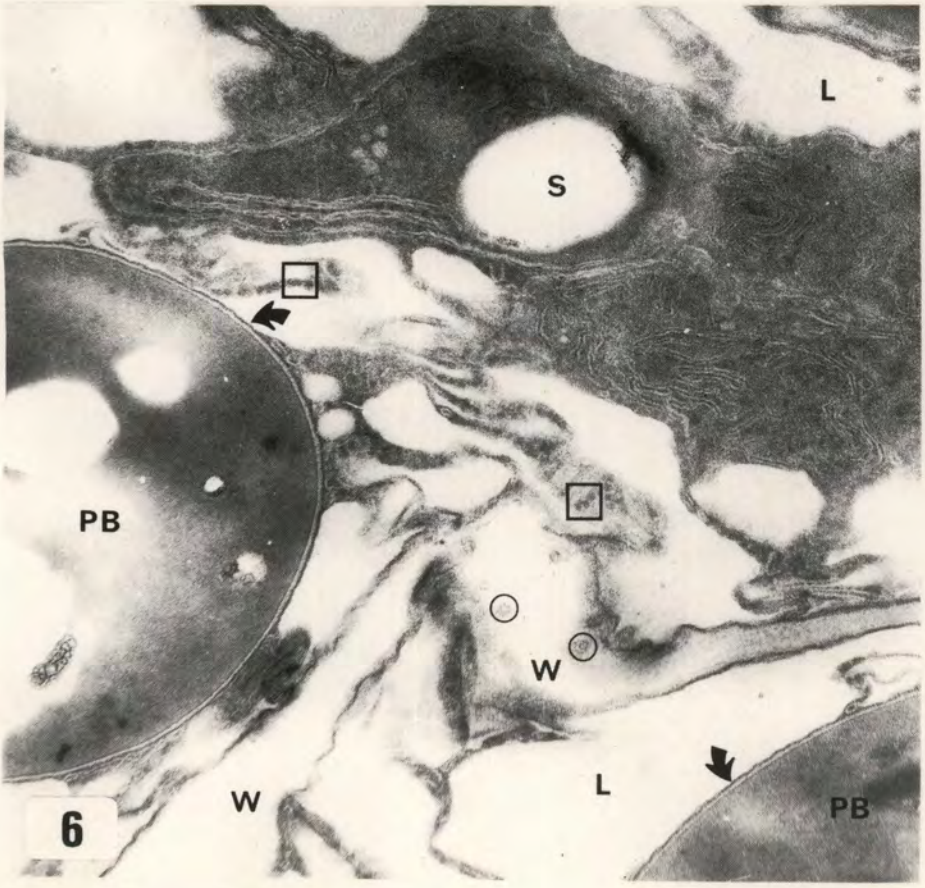

6

7

Figure 8 : Illustrates irregularly shaped nucleus with discontinuous regions in the nuclear envelope (highlighted arrowheads) which may represent nuclear pores. Tubule-like structures are evident in association with some of the lipid droplets (L) as indicated by double arrowhead. Tissue preparation as above. Stained with alcoholic uranyl acetate. X 56 000.

Figure 9 : Illustrates tubule-like structures associated with lipid bodies (double arrowheads). Tissue preparation as above, but stained with lead citrate. X 53 760.

Figure 10 : Illustrates tubule-like structures associated with lipid bodies in cotyledonary cell after fixation with formaldehyde and osmium tetroxide vapour. Section stained with lead citrate. Irregular membrane profiles evident at the darkly stained cell wall (curved arrow). X 24 700.

Figure 11 : Illustrates negatively stained ER-like profiles in cotyledonary section collected on a holey film. Compare with Figure 6. Formaldehyde-acrolein vapour fixation, and section stained with alcoholic uranyl acetate. X 100 800.

Figure 12 : Illustrates appearance of aqueously fixed preparation comprising bovine serum albumin and brain phospholipid. Within the lamellar myelin-like structure are regions where the membrane appears non-lamellar (squares). Lead citrate staining. X 172 640.

Figure 13 : Illustrates appearance of cotyledonary cells after fixation by osmium tetroxide in acetone. Some protein bodies have been lost from the sections as can be seen by electron translucent circles. Although wall (W) detail is absent their highly convoluted nature is clearly evident. Nuclei (N) are highly irregular in outline and vascular tissue is greatly compressed. Section stained with lead citrate. X 5 600.


L
L
8


9


L
W
10


11

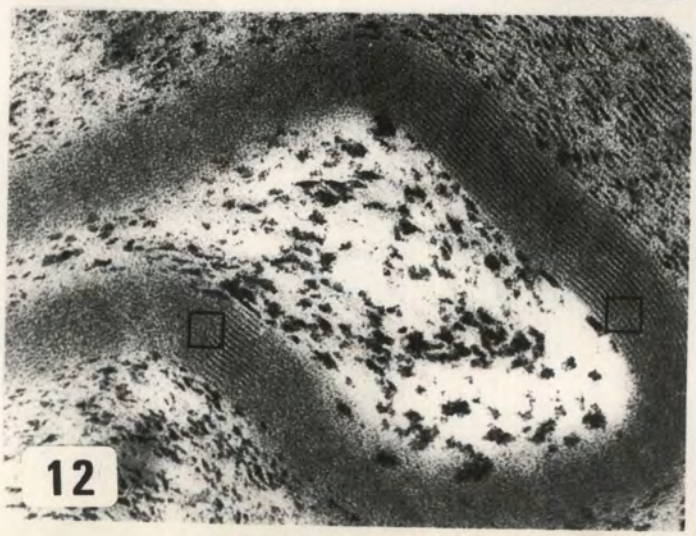
12

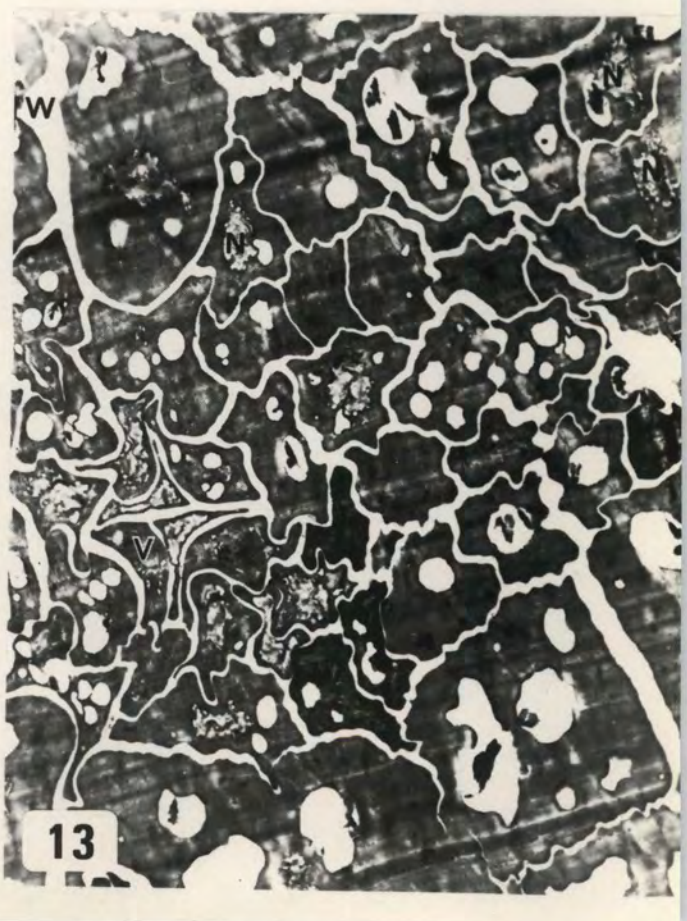
W
N
V
13

Figure 14 : Cardiolipin (diphosphatidylglycerol) precipitated by calcium chloride and fixed with osmium tetroxide, showing numerous hexagonal profiles. Lanthanum nitrate staining. X 198 000.

Figure 15 : Phosphatidylethanolamine-bovine serum albumin model system fixed with aqueous osmium tetroxide at 30°C, showing predominantly hexagonal images. Uranyl acetate and lead citrate staining. X 198 000.

Figure 16 : Brain phospholipid fixed according to the anhydrous technique of Thompson showing clear evidence of dispersion of phospholipid by the preparative technique.
Uranyl acetate and lead citrate staining. X 15 960.

Figure 17 : High-power micrograph of sample prepared as above showing rather atypical bilayer structure of phospholipids. X 172 640.

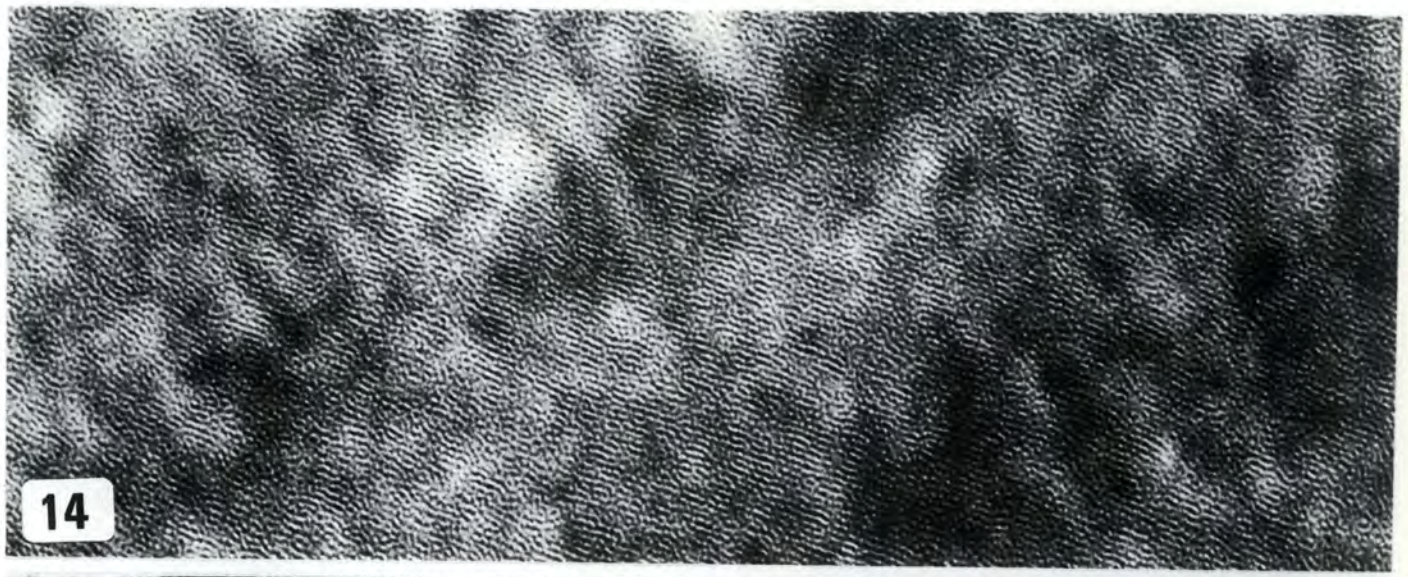
14


15


16


17

Figure 18 : Illustrates appearance of cotyledonary cells after fixation according to the anhydrous technique of Thompson. There is some evidence of tissue hydration; compare, for instance with Figure 3 earlier. Both nuclei (N) and nucleoli (NO) are evident. Tissue compression as indicated by irregularly shaped lipid bodies (L) , and withdrawal of the plasmalemma is evident (curved arrows). Uranyl acetate and lead citrate staining. X 7 840.

Figure 19 : Illustrates plasmalemma withdrawal from the cell wall and material in extracytoplasmic space (asterisks) after fixation according to the technique of Thompson. Uranyl acetate and lead citrate staining. X 29 250.

Figure 20 : Shows appearance of cotyledonary cell after imbibe-fixation, showing somewhat more expanded cytoplasm than the above figure. Nucleus (N), lipid (L) and protein bodies (PB) indicated. Some artefactual damage results from using this technique as indicated by the adjacent ruptured cell (asterisk). Uranyl acetate and lead citrate staining. X 10 080.

Figure 21 : Illustrates appearance of nucleolus (NO) and adjacent nucleoplasm after fixation according to the technique of Thompson. the nuclear envelope is not resolved and appears to have dilated (arrowheads). Membranous elements of mitochondria (M) are atypical. Lipids (L) and ribosomes (circles) are indicated. Uranyl acetate and lead citrate staining. X 29 250.

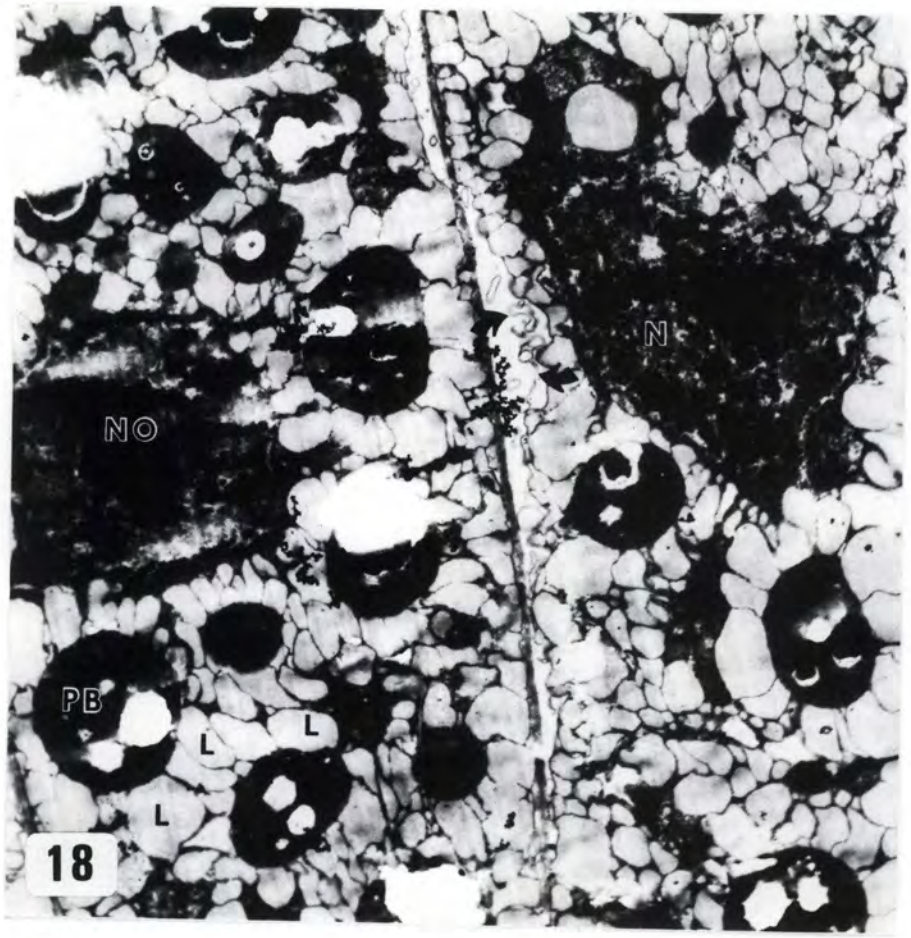
N
NO
PB
L
L
L
18


L
L
19

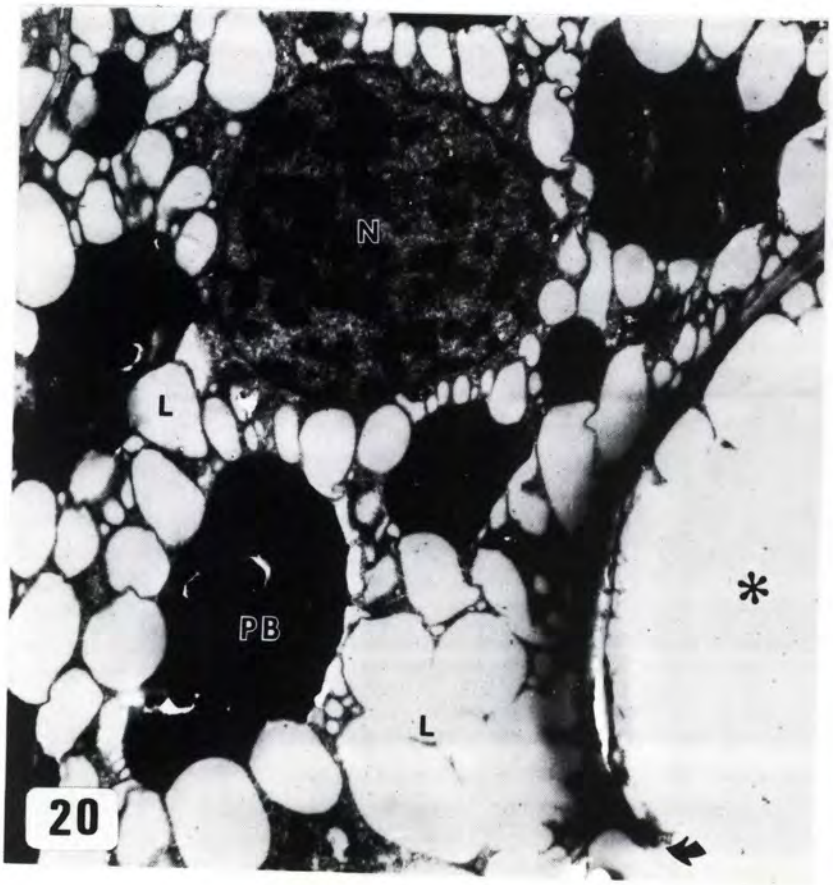
N
L
PB
L
*
20


L
M
L
NO
21

CHAPTER 4 : ULTRASTRUCTURE OF COTYLEDONARY NECROSIS

NOTE: The sections of all material presented in this chapter were stained with uranyl acetate and lead citrate.

Figure 1 : Illustrates palisade cell from cotyledon of a high vigour embryo after 2 days imbibition. Although apparently metabolically competent large-scale mobilization has not yet commenced. Phytin (asterisks) which was present in the protein bodies (PB) has been lost from the section during staining. Also illustrated are nucleolus (NO), heterochromatin in the nucleoplasm, numerous plastids (P), elongate mitochondria (M) and numerous lipid droplets (L). X 7 400.

Figure 2 : Illustrates apparent digestion of protein body (PB) content in epidermal cell of high vigour embryo after 2 days imbibition by fusion of numerous cytoplasmic vesicles with the limiting membrane of the protein body. X 14 960.

Figure 3 : Illustrates the more advanced stage of reserve mobilization seen in a marginal mesophyll cell of a high vigour embryo after 2 days imbibition. Fusion of depleted protein bodies has resulted in the production of large vacuoles (V) with a sparsely distributed fibrillar content and residual electron-dense material (D). Chloroplasts (C) are differentiated and numerous glyoxysomes (G) and mitochondria (M) are present. X 10 080.

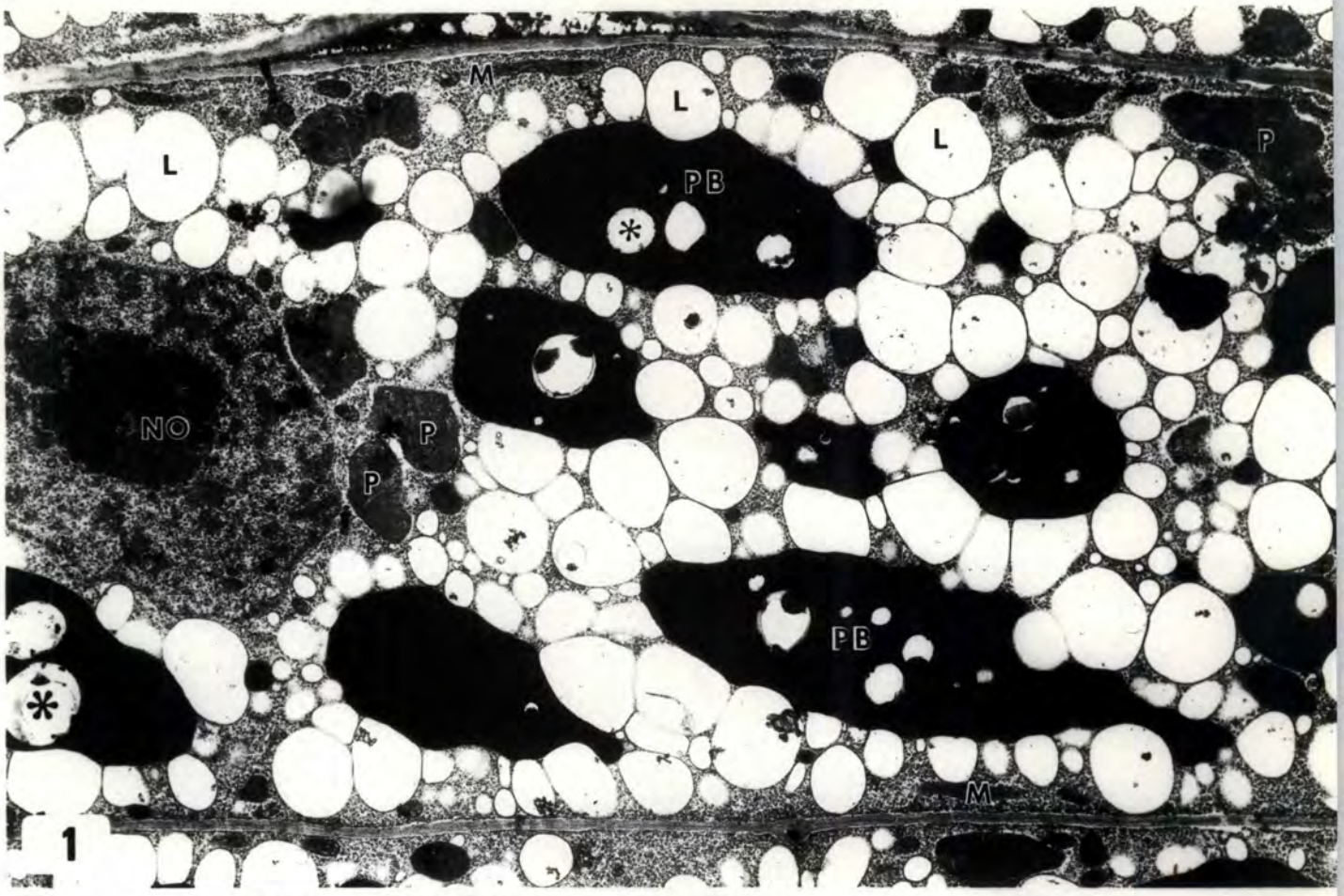

1

2

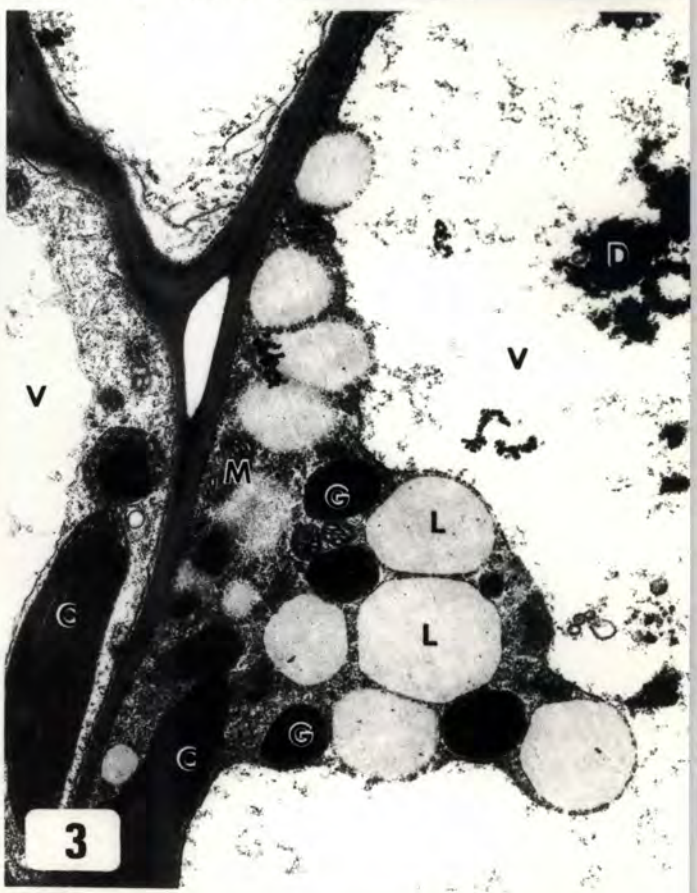

3

Figure 4 : Shows delayed mobilization of protein bodies in mesophyll cells of low vigour embryo after 5 days imbibition. The presence of membranous elements may be implicated in the digestion process (arrowheads). The mobilization of the content of the protein body (PB) appears to precede large-scale lipid (L) mobilization. Elongate mitochondria (M) are also evident. X 9 850.

Figure 5 : Illustrates damage seen in the vascular tissue of cotyledons of low vigour embryos after 2 days imbibition. Dilation of the ER (highlighted arrow-heads) and nuclear envelope is evident as well as darkly-staining nucleolus and heterochromatin. X 4 800.

Figure 6 : Illustrates appearance of palisade cells of low vigour embryo after 7 days imbibition. The delayed mobilization of lipid reserves (L) and limited vacuolation is evident in one cell, while in another the vacuole appears to contain engulfed cytoplasmic elements (arrowheads). Some chloroplasts (C) are of abnormal morphology. Glyoxysome (G) indicated. X 6 040.

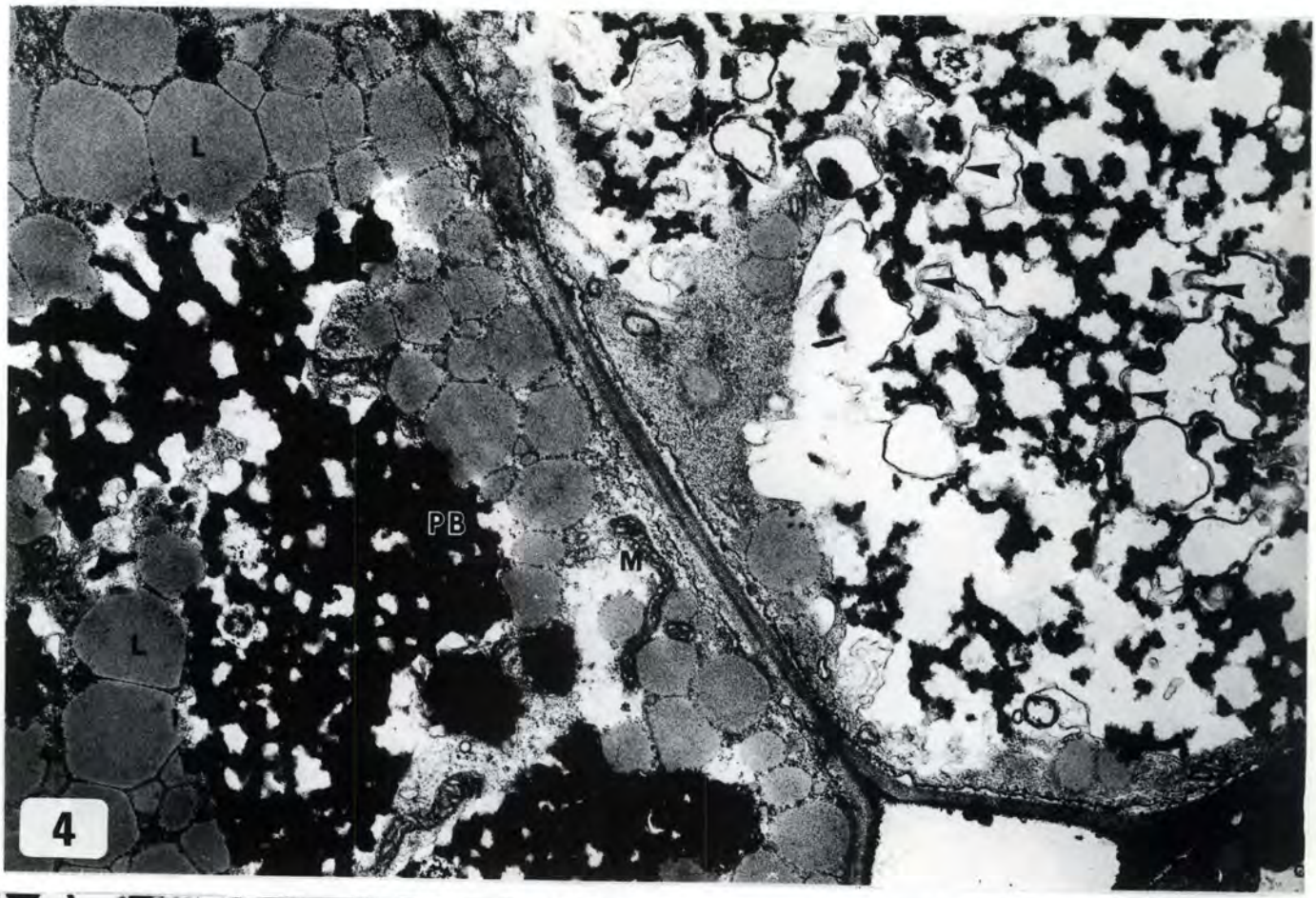
L
PB
M
L
4

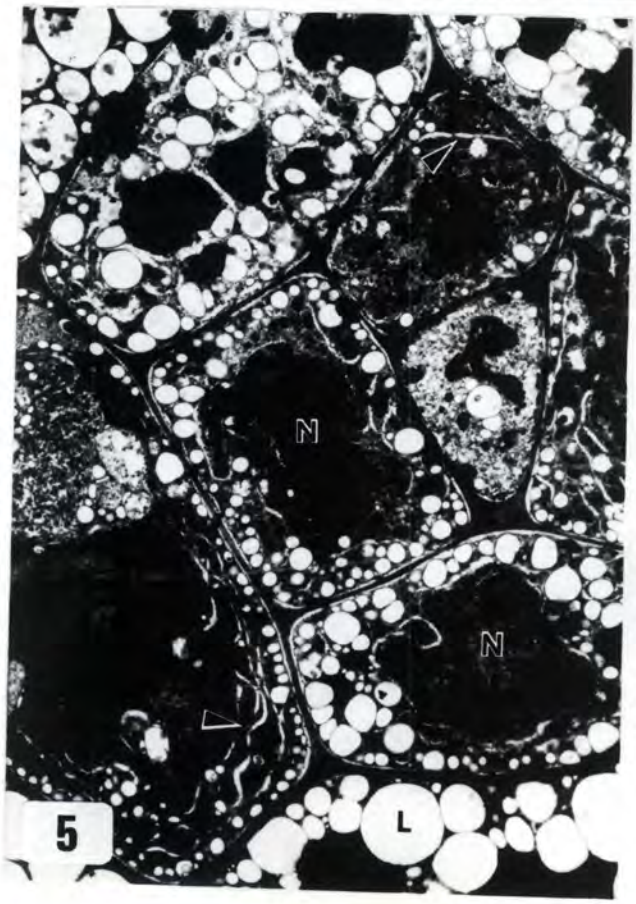
N
N
L
5


L
V
L
G
L
G
G
L
V
6

Figure 7 : Illustrates limited mobilization of protein body (PB) and lipid (L), reserves in a palisade cell of a low vigour embryo after 5 days imbibition. Partial mobilization of phytin reserves (P) has taken place and amyloplast (A) differentiation has occurred. X 7 400.

Figures 8-11: Illustrates widely divergent appearance of cotyledonary cells in low vigour embryos ranging from severe delay in mobilization (Figure 8, 7 days after imbibition); partial delay (Figure 9, 5 days after imbibition); cell plasmolysis (arrowheads Figure 10, 5 days after imbibition); variable pattern of mobilization between contiguous cells (Figure 11, arrows and vacuolation (V) of vascular tissue; Figure 9, vacuolation (V) and absence (highlighted asterisks) of mobilization).

Figure 8: X 3 300. Figure 9: X 3 300.

Figure 10: X 2 000. Figure 11: X 2 000.

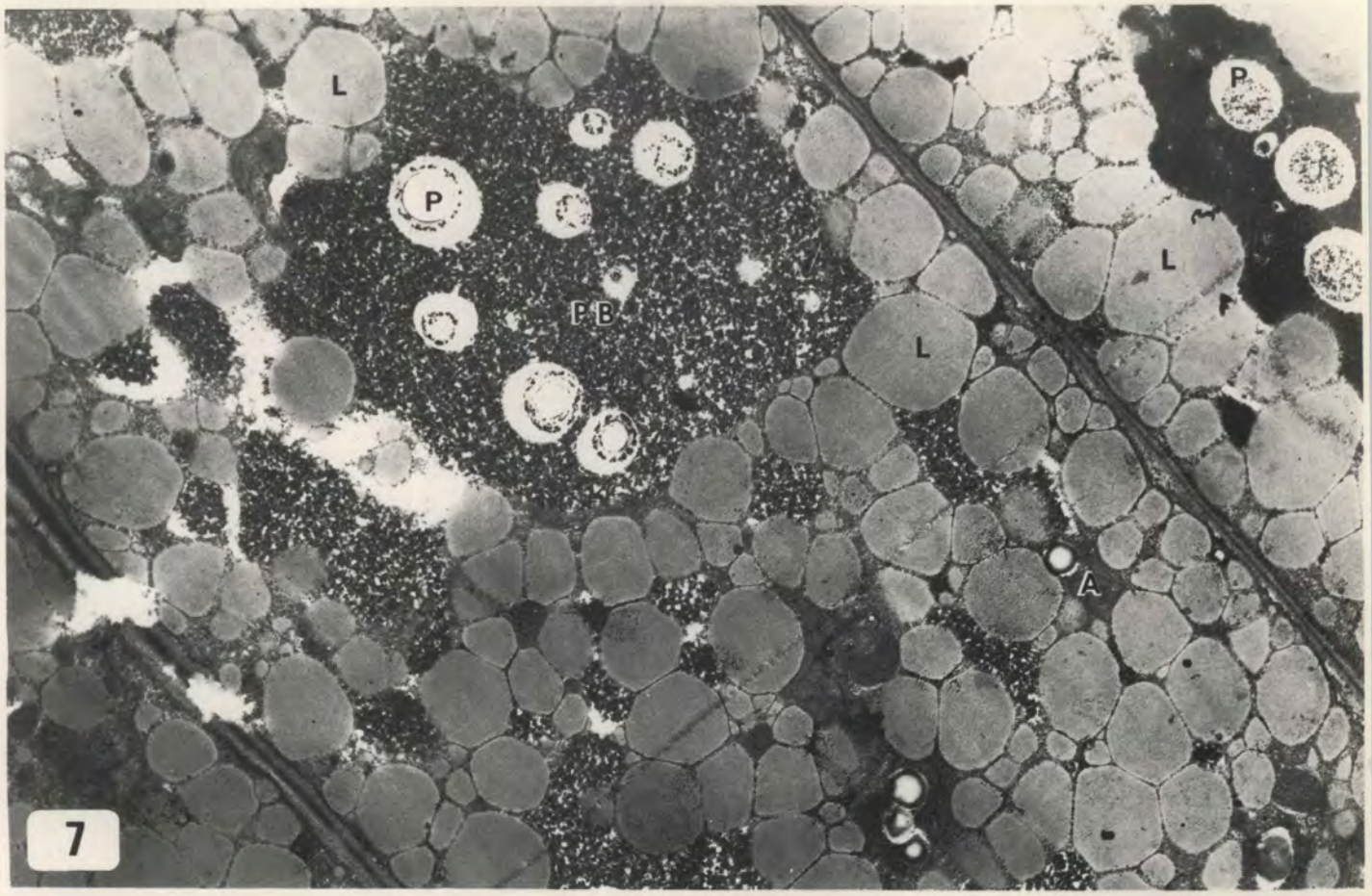
L
P
PB
L
P
L
L
A
7

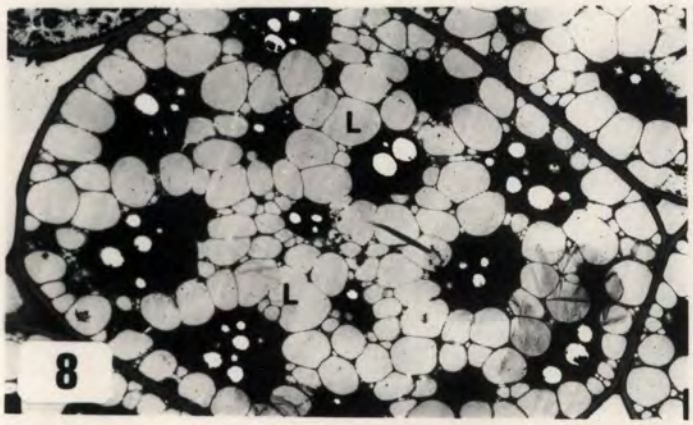
L
L
8

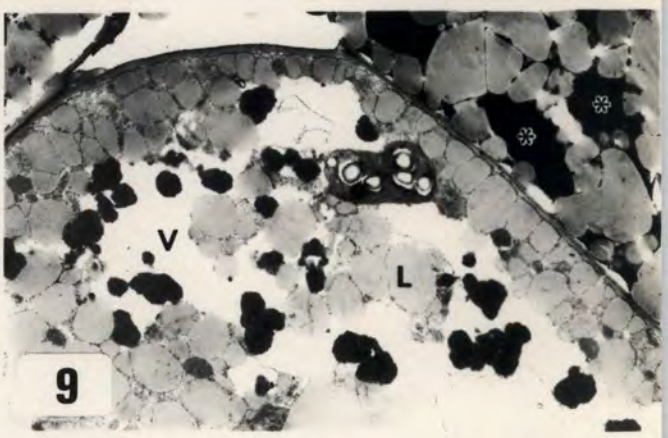
V
L
9

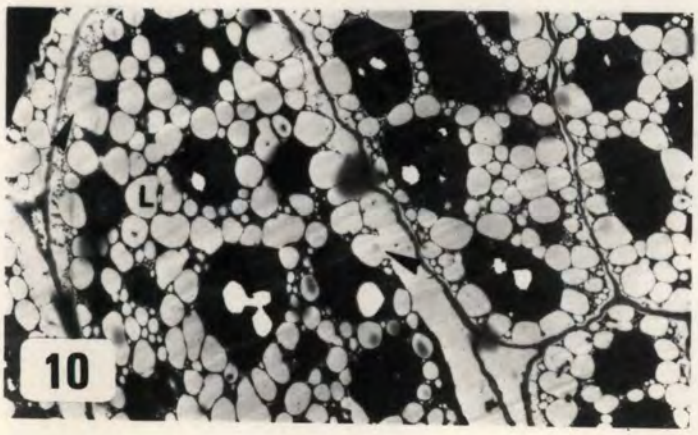
L
10

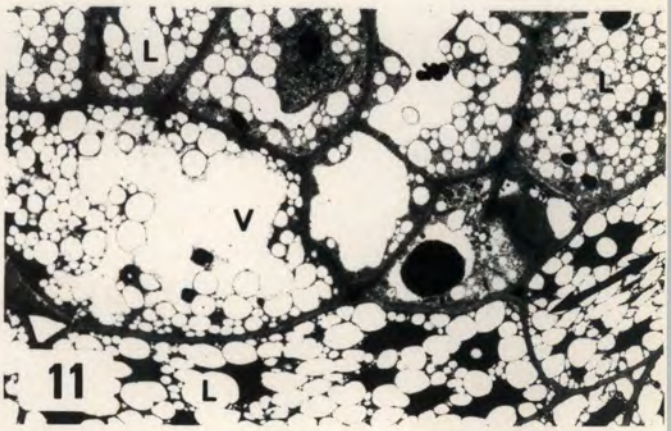
L
L
V
11
L

Figure 12 : Illustrates appearance of epidermal cells of high vigour embryo after 2 days imbibition. The early stages of vacuolation are discernible (asterisks) and apparent division and differentiation of plastids (P) has occured. Nuclei (N) of active appearance and stellate mitochondrion (M) are illustrated. X 2 600.

Figure 13 : Shows divided epidermal cell of a high vigour embryo after 5 days imbibition. Vacuolation (V) is at an advanced stage and characteristic dense deposits (D) are seen in the vacuole. The plastids have developed into amyloplasts (A) in the perinuclear region. Mitochondria (M) with well developed cristae evident in cytoplasm. X 7 860.

Figures 14, 16 & 17: Illustrate abnormal chloroplast images seen in cotyledonary cells of low vigour embryos after 7 days imbibition which principally involve dilation of and vesiculation of granal membranes (highlighted arrowheads).
Figure 14 X 15 475.
Figure 16 X 11 250.
Figure 17 X 9 780.

Figure 15 : Shows well-differentiated amyloplasts in mesophyll cell of a high vigour embryo after 2 days imbibition at a time when lipid (L) and protein reserves remain abundant. X 11 600.
Compare also with Figure 1.

Figure 18 : Illustrates mesophyll cells of a low vigour embryo after 5 days imbibition where cells of varying degrees of mobilization lie adjacent to a necrotic (N) cell.See also Figure 26. X 2 000.

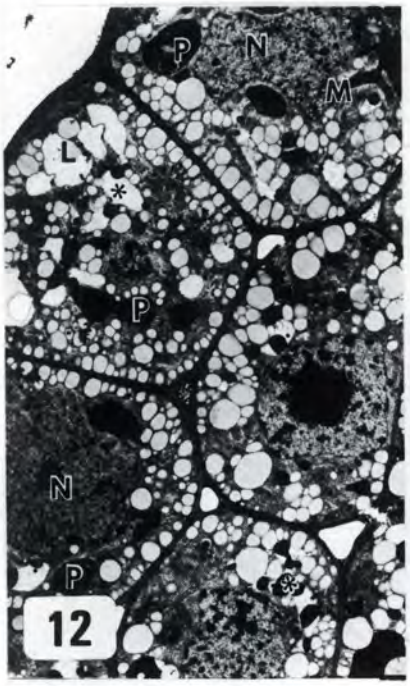
P
N
M
L
P
N
P
12

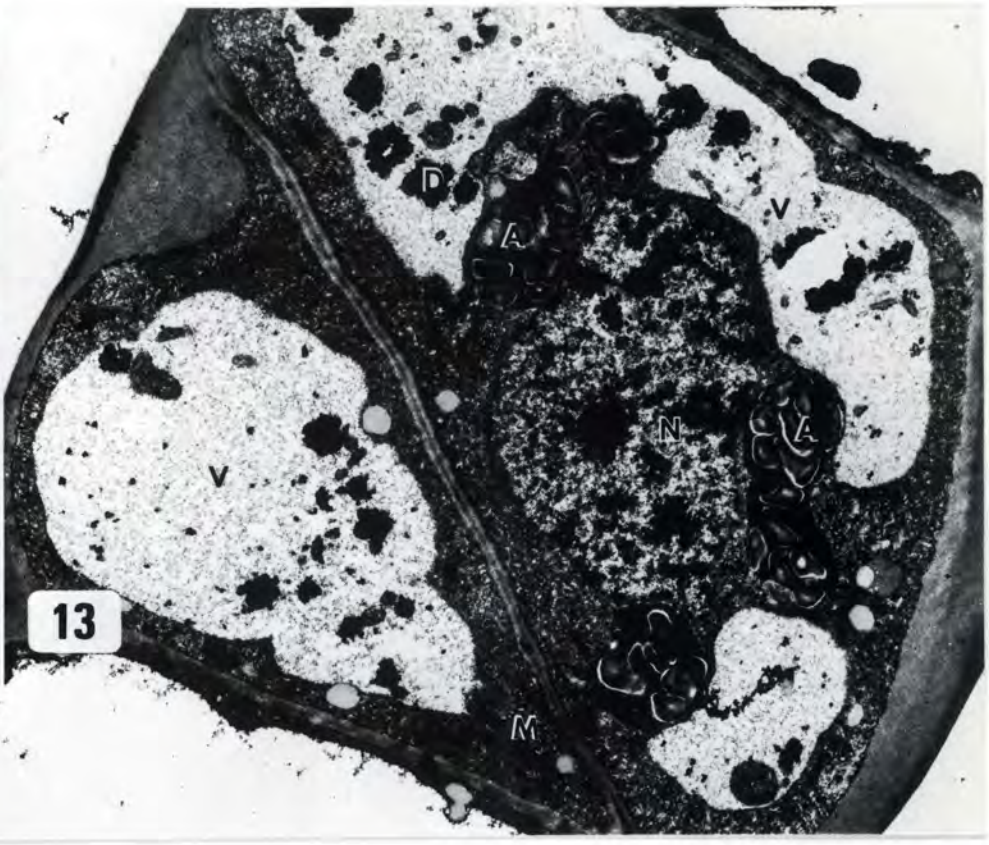
D
A
V
V
N
A
M
13

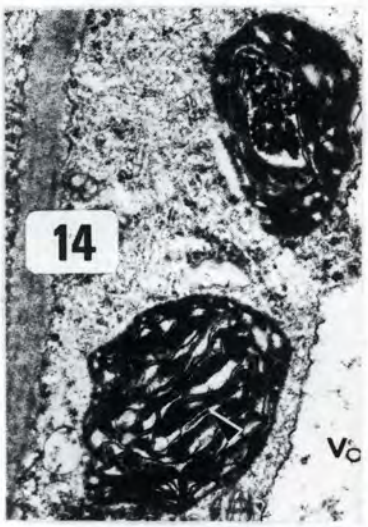
14
Vc

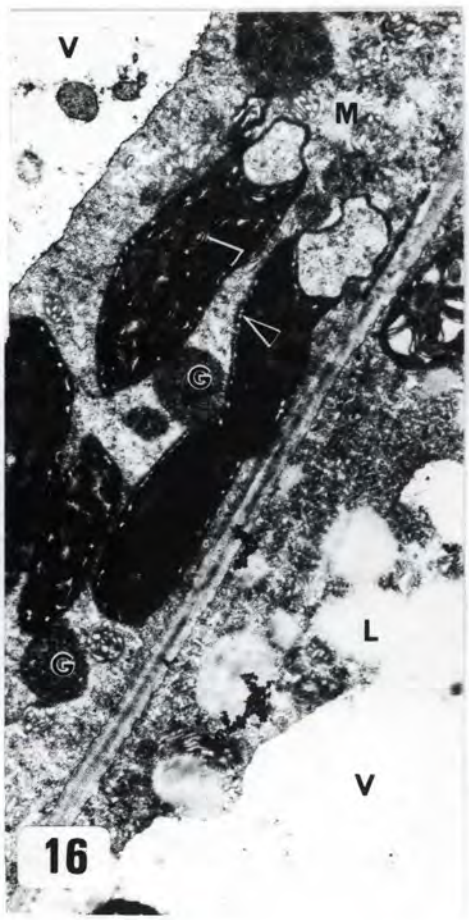
V
M
G
G
L
V
16

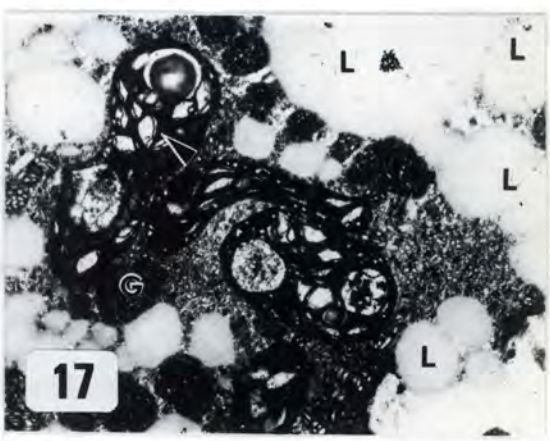
L
L
L
L
G
17

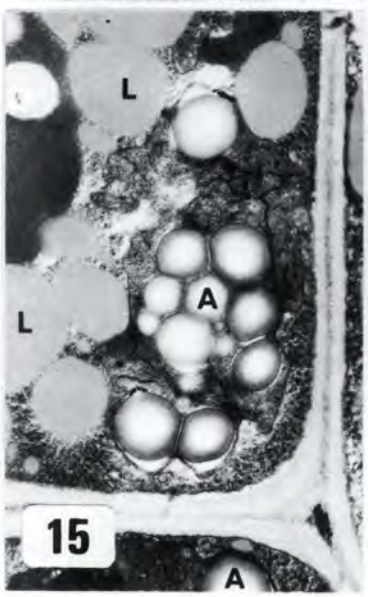
L
A
L
15
A

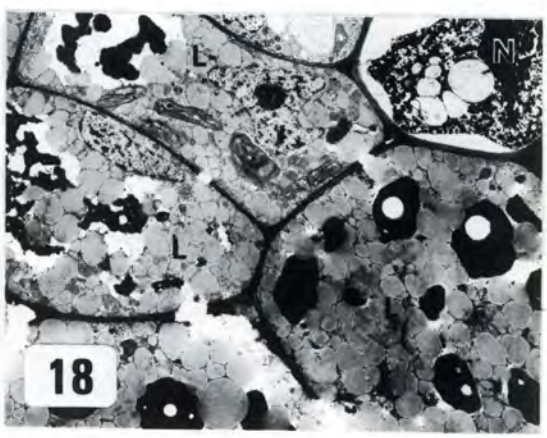
L
N
L
18

Figure 19 : Illustrates extensive wall (curved arrows) and cytoplasmic distortion (double headed arrow) in cotyledonary cells of low vigour embryo after 7 days imbibition. Epidermal cell vacuoles contain finely floccular material (E) suggesting impaired mobilization of protein content (compare with Figure 13). Chloroplasts (C) of abnormal appearance. Vacuolation (V) in a subepidermal cell of more normal appearance with typical vacuolar electron-dense deposits (D). The inferred distortion caused the rupture of one of the subepidermal cells (Star). X 7 800.

Figure 20 : Detail of abnormal chloroplast structure seen in Figure 19 between highlighted arrowheads. The limiting membrane of the chloroplasts is poorly resolved (interrupted lines) as are the plasmalemma (PM) and mitochondrial membrane (M). Dilation of some of the poorly developed grana appears to give rise to vesicle-like structure (asterisks). Unusual myelin-like figures (arrowheads) are thought to be chloroplast derived. X 24 900.

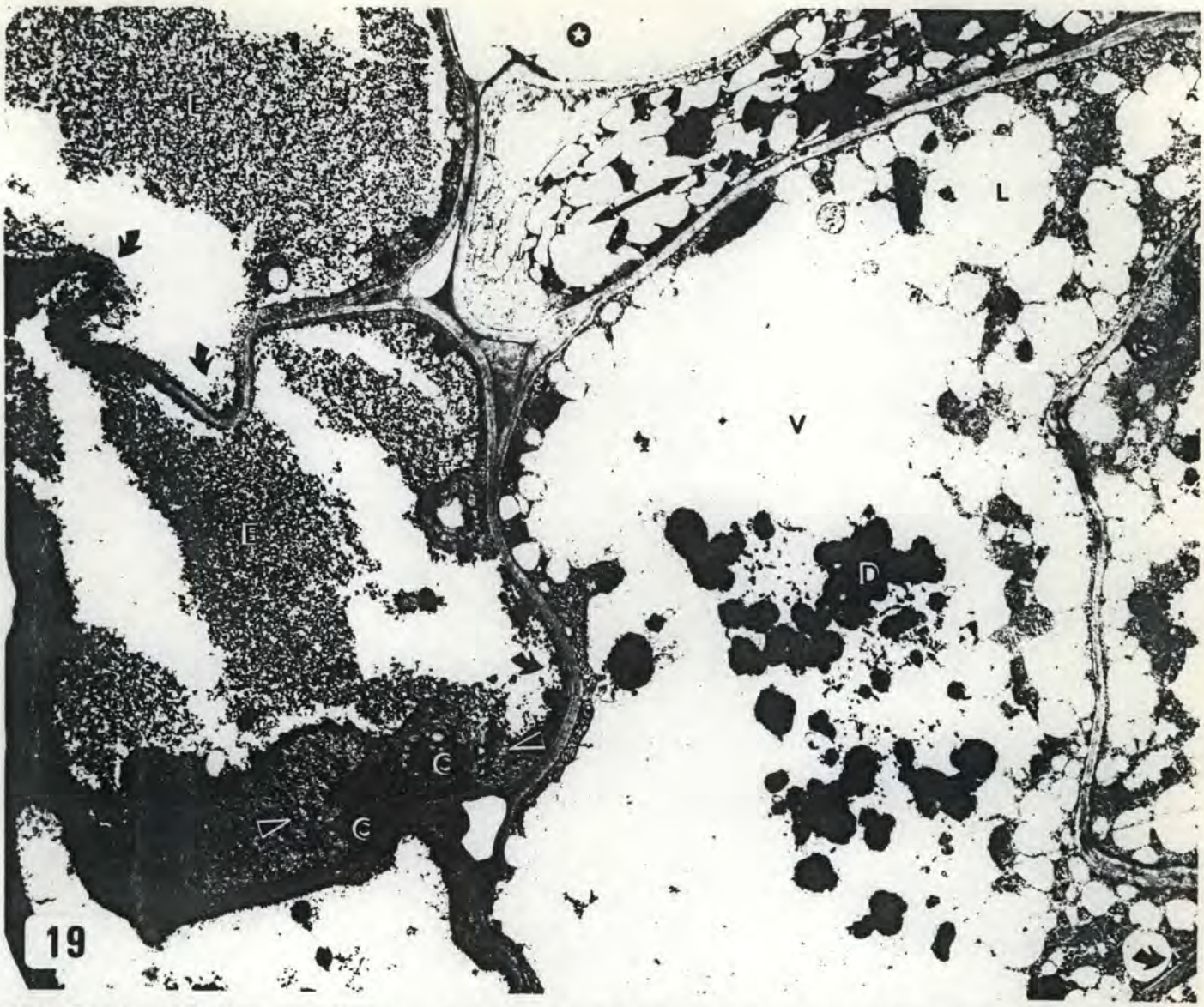
E
L
V
E
D
C
C
19

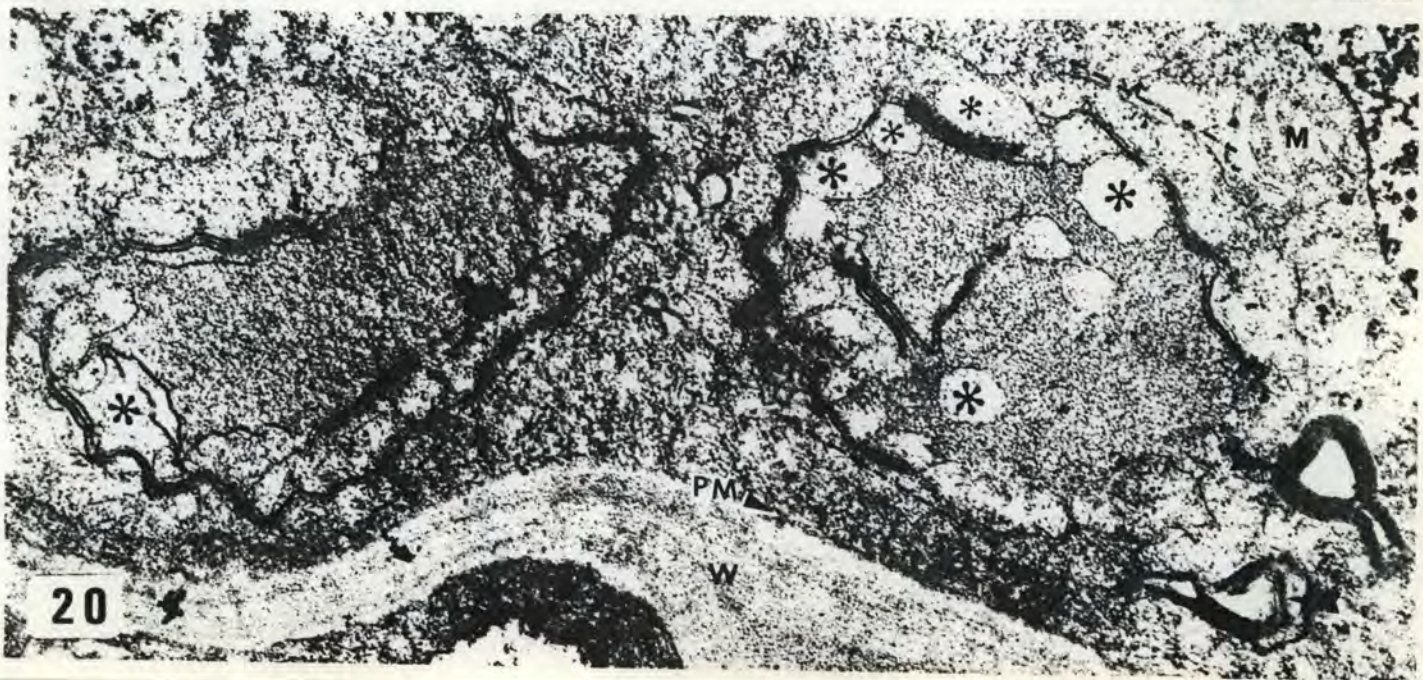
M
PM
W
20

Figure 21 : Cryosection of aldehyde-fixed cotyledon of low vigour embryo at 7 days after imbibition. Functional chloroplasts were evident in all areas of the section except for areas of localized necrosis which appeared dark yellow-orange (arrowheads). Such necrosis was absent in the region of the vascular trace (VT). Bright-field optics. X 220.

Figure 22 : Resin embedded section from the cotyledon of a low vigour embryo 7 days after imbibition showing extensive wall buckling (arrowheads). Note extensive vacuolation (V) of all marginal cells. Phase contrast optics. X 600.

Figure 23 : Illustrates marginal development of cotyledonary vascular supply in a low vigour embryo 7 days after imbibition. Necrotic zone demarcated by highlighted dots, although mobilization is evident in the vicinity of the vascular supply (highlighted) arrowheads . Formalin acetic alcohol fixed cotyledon, cleared to showed vascular supply and stained with safranin. X 32.

Figure 24 : Resin embedded section of the margin of the cotyledon of a control, unaged embryo 7 days after imbibition showing evidence of cell division in mesophyll cells (arrowheads) and the development of intercellular spaces (asterisks). Epidermal hair cell (H) and vacuoles (V) indicated. Numerous ellipsoidal chloroplasts (C) can be seen at the periphery of many of the mesophyll cells. Phase contrast optics. X 4 000.

Figure 25 : Illustrates sequence of vascular development and cotyledonary expansion at 2, 4, 6 and 8 days after imbibition in control, unaged cotyledons. Some indication of marginal cotyledonary growth is indicated by areas between arrowheads. Material prepared as Figure 23. X 16.

Figure 26 : Resin embedded section of a cotyledon from a low vigour embryo after 7 days imbibition showing mobilization of marginal reserves (M), an intensely osmiophilic necrotic region (N) demarcated by highlighted dots, and gradation of delayed mobilization in the region of the vascular trace (VT). Protein bodies with a surrounding shell of lipid droplets are still clearly evident in some cells in this region. Phase contrast optics. X 675.

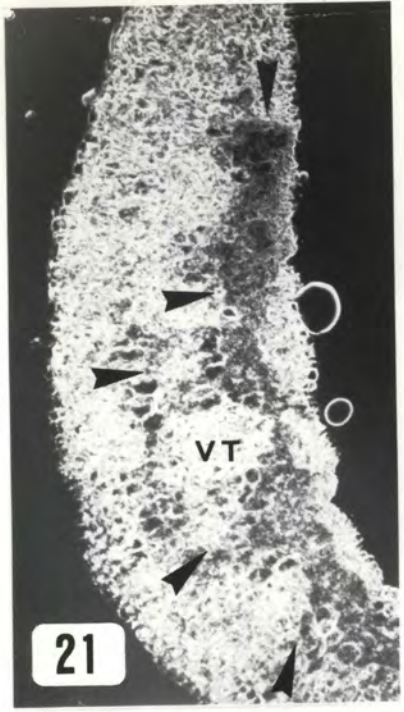
VT
21

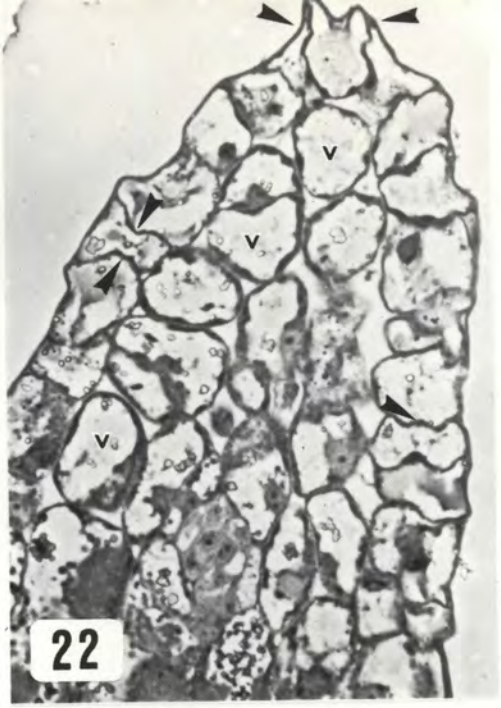
V
V
V
22

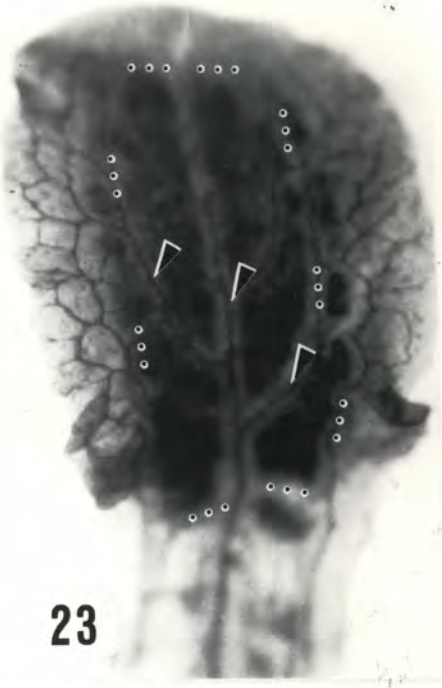
23

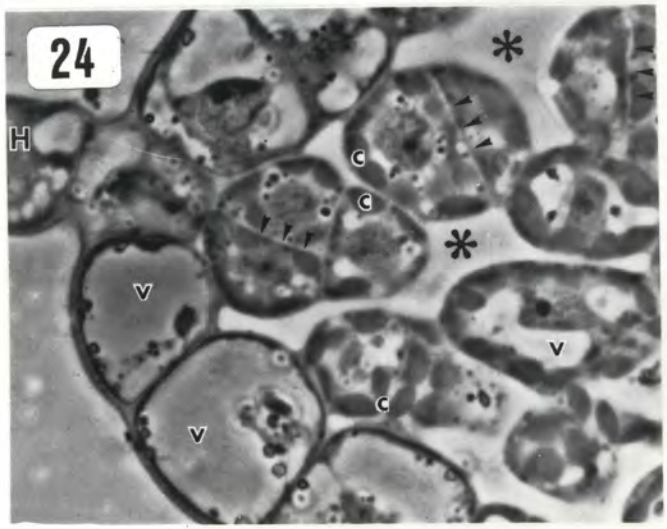
24
H
C
C
V
V
V
C

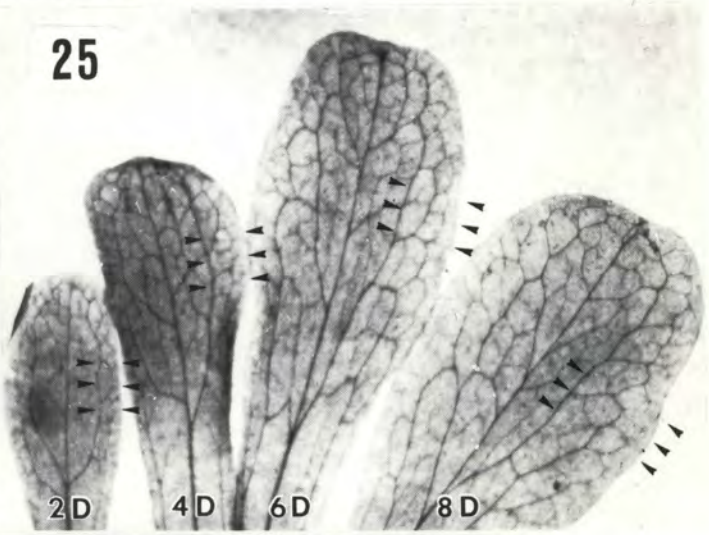
25
2D
4D
6D
8D

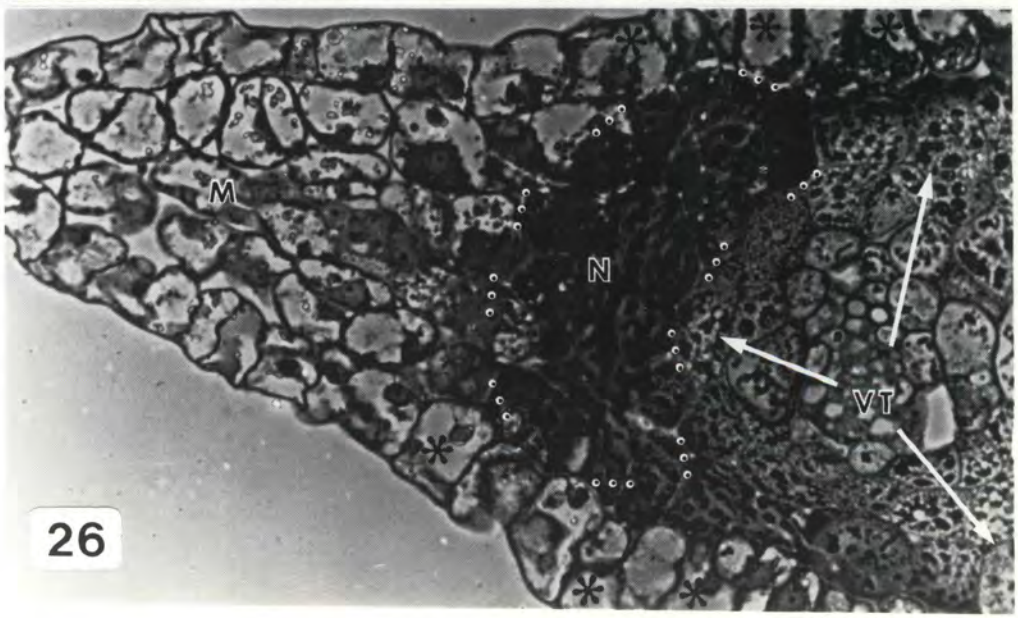
M
N
VT
26

Figure 4 : Shows the appearance of the nuclear envelope of an imbibe-fixed cell from the root tip of an embryo drawn from a sample of lowered viability (89% germination; 8 months at 60% RH and 20°C). This cell may have sustained some imbibition - related damage as evidenced by the absence of a continuous plasma membrane (highlighted arrow) and the dilated appearance of the contents of protein bodies (asterisks). X 11 400.

Figure 5 : Shows discontinuity in the staining of the nuclear envelope (arrowheads) and some plasmalemma breaks (arrowheads, top right) of imbibe fixed tissue from an embryo drawn from a sample of lowered viability. (Details as for Figure 4, above). Note dilated, cristae-less mitochondria. X 19 500.

Figure 6 : Illustrates discontinuity in the nuclear membrane of a cell near the cut surface of an embryo drawn from a sample of high viability(arrowheads). There is evidence for rupture of membrane of the protein body (asterisk). Compare also with Figures 3,4,5, 7 & 9. X 11 400.

CHAPTER 5 : ULTRASTRUCTURAL CHANGES DURING IMBIBITION - (A) STUDIES USING TISSUE SLICES

Note: All section staining by uranyl acetate and lead citrate unless otherwise indicated.

Figure 1 : Illustrates appearance of cells in the meristematic region of the root cap of unaged, high viability embryos after placing air-dry roots directly into glutaraldehyde fixative and processing according to standard techniques. Material prepared in this manner will be referred to as imbibe-fixed to distinguish it from root tips or slices which were allowed to imbibe in contact with water, however briefly, before fixation. The dispersed nature of the ground cytoplasm (asterisks) may be the result of localized rupture of vacuolar membranes and/or rapid, uncontrolled imbibition. Mitochondria of dilated appearance may also be seen, although the plasmalemma appears intact. X 11 960.

Figure 2 : The dilated appearance of cytoplasmic membranous components is evident in the undamaged cells at the cut surface of a sliced, imbibe-fixed root tip of control, high viability embryos. Plasmalemma integrity is not altered by the treatment (arrowheads) and full cell turgidity is apparently attained. Note the relative integrity of the nuclei of the cut cells. X 5 880.

Figure 3 : Illustrates the discontinuous nature of staining (arrowheads) seen in the nuclear envelope of a meristematic cell of an imbibe-fixed, non-viable embryo (22 months storage at 60% RH and 20°C). Note intense staining of lipid bodies (L) and poor differentiation between the staining of nucleoplasm (N) and ground cytoplasm obtained with only lead citrate staining. X 67 900.

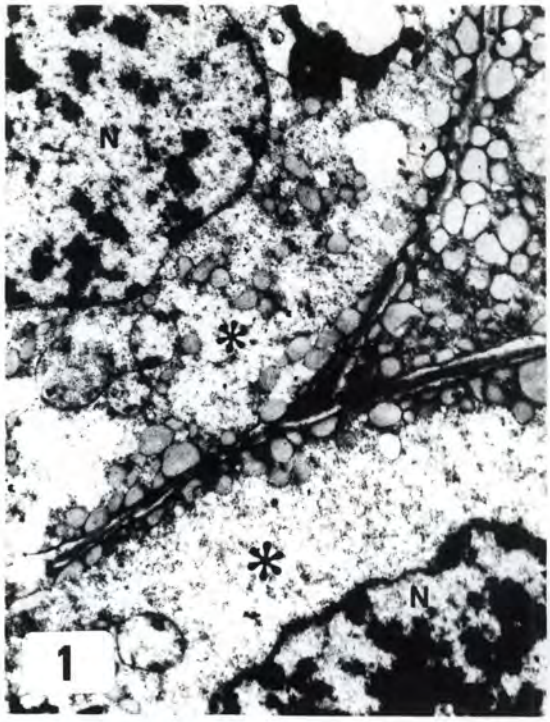
N
N
1

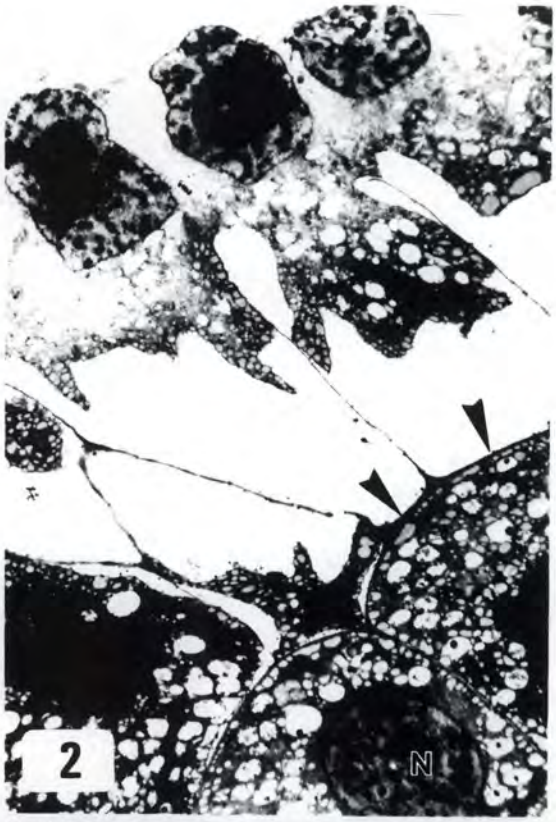
N
2

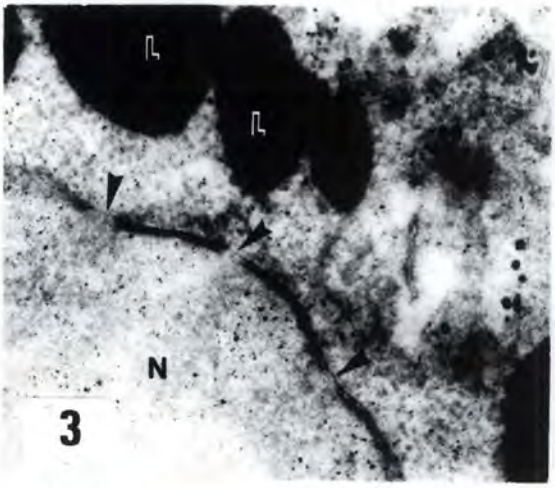
L
L
N
3


4

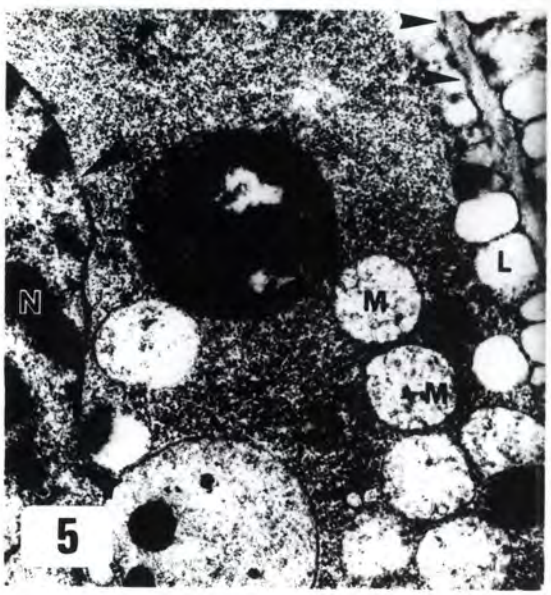
N
M
M
L
5

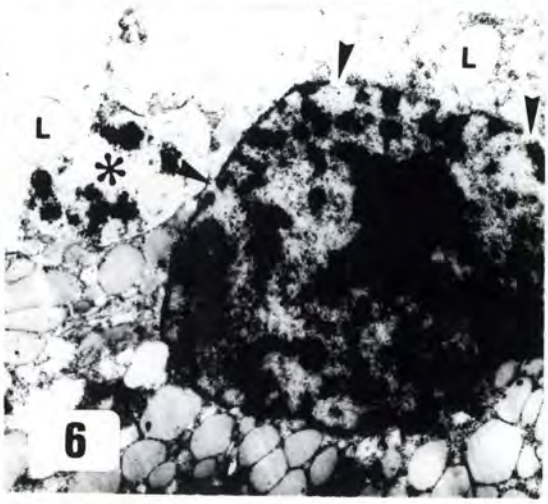
L
L
6

Figure 11 : Illustrates greater continuity of the plasmalemma in the cortical cell of an embryo drawn from a sample of high vigour in which the embryo was allowed to imbibe for 1 hour before fixation. A close association is evident between the lipid bodies and the plasmalemma (arrowheads). The nucleolus (NO) is compact and the heterochromatin fibrillar and disperse. (Compare Figures 4 & 7). X 15 960.

Figure 12 : Undifferentiated mitochondria (M), some of which may have suffered membrane damage (asterisk), from an imbibe-fixed root tip of an embryo drawn from a seed sample of lowered viability. Electron-dense deposits (arrowheads) are thought to be phosphate deposits. X 39 200.

Figure 13 : Illustrates conjoined nature (arrowheads) of mitochondria (M) in a meristematic cell of an imbibe-fixed root from a high vigour sample. Short cristae-like structures (asterisks) were seen to span a small part of the electron translucent mitochondria. X 42 560.

Figure 7 : Illustrates discontinuities and the poorly resolved nuclear envelope from an embryo drawn from a non-viable sample. (Storage details as for Figure 3). In this instance the root tissue slice was allowed to imbibe on filter paper for 30 minutes before fixation and preparation for electron microscopy. Note formless, patchy staining of nucleolus (N) and nucleoplasm. X 22 750.

Figure 8 : Shows rupture of nuclear envelope (top right) and apparent blebbing of both elements of the membrane bilayer (asterisks) in seed from a non-viable sample which was imbibed for 30 minutes before fixation (compare with Figure 3 in which sample was imbibe-fixed). Note rather homogenous nature of cytoplasm and dilated mitochondria (M). Lead citrate staining. X 10 150.

Figure 9 : Nuclear envelope at higher magnification from a non-viable sample which was imbibed before fixation. The membrane blebbing (highlighted arrow-heads) may be a precursor of the condition illustrated in Figure 8 (asterisks). Note the absence of clear bilayer structure in the envelope, which contrasts markedly with that seen in imbibe-fixed material (Figure 3). X 67 900.

Figure 10 : Illustrates the close association between the plasmalemma and lipid bodies (L) in the cortical cell of an unsliced, imbibe-fixed radicle drawn from a sample of high vigour. Plasmalemma continuity is less evident in the regions between adjacent lipid droplets (arrowheads). X 31 200.


N
7

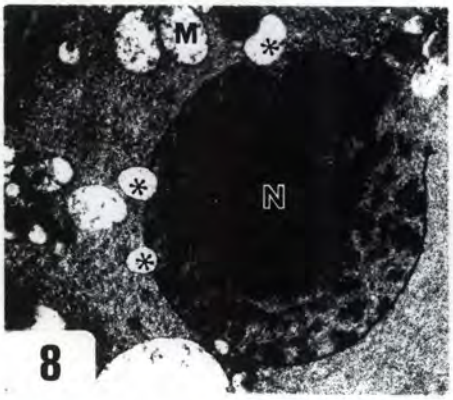
M
N
8


N
9

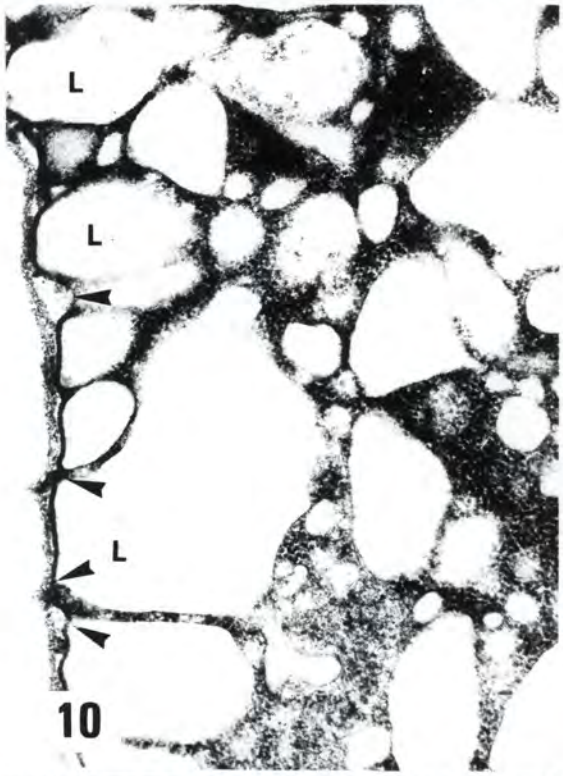
L
L
L
10


NO
11

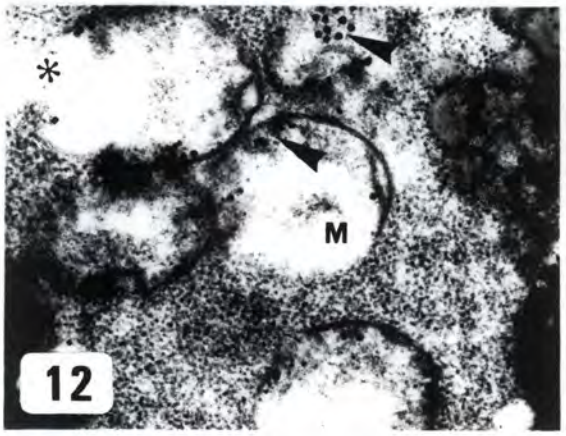
M
12

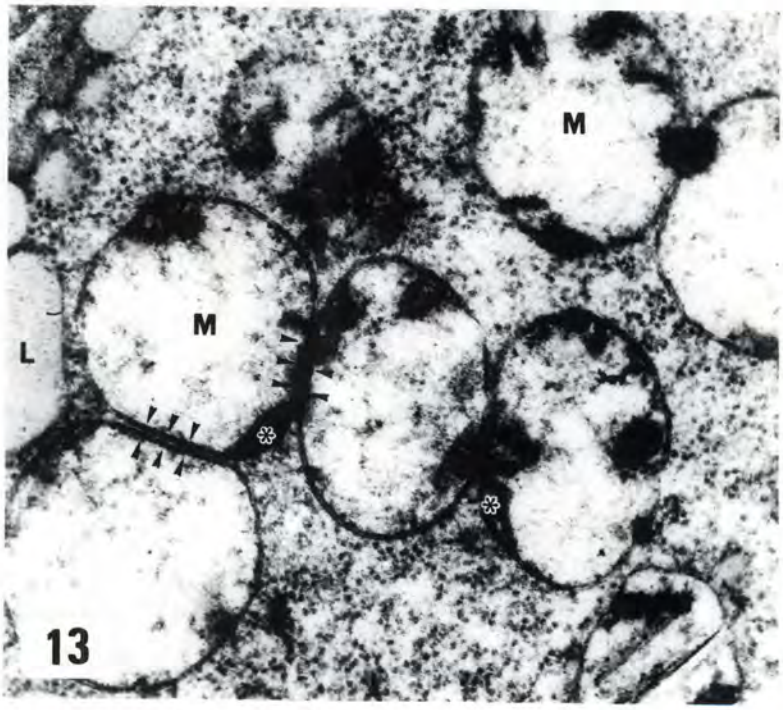
M
M
L
13

Figure 18 : Appearance of mitochondria (M) in freeze-substituted tissue of high vigour embryos showing uniformly electron dense matrix and a single cristae-like structure spanning part of one organelle. The appearance of a regular array of small particles along the membrane is indicated (arrowheads) and adjacent lipid body (L). X 146 080.

Figure 19 : Illustrates regular array of ribosome-like particles along the margins of lipid bodies (L) in freeze substituted tissue (arrowheads) and in surface view (R). X 89 640.

Figure 20 : Epidermal cell of an imbibe-fixed root tip from an embryo drawn from a sample of non viable embryos (see also Figure 21) which may have suffered imbibition-associated injury as indicated by the dilated and possibly fused protein bodies (asterisks). Some of the smaller electron translucent vesicles are thought to be mitochondria. A small degree of plasmolysis is evident (arrowheads). X 4 900.

Figure 21 : Imbibe-fixed radicle cells of a non viable embryo (22 months storage at 60% RH and 20°C) in which plasmalemma withdrawal is more extensive and in which little evidence for dilation of mitochondria and protein bodies is seen. The absence of clearly discernible nuclear (N) detail suggests that this may represent a more advanced stage of deterioration than that illustrated in Figure 20 where some measure of osmotic regulation appears evident. Numerous lipid droplets (L) are clearly evident at the membrane (arrowheads). X 4 900.

Figure 14 : Illustrates appearance of an imbibe-fixed cells from seeds crushed in liquid nitrogen before imbibe fixation. The sample was of high vigour seed and shows little evidence of plasmalemma breaks. Although some mild plasmolysis is evident by the withdrawal of the protoplast from the cell wall (W), the overall image obtained is not unlike that of Figure 10 with a close plasmalemma-lipid body (L) association (arrowheads). Note tubule-like structures (curved arrow) previously reported using anhydrous fixation techniques (Chapter 3; Figures 8-11). X 26 650.

Figure 15 : Illustrates appearance of imbibe-fixed cells from non-viable seed, prepared as for Figure 14. Although the plasmalemma is apparently only partly withdrawn from the cell wall (W) cytoplasmic disorganisation has occurred as evidenced by the loss of ground cytoplasm. Mitochondria (M) show loss of membrane structure and severe dilation. Nuclear lobing, dispersal of the heterochromatin of the nucleoplasm (N), and a compact nucleolus (N) are evident. The integrity of the protein body (PB) membrane is maintained. X 15 580.

Figure 16 : Shows intact plasmalemmae in radical cells of a high vigour embryo after 10 minutes imbibition before being prepared for electron microscopy by using a freeze substitution technique. A close association between the lipid bodies (L) and the membrane are clearly evident, and plasmodesmatal continuity is evident (arrowheads). Although the exact extent of tissue hydration is unknown, the ultrastructural appearance of the tissue is similar to that of anhydrously fixed material. (See Figures 3 & 6, Chapter 3). Note ribosome-like particles between the lipid (L) droplets (squares). X 42 560.

Figure 17 : A more deeply-seated cells from radicle tissue prepared by freeze substitution (as above) showing withdrawal of the plasmalemmae from the wall (W). Lipid (L) and nucleus (N) indicated. X 7 590.

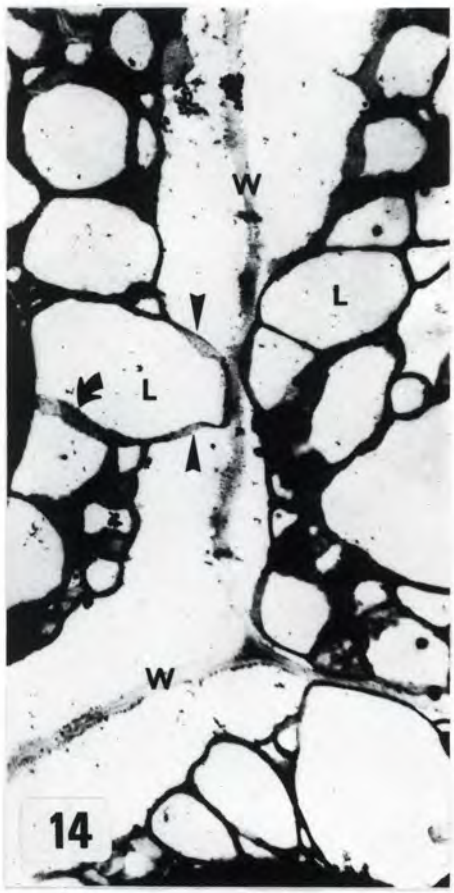
W
L
L
W
14

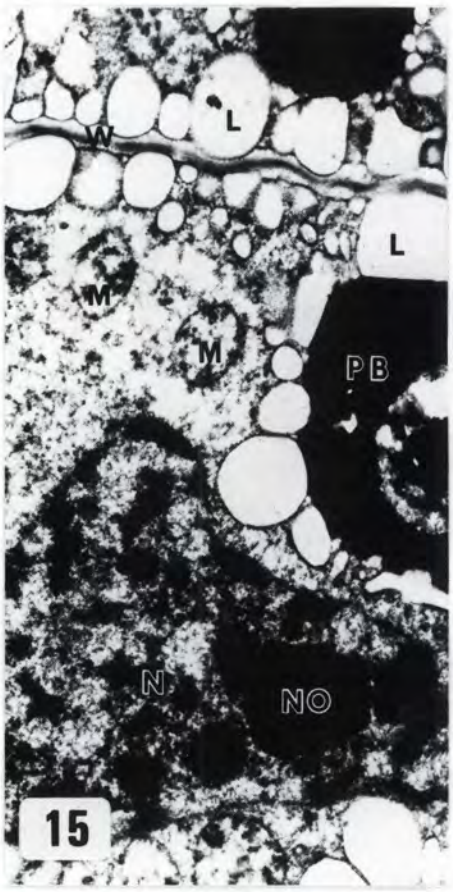
W
L
L
M
M
PB
N
NO
15

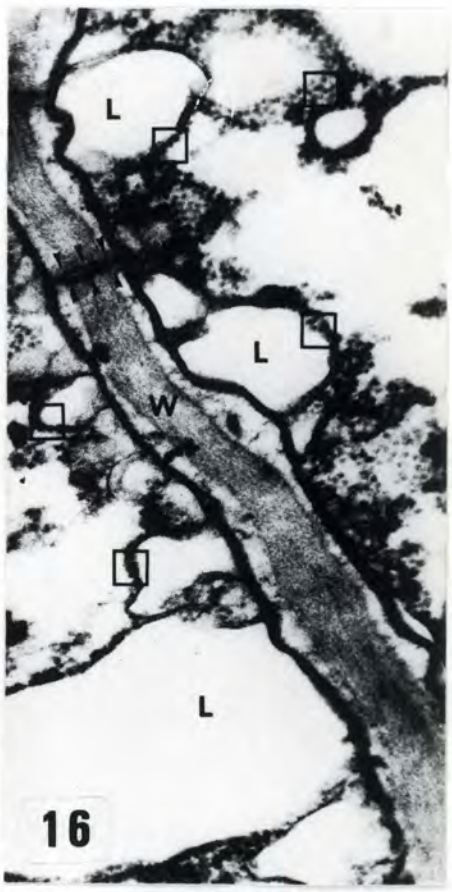
L
L
W
L
16

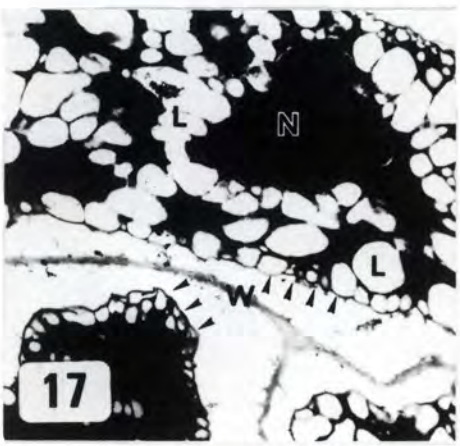
L
N
L
W
17

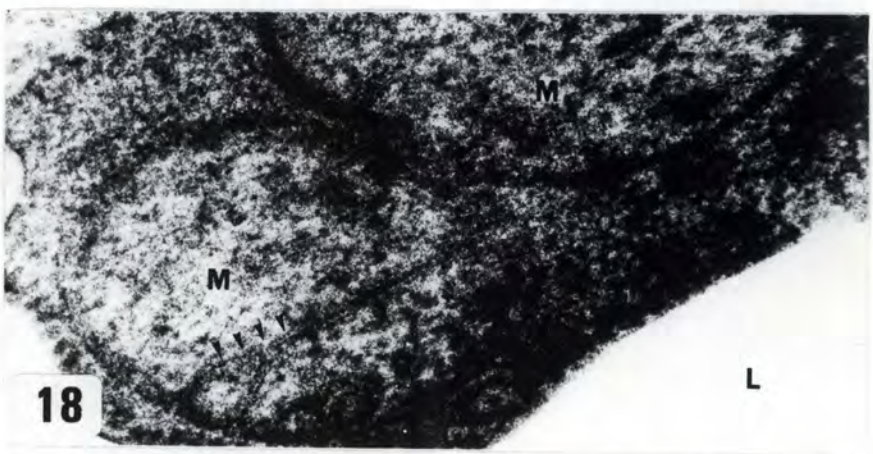
M
M
L
18

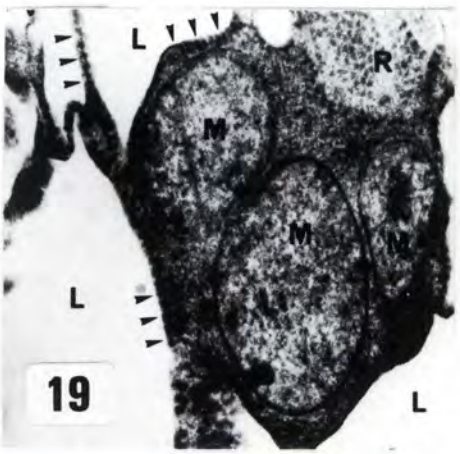
L
R
M
M
M
L
L
19

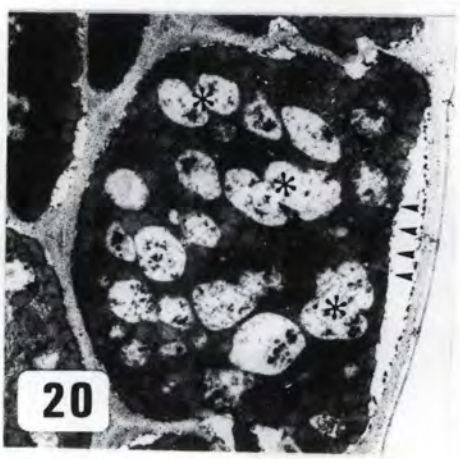
20


L
L
L
N
21

Figure 22 : After 1 hour of imbibition some evidence is seen of a separation of the lipid bodies (L) from the plasmalemma (arrowheads), unlike that prevailing in imbibe-fixed material (Figure 10). Unaged, high-vigour sample. X 47 040.

Figure 24 : Illustrates the plasmolysed appearance of a non-viable root tip cell of an imbibe-fixed tissue slice. A clearly-defined plasmalemma is not evident except for a small region (arrows). Within the cytoplasm two vacuoles appear largely devoid of contents with discontinuous or poorly-defined membranes. Note the closely appressed lipids (L) at the periphery of the cytoplasm. X 42 560.

CHAPTER 5 : ULTRASTRUCTURAL CHANGES DURING IMBIBITION - (B) STUDIES ON INTACT RADICLE TISSUES AFTER 12 HOURS IMBIBITION

Figure 23 : Appearance of root cap cell after 13 hours imbibition in an embryo drawn from a high vigour sample showing numerous vesicles (VE), thought to be Golgi-derived, fusing with the plasmalemma. The vesicles appear devoid of contents which may be the result of the potassium permanganate treatment of sections before staining with uranyl acetate and lead citrate. Wall (W) fibrillar structure is poorly resolved, while amyloplasts (A) are exceptionally electron dense. X 35 840.

Figure 25 : Illustrates active appearance of nucleolus and cytoplasm in an inner root cap of control, high vigour embryo after $17\frac{1}{2}$ hours imbibition. The nucleolus (NO) is seen to possess a vacuole (V), and numerous profiles of ER are visible in the cytoplasm (highlighted arrowheads). The nuclear envelope is clearly defined (arrowheads) and several amyloplasts (A) are evident. X 15 200.

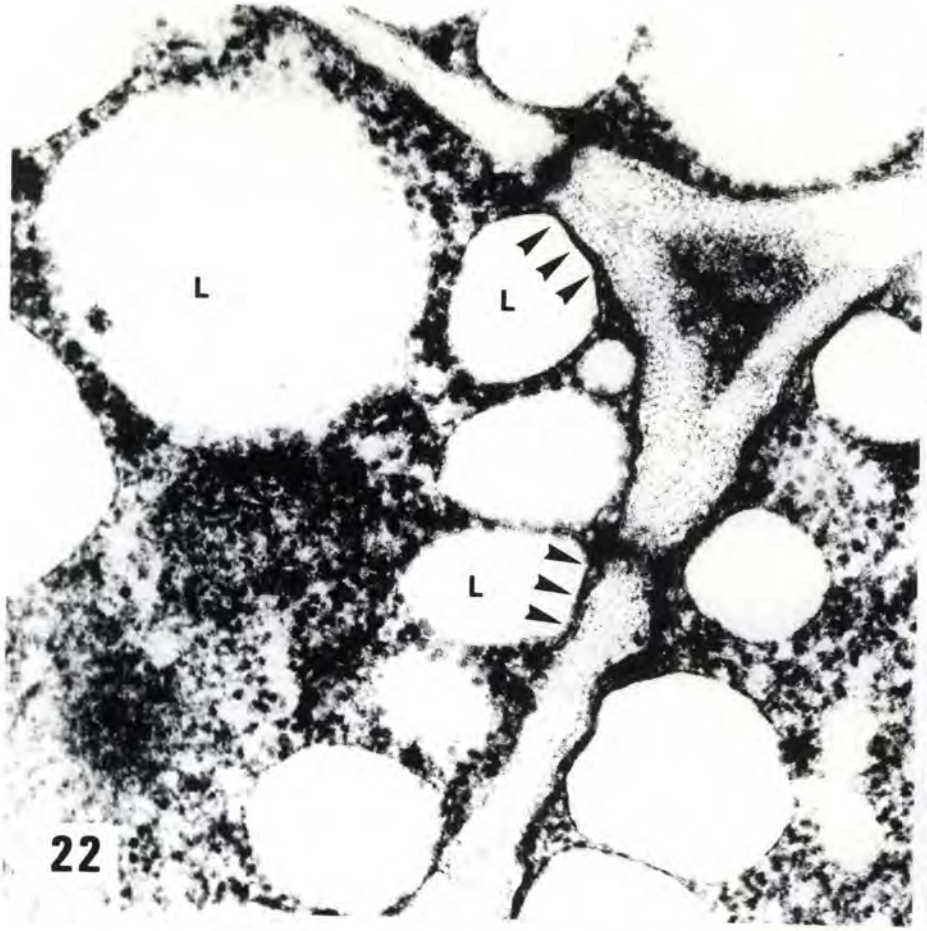

22

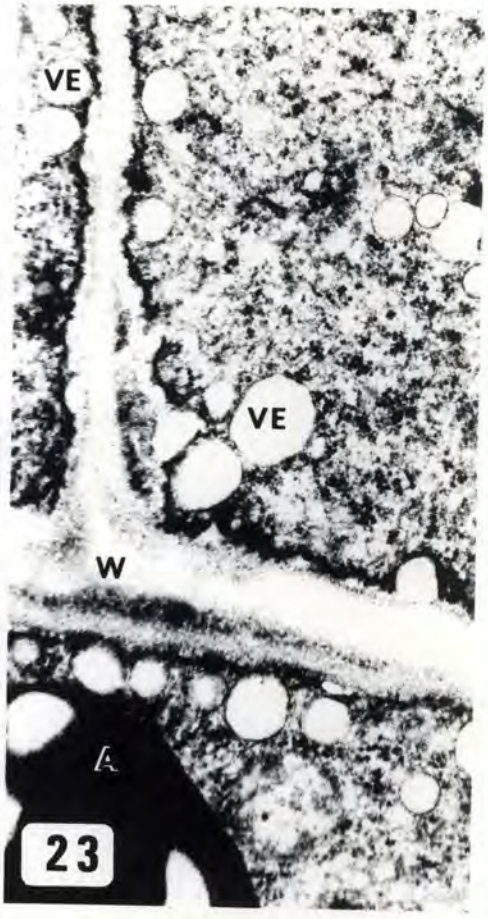

23

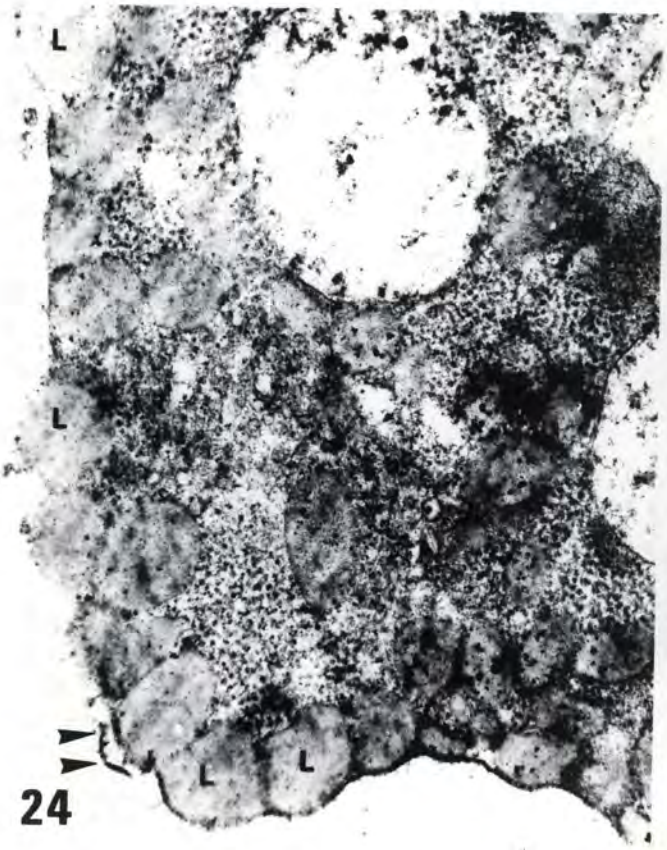

24

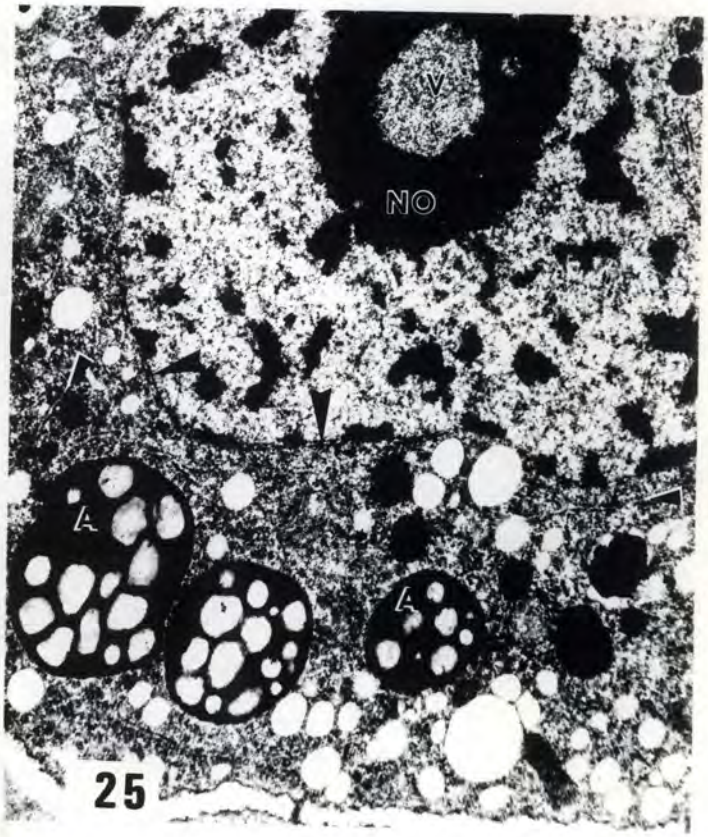

25

Figure 26 : A root cap cell from an embryo drawn from a seed lot of low viability (3 months storage at 60% RH and 20°C) showing the extensive dilation of the ER (arrowheads). The nucleus and nucleolus are of normal appearance and only slight withdrawal of the plasmalemma is evident. An adjacent necrotic cell (asterisks, top right) shows extremely electron dense cytoplasm. X 9 660.

Figure 27 : Illustrates dilation of the ER (arrowheads) and loss of defining boundaries around amyloplasts seen in low viability samples. Protein bodies (PB) appear relatively intact, as do mitochondria. Note the appearance of electron translucent 'halos' around the starch grains (S), which contrasts markedly with Figure 25. No cell plasmolysis evident. X 15 200.

Figure 28 : Illustrates what is thought to be a more advanced stage of cytoplasmic disorganisation in a root cap cell from a sample drawn a non-viable seed lot (3 months storage at 100% RH and 20°C) after 13 hours imbibition. Confluence of the lipid droplets (L) and withdrawal of the plasmalemma (arrowheads) from the cell wall can be seen. It is impossible to distinguish clearly a definable boundary between the amyloplast, ground cytoplasm and vacuole-like bodies within the area demarcated by the white arrows. The ground cytoplasm and nucleoplasm (N) are electron-dense and floccular, and the nucleolus (NO) is compact. X 18 240.

Figure 29 : Illustrates dilation of ER seen in a cortical cell from an embryo of low viability after $17\frac{1}{2}$ hours imbibition. Anastomoses between the dilated elements is evident (arrowheads) and dilation of the Golgi cisternae are also evident (asterisks). The plasmalemma is intact and continuous (curved arrows). X 16 340.

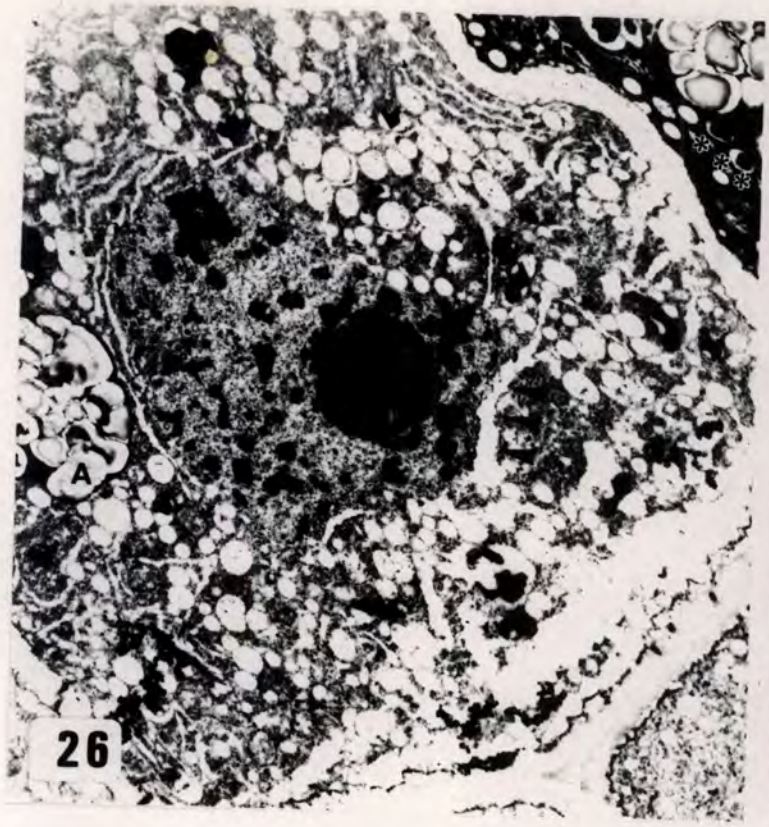

26

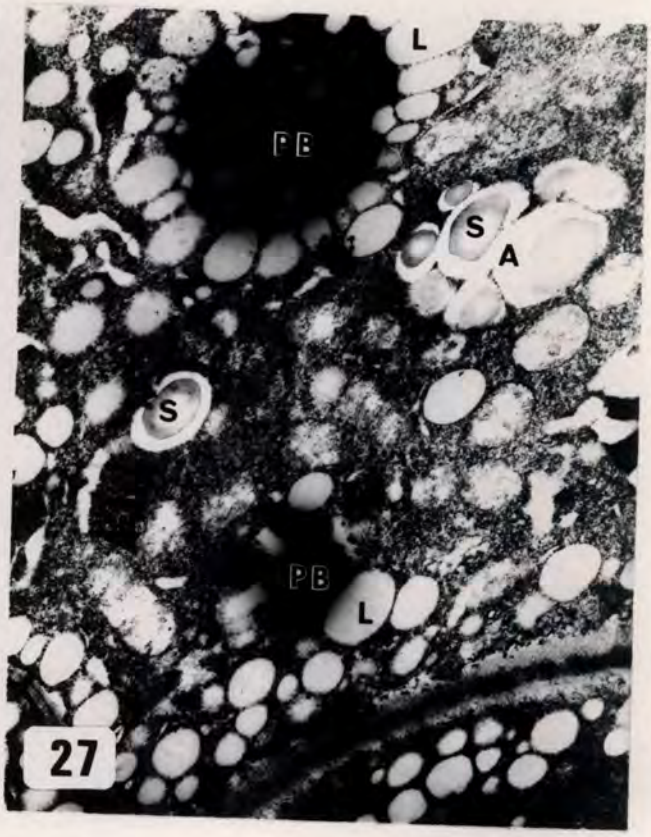

27

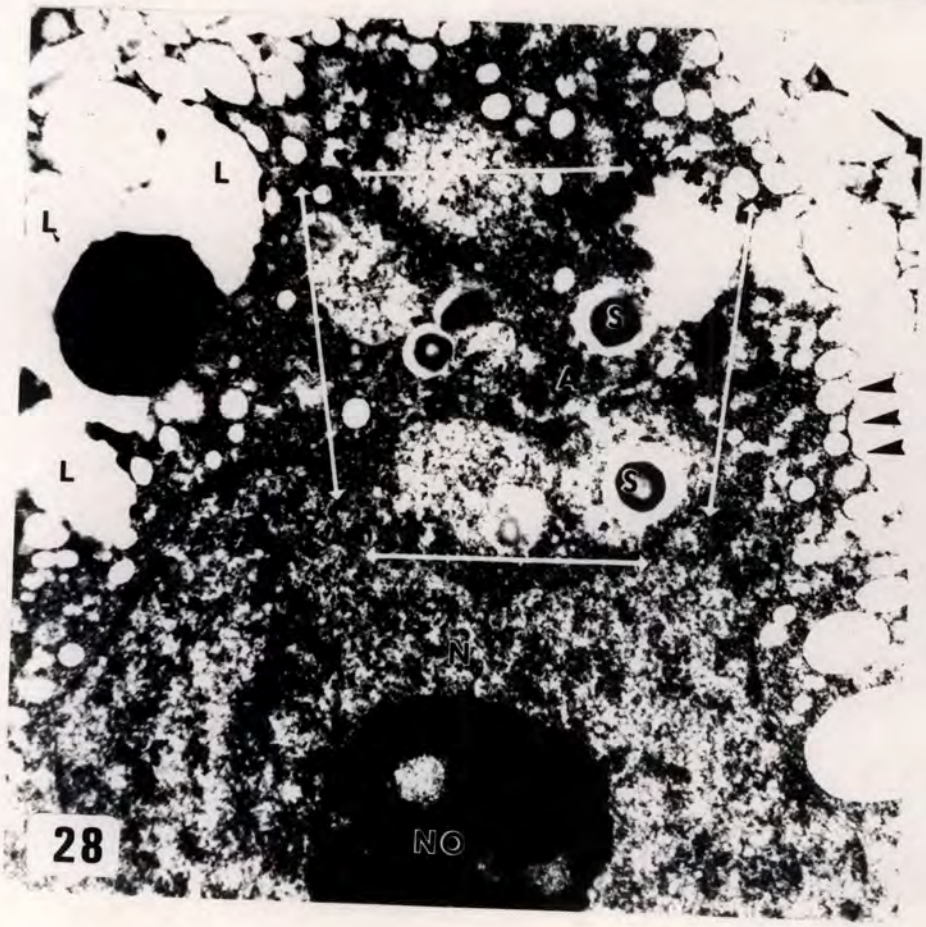

28

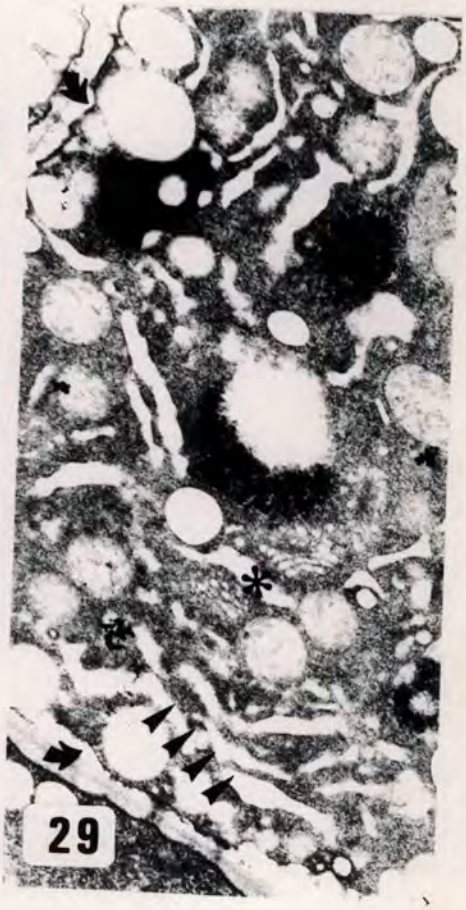

29

Figure 30 : Nucleus from a meristematic cell of a control, high viability embryo after 17½ hours imbibition. A fibrillar nucleolus (NO) and sparsely clumped heterochromatin in the nucleoplasm are evident. An elongate plastid (P) profile is illustrated. X 17 100.

Figure 31 : Nucleus from the meristematic region of a non-viable embryo after 17½ hours imbibition. Localized breaks are evident in the nuclear envelope (arrowheads), the nucleoplasm is sparsely floccular and the nucleolus (NO) electron-dense and compact. Note nuclear lobing. X 17 100.

Figure 32 : Pith cells from the radicle of an embryo from a seed lot of low viability after 17½ hours imbibition. Dilation of the nuclear envelope is evident (arrowheads) and the plasmalemma is poorly resolved along the wall (W). Mitochondria (M) appear intact with clearly-defined membranes and plastids (P) appear intact. Vacuole-like bodies (V) are evident in the vicinity of the nucleus. Note marked nuclear (N) lobing. X 15 200.

Figure 33 : Further vacuole-like bodies (V) adjacent to the nucleus of a low viability embryo. Some membrane profiles (arrowheads, right) are evident where the vacuole abuts against the nucleus. Discontinuous plasmalemma (arrowheads) evident along the cell wall (W). X 26 000.

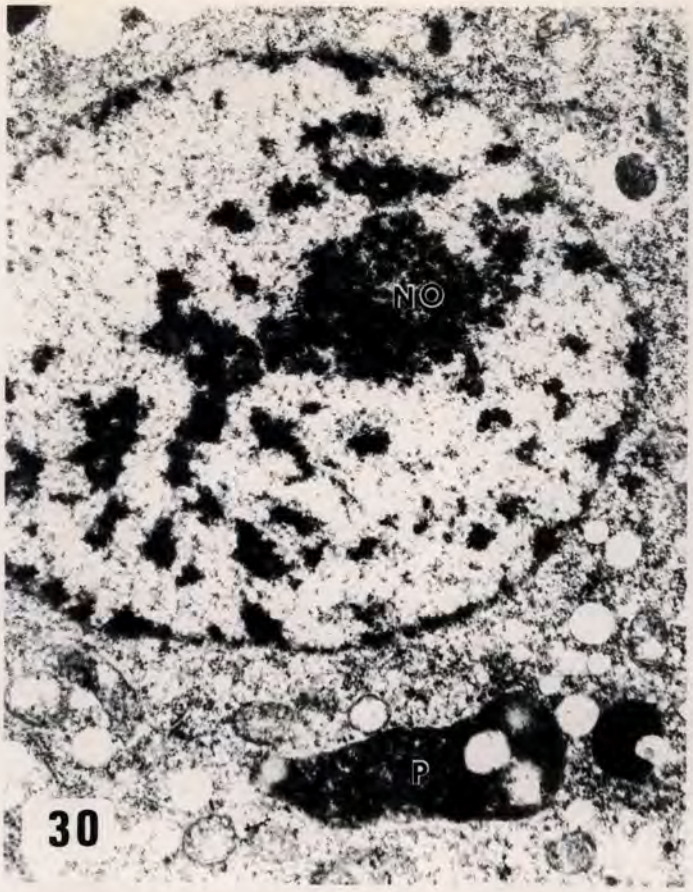

30

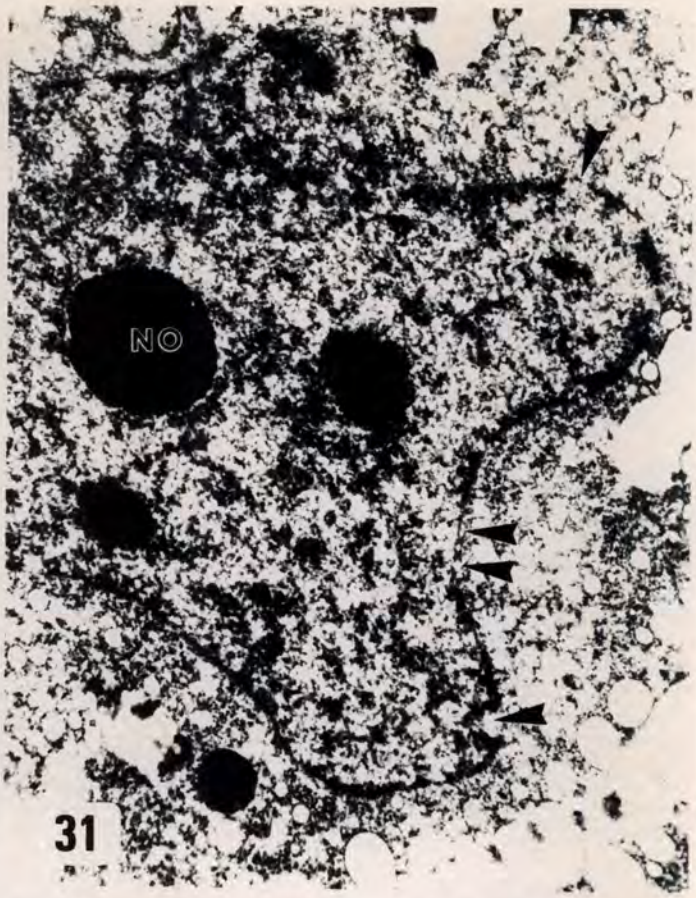

31

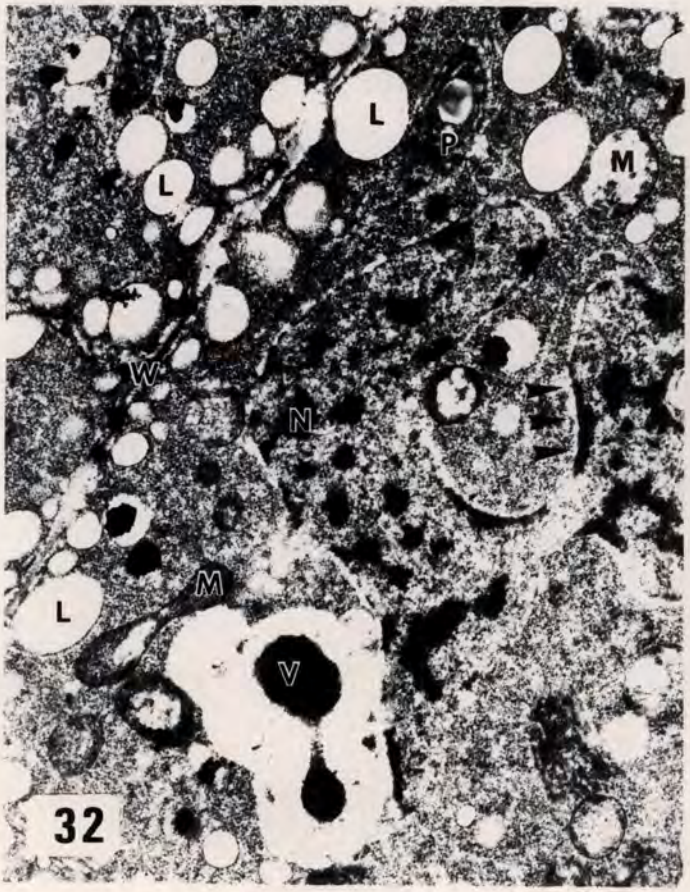

32

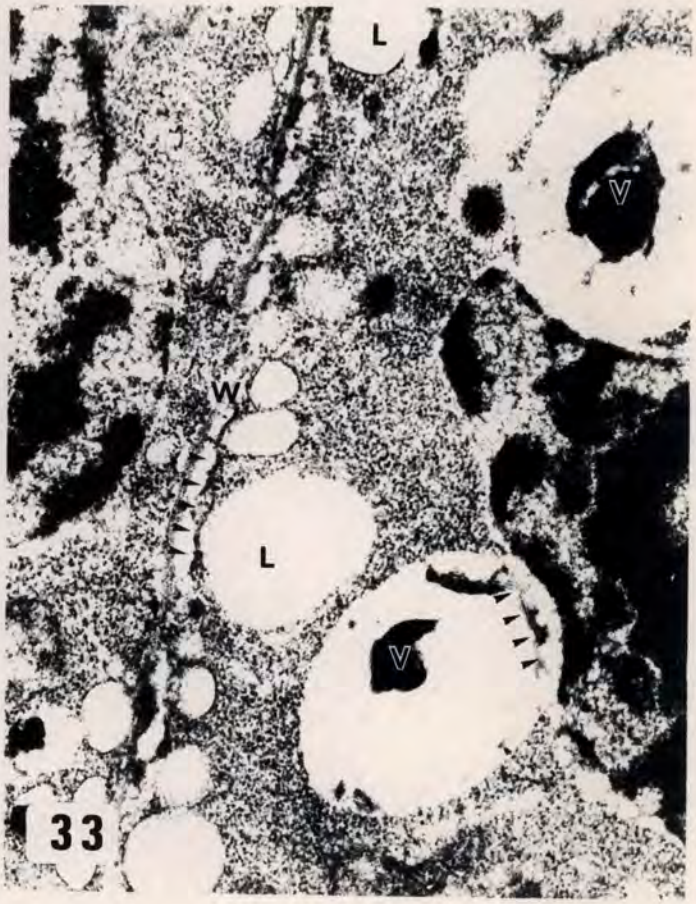

33

Figure 34 : Shows the normal appearance of cortical cells in the root tip of embryos drawn from a sample of low viability at 17½ hours imbibition. The large lipid body (L, bottom right) is thought to have arisen from the fusion of several smaller lipid bodies. Note the active appearance of the nucleoli (NO) and well-defined plasmalemmae (arrowheads) which suggest that little deterioration has occurred. X 9 200.

Figure 35 : Protein bodies (PB) in the cortical tissue of low viability embryos after 17½ hours imbibition showing little suggestion of digestion and mobilization of the contents. Lipid (L) is indicated, and there is no clearly-defined plasmalemma at the cell wall (top right). X 9 200.

Figure 36 : Illustrates the appearance of protein bodies in the cortical tissue of a control, high viability sample at 17½ hours imbibition. Note the vesicle-like elements within the protein body which are thought to be implicated in reserve mobilization. X 9 200.

Figure 37 : Wall buckling and an absence of a defined plasma membrane (curved arrows) seen in the cortical cells of an embryo drawn from a sample of low viability at 34 hours imbibition. Although disorganisation of the cytoplasm has not occurred it is assumed that embryo would have been non-viable. X 9 200.

Figure 38 : Illustrates the partial envelopment of a protein body (PB) from an epidermal cell by ER studded with ribosomes in a sample of high viability at 17½ hours imbibition. The plasmalemma is seen to be intact. X 25 350.

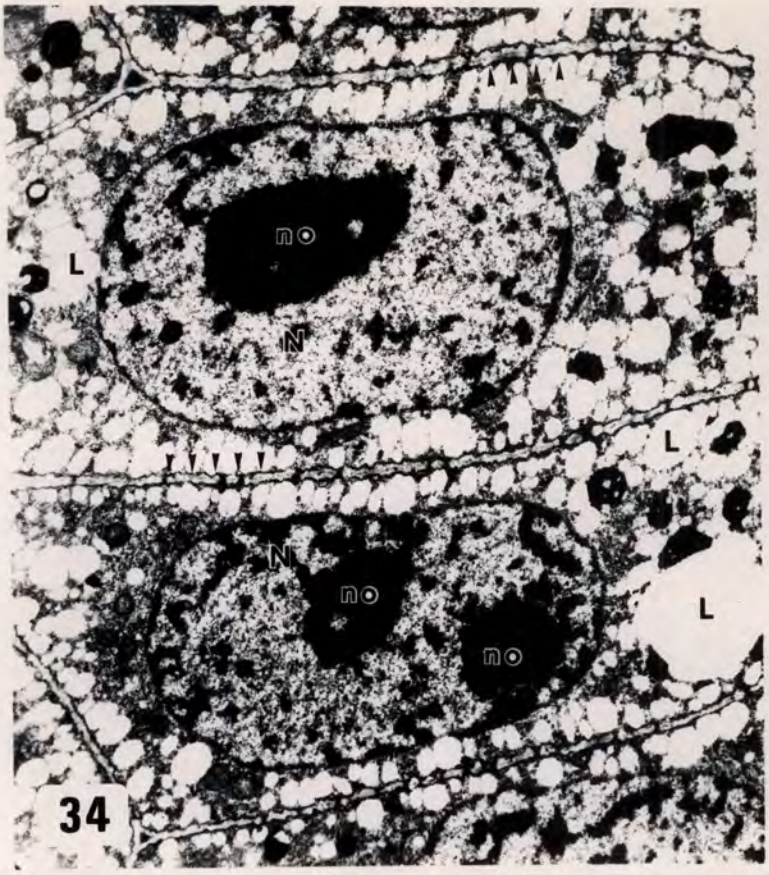

34

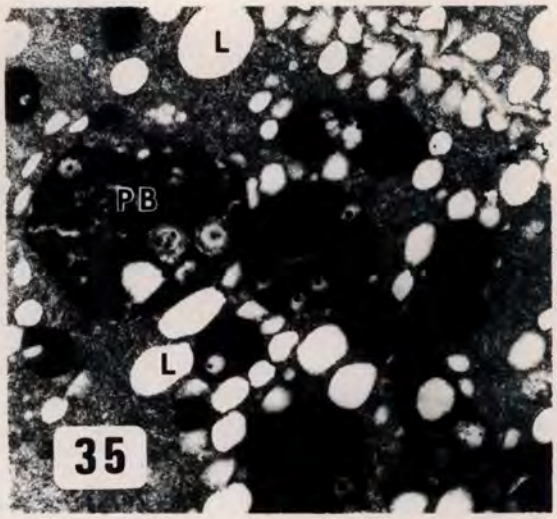

35

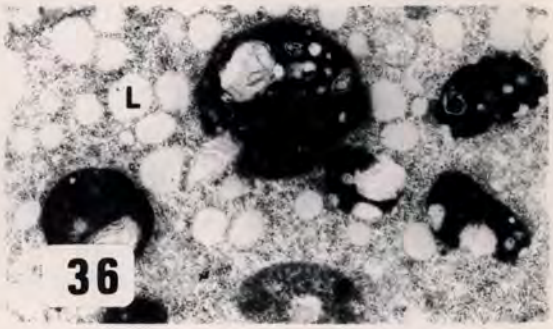

36

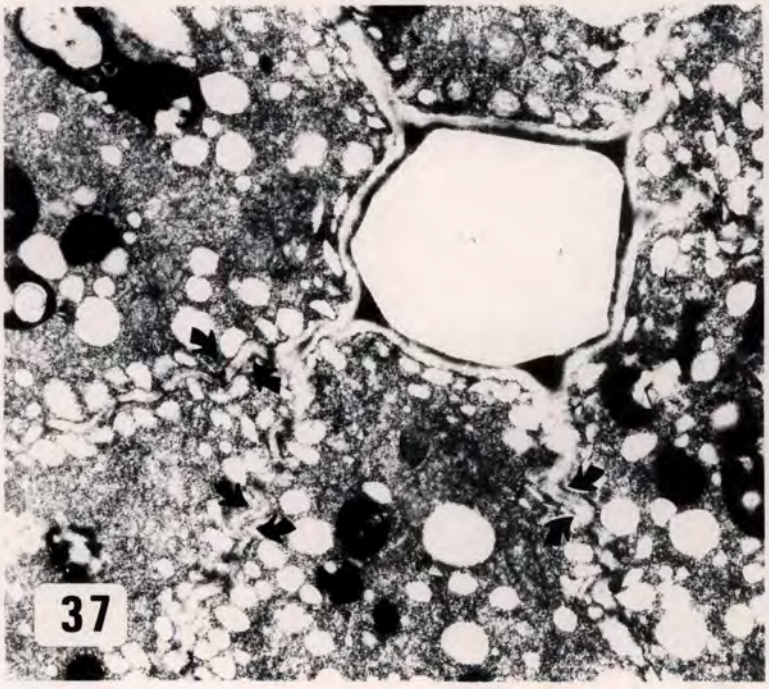
37

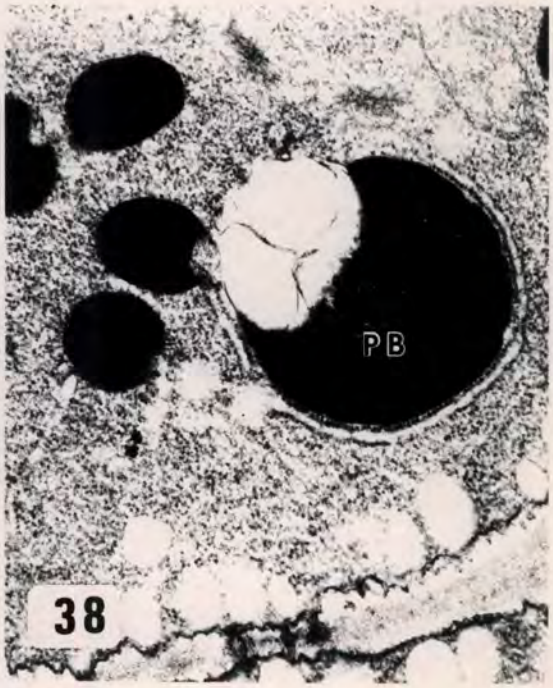

38

Figure 39 : Illustrates the appearance of a cortical cell in the root tip of a seed drawn from a sample of high viability after 13 hours imbibition. the plasma membrane is discrete (arrowheads) and protein bodies (PB) are surrounded by a shell of lipid droplets (2). X 9 200.

Figure 40 : Illustrates the appearance of a cortical cell from a non viable sample after 13 hours imbibition. Some lipid droplets (L) have become confluent and lie adjacent to the presumed contents of the protein bodies (P). Note the "frothy" appearance of the cytoplasm caused by the presence of numerous small vesicles, and the absence of a clearly defined plasmalemma at the densely staining cell wall (upper left). X 9 200.

Figure 41 : Shows a fibrillar structure (F), which may be a cytoskeletal element, in the cytoplasm of a pith cell from an embryo of low viability at 17½ hours imbibition. Numerous mitochondria (M) of dilated appearance with internal vesicles can be seen. X 26 000.

Figure 42 : Enlarged nucleolus (NO) seen in the procortical cell of an embryo drawn from a non viable sample after 17½ hours imbibition. Pools of confluent lipid (L) may be seen. x 8 740.

Figure 43 : Illustrates the elongate, branched mitochondria (M) seen in the cortical tissue of seeds drawn from a sample of low viability. The plasmalemma is poorly defined and the ground cytoplasm rather irregular and floccular. X 18 240.

Figure 44 : Illustrates a necrotic cell from the root cap of a non-viable embryo sample at 13 hours imbibition. Plasmalemma withdrawal is evident (arrowheads) and most of the confluent lipid (L) lies outside of the cytoplasm. Numerous electron transparent vesicles lying in the cytoplasm have their origin in the dilation and vesiculation of the membranes of the protein bodies. The nucleus is lobed and contains a rather formless electron-dense content. X 8 740.

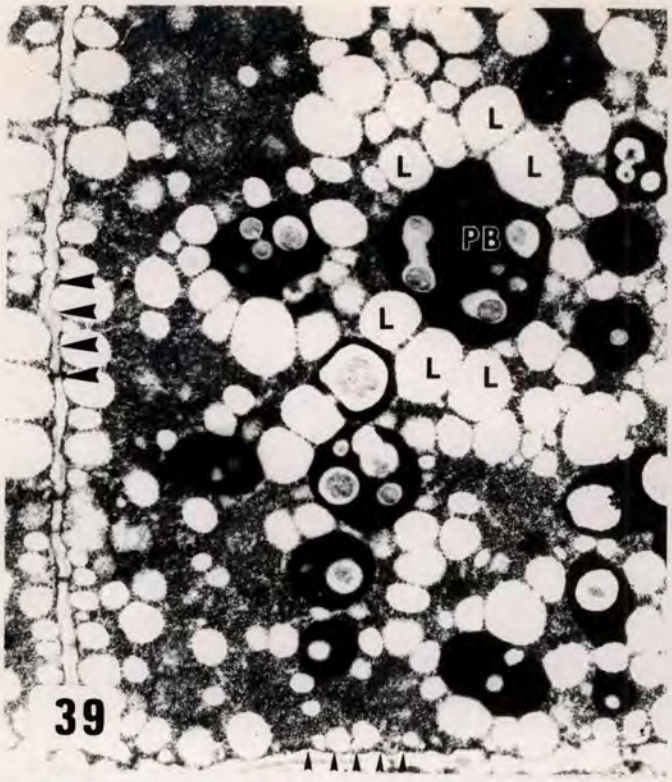
L
L
L
L
PB
L
L
L
39


P
L
L
L
P
L
L
P
L
40

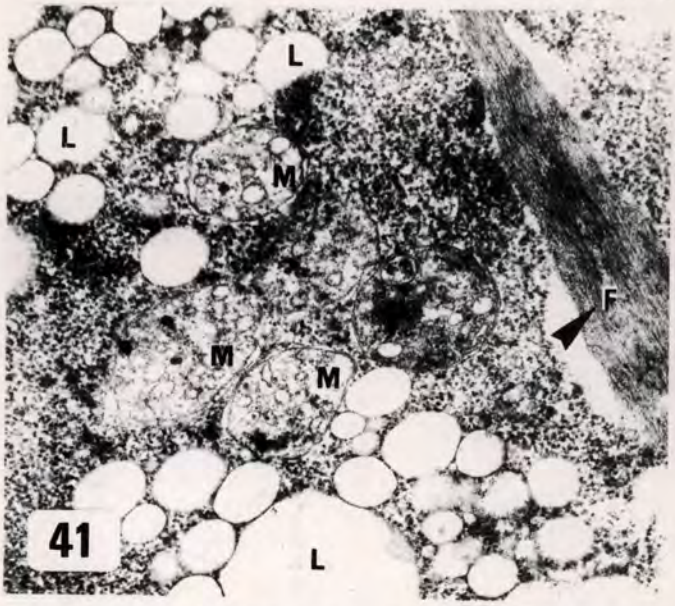
L
L
M
F
M
M
L
41

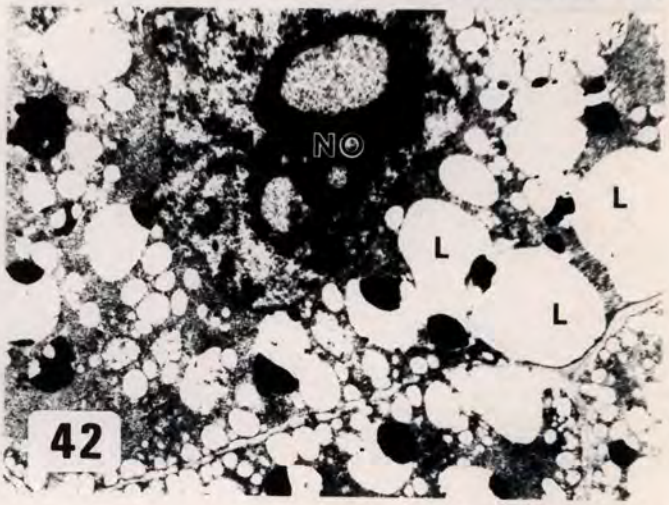
NO
L
L
L
42

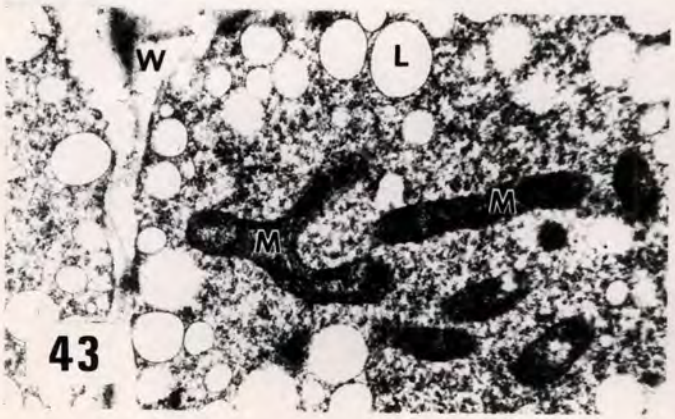
W
L
M
M
43


N
L
44

Figure 45 : Illustrates appearance of pith cells in an embryo drawn from a sample of high viability after 34 hours imbibition. Damage was restricted to only a few cells in this region, and cells in the other tissues were of normal appearance. Note the presence of myelin-like figures (My) in a cell which is presumed to have autolysed flanked by one cell with a nucleus (N) of normal morphology and another in which the mitotic apparatus is presumed to have been defective. Chromosomes (C) have not apparently migrated to opposite poles, and the cytoplasm contains numerous dilated vesicles. Some of these appear to be closely associated with the chromosomes. Note the absence of cell plasmolysis and an intact plasmalemma. X 6 440.

Figure 46 : Shows an island of apparently viable cells (V) surrounded by numerous electron-dense necrotic cells in the root cap of a low viability embryo after 13 hours imbibition. Some cell plasmolysis is evident. X 5 600.

Figure 47 : Illustrates appearance of cortical cells from the root tip of an embryo drawn from a non viable seed lot at 13 hours imbibition. Note floccular nucleoplasm (N) and cytoplasm containing numerous small vesicles. Confluent lipid (L) and associated protein (P) of the protein bodies are shown. The plasmalemma is partially continuous (arrowheads), and an adjacent necrotic cell (asterisks) is illustrated. X 9 200.

Figure 48 : A localized region of necrotic cells (asterisks) seen in the cortical-epidermal junction of an embryo drawn from a low viability sample at 13 hours imbibition. The adjacent viable cells appear metabolically competent as evidenced by the active nucleolus (N) numerous small amyloplasts (P) and mitochondria. Some plasmalemma withdrawal is evident but it is not clear whether this necessarily represents the in vivo condition. X 5 320.

Figure 49 : Procortical cell from a non-viable embryo at 13 hours imbibition showing an electron dense nucleus (N) which lacks a membrane and contains what appear to be small islands of cytoplasm (arrowheads). Confluent lipid (L) is evident in a uniformly floccular cytoplasm. X 8 740.

Figure 50 : Illustrates pattern of protein body (PB) digestion seen in an endosperm cell of a low viability seed after 20 hours imbibition. X 29 990.

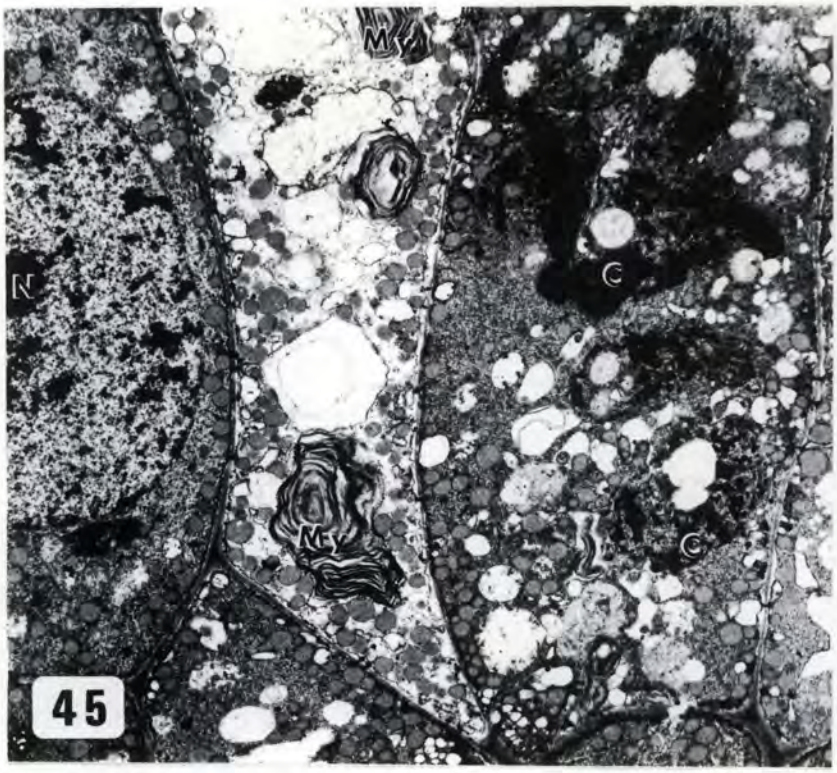
N
M
C
M
C
45

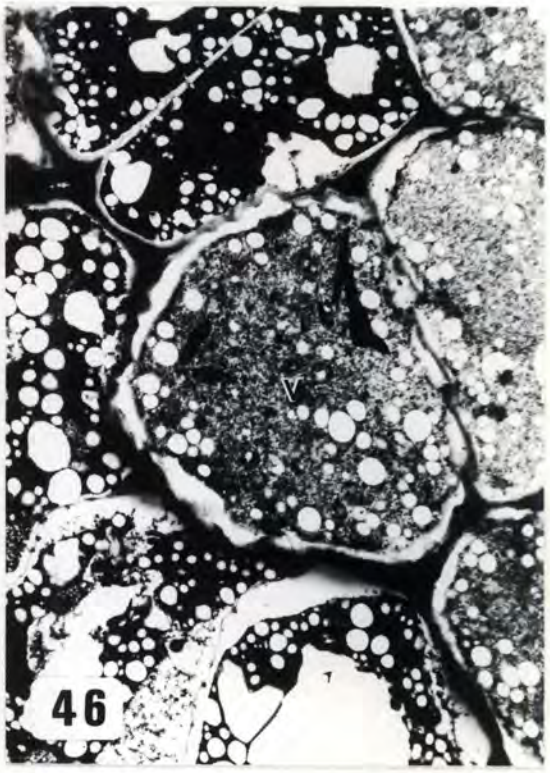
V
46

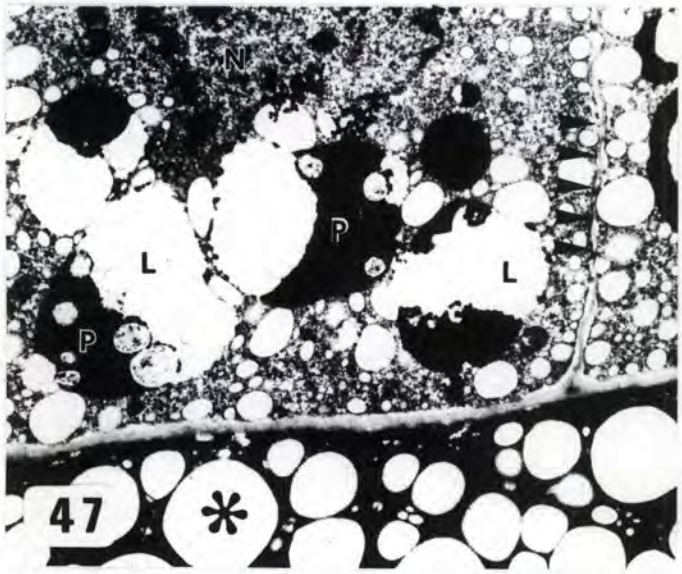
N
P
L
L
P
47
*

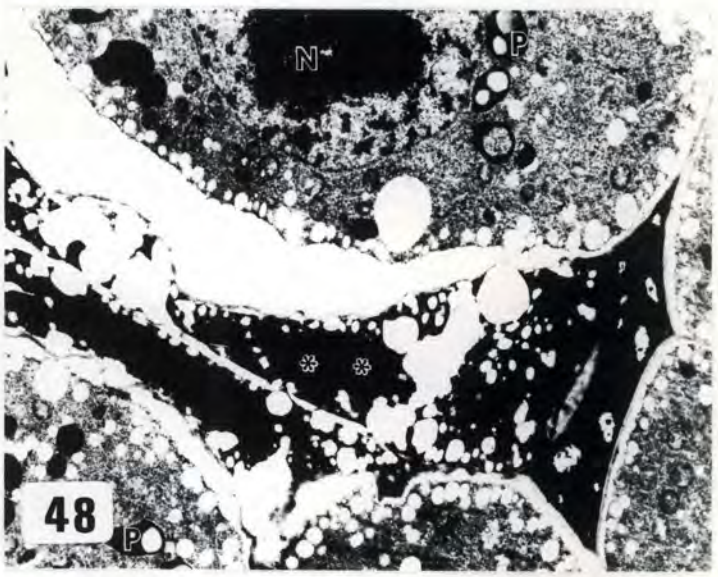
N
P
48
PD

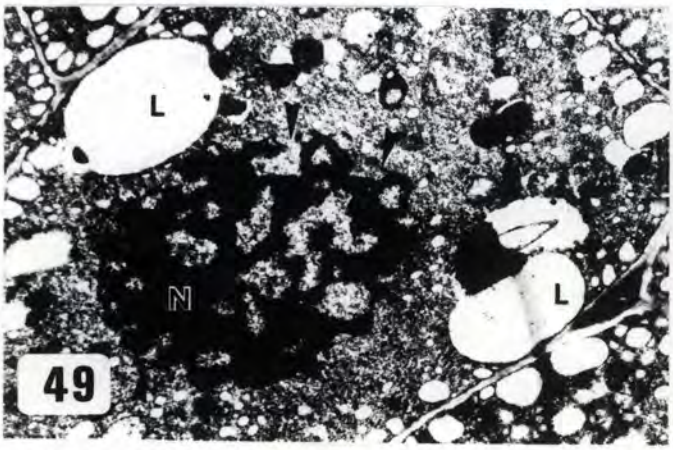
L
N
L
49

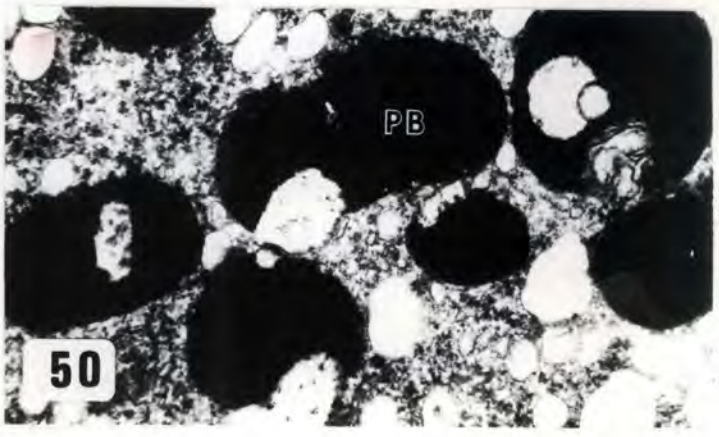
PB
50

Figure 51 : Illustrates the embryo (EM) -endosperm junction in the root cap region of a low viability seed at 20 hours after imbibition. Note the comparable size and structure of the protein bodies (asterisks), and nuclear (N) structure between embryo and endosperm tissues. The junction between the endosperm wall (W) and the pericarp (bottom right) is seen to be very thick. X 5 460.

Figure 52 : Typical peg-like (P) intrusions of the endosperm wall into an endosperm cell of a seed drawn from a low viability sample after 20 hours imbibition. The intense metabolic activity of the cell is evident from the mitochondria (M), microbodies (asterisks), elements of RER and numerous vesicles. X 14 820.

Figure 53 : Illustrates adjacent viable and non viable (D) endosperm cells in a sample drawn from a seed lot of low viability at 20 hours imbibition. Although the viable cell is not of entirely normal ultrastructure as indicated by the somewhat lobed nucleus (N) general cellular integrity if maintained. X 8 970.

Figure 54 : Degenerate cytoplasm in an endosperm cell from the cotyledonary region of an embryo after 4 hours imbibition showing plasmalemma withdrawal, lipid (L) coalescence, and nucleus (N) with clumped chromatin. The endosperm wall structure is apparently unchanged (compare with peg-like ingrowths in Figure 52, above). X 8 740.

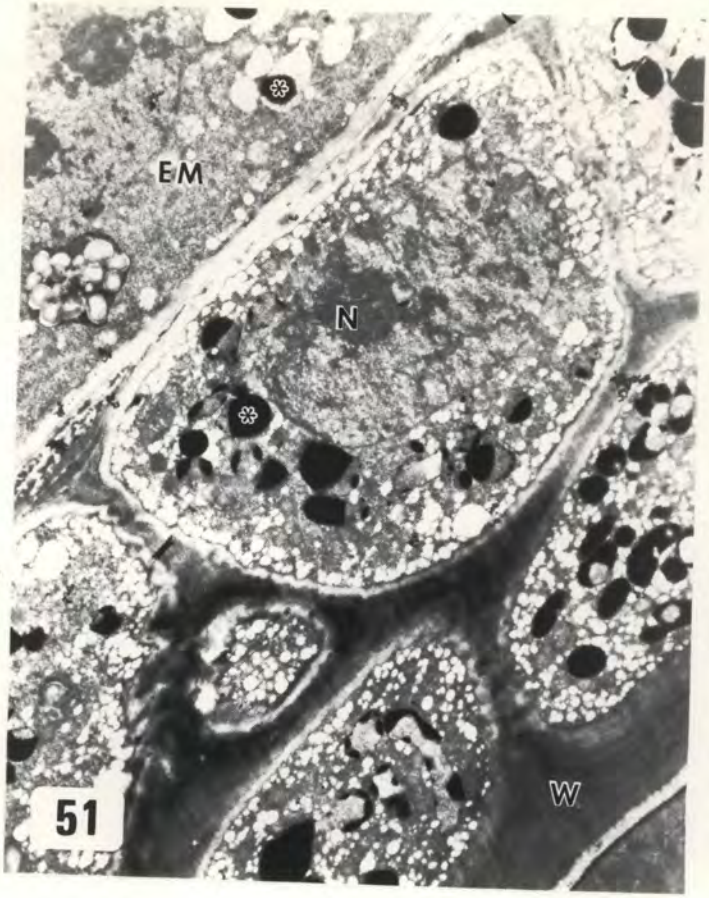
EM
N
W
51

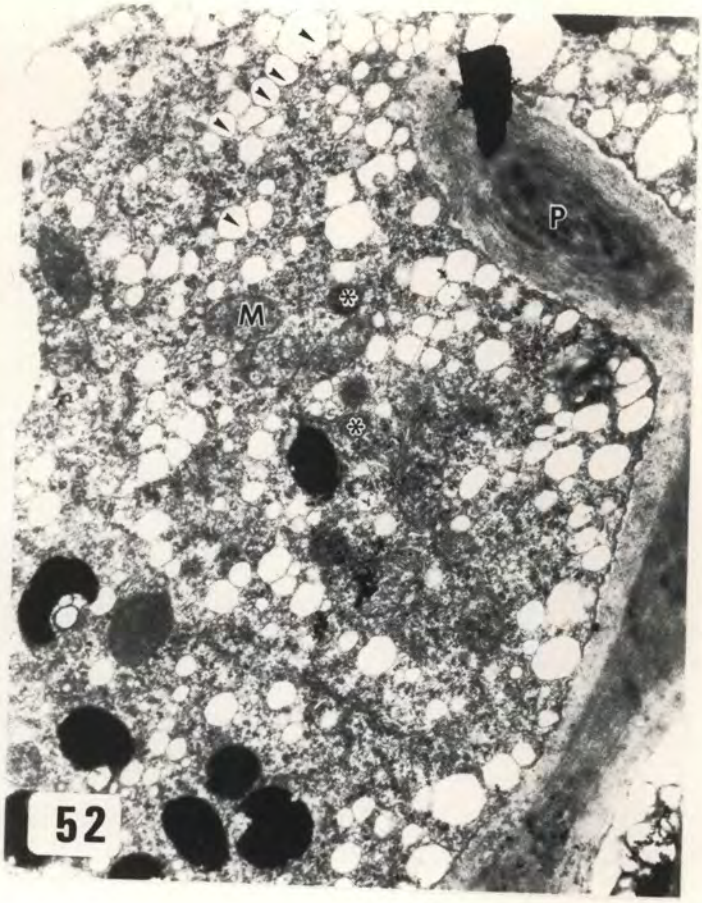
P
M
52

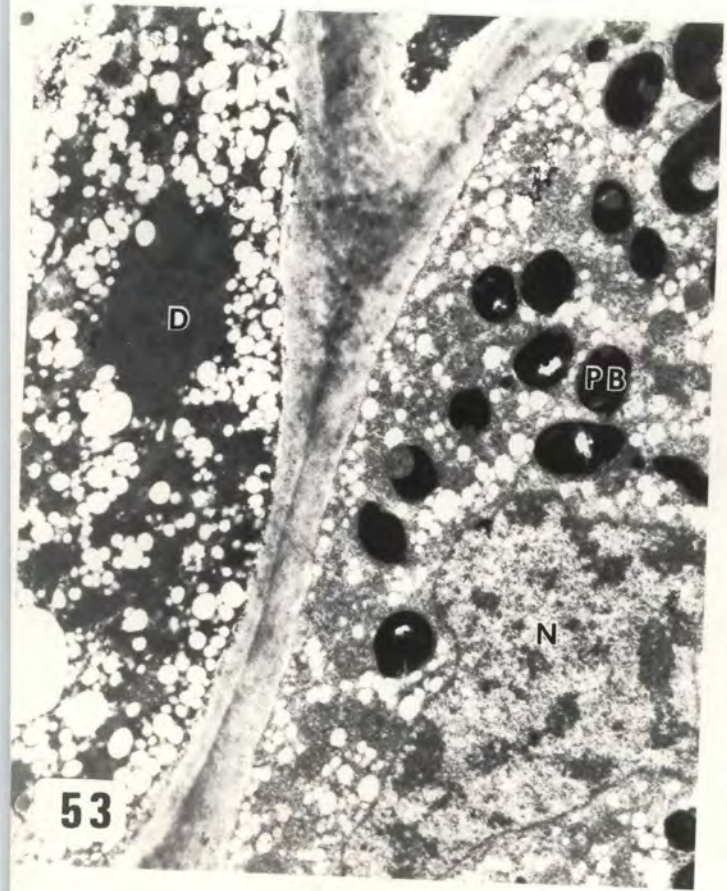
D
PB
N
53

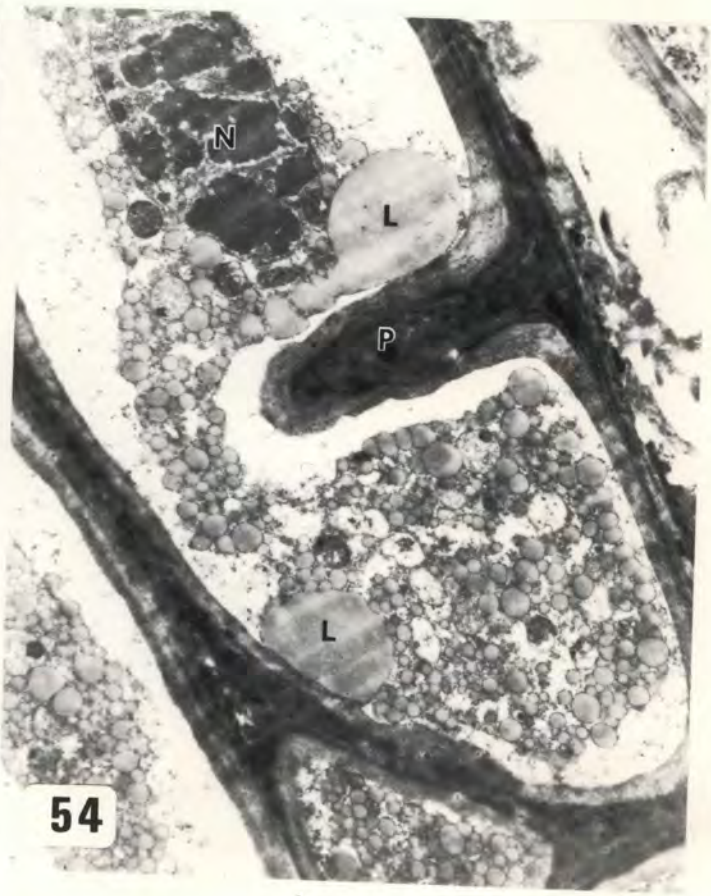
N
L
P
L
54

Figure 55 : Section through portion of a non viable seed after 20 hours imbibition showing total loss of cellular organisation seen in the cytoplasm of embryonic (EM) and endosperm (EN) cells, the limits of which are demarcated by arrowheads. The schlerenchymatous (SC)pericarp is also evident. It is notable that while the cell walls of embryonic tissue show signs of deformation and possible dissolution, the walls of the endosperm are apparently unchanged. X 4 000.

Figure 56 : Illustrates the intense metabolic activity in an endosperm cell of low-viability seed at 20 hours imbibition showing numerous cytoplasmic vesicles, ribosomes and ER (arrowheads). As in embryonic tissue numerous lipid droplets (L) are seen at the plasmalemma. The cell wall (W) is typically composed of two distinct layers. (See also Figure 52). X 25 350.


SC
55
EN
EM

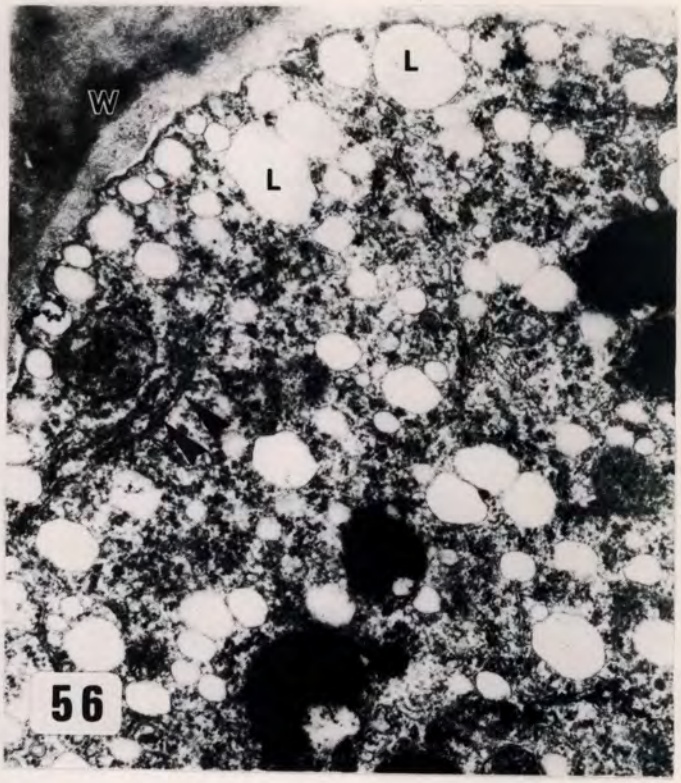
W
L
L
56

Figure 60 : Cortical cells in the root tip after 4 hours imbibition of an embryo drawn from a seed sample held at 20°C and 80% RH for 2 months. Plasmalemma-derived vesicles are evident at the cell boundary at the expense of membrane continuity while the close plasmalemma-lipid body association previously observed is noticeably absent. (Figures 10, 11 & 16). Nucleus (N) with heterochromatin of normal appearance. X 47 040.

Figure 61 : Illustrates similar, though less severe, plasma/membrane abnormalities than the above seen after 4 hours imbibition in cortical cells of the root tip of an embryo stored for 2 months at 40°C and 40% RH. Nucleus (N) of normal appearance. X 35 840.

Figure 62 : Myelin-like whorls seen after 4 hours imbibition at the plasmalla of a cortical cell from an embryo stored for 2 months at 40°C and 40% RH. Cytoplasm of normal appearance although the plasmalemma was not always well-defined. X 20 800.

CHAPTER 5 : ULTRASTRUCTURAL CHANGES DURING IMBIBITION - (C) COMPARATIVE STUDIES ON EMBRYOS OF DIFFERING VIGOUR

Figure 57 : Appearance of root tip cells from embryo after 4 hours imbibition showing cytoplasmic degeneration. The seed had been stored at 20°C and 100% RH for 2 months and although 78% germination was recorded it must be assumed that the seed sampled for microscopy was non viable. Numerous plasmalemma breaks are indicated (arrowheads) and the densely-staining nucleus is without a discernible envelope. X 24 700.

Figure 58 : Illustrates the variable appearance of mitochondria some of which have sustained damage (denoted M) while others are of somewhat normal appearance (centre and bottom right) after 4 hours of imbibition. The beginnings of lipid body (L) confluence may be seen. The ground substance of the cytoplasm contains numerous small areas devoid of ribosomes (arrowheads). Storage conditions as for Figure 57. X 29 900.

Figure 59 : A further view of a non-viable embryo after 4 hours imbibition showing atypical negative nuclear envelope images (large arrowheads) and discontinuous regions (smaller arrowheads). The nuclear matrix is uniformly electron dense while electron transparent regions are seen in the ground cytoplasm. (See also Figure 58). X 87 300.

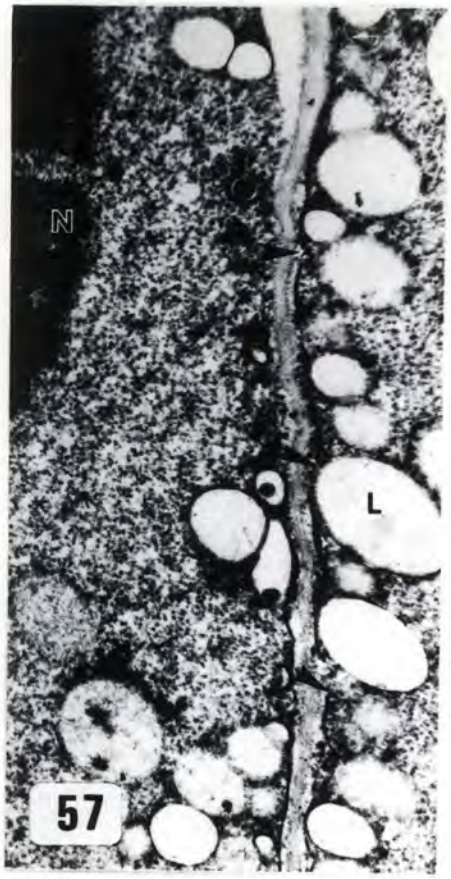
N
L
L
57

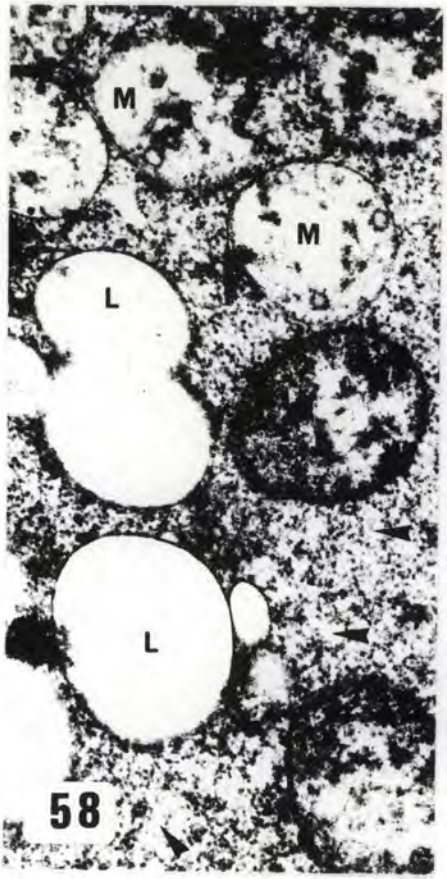
M
M
L
L
58

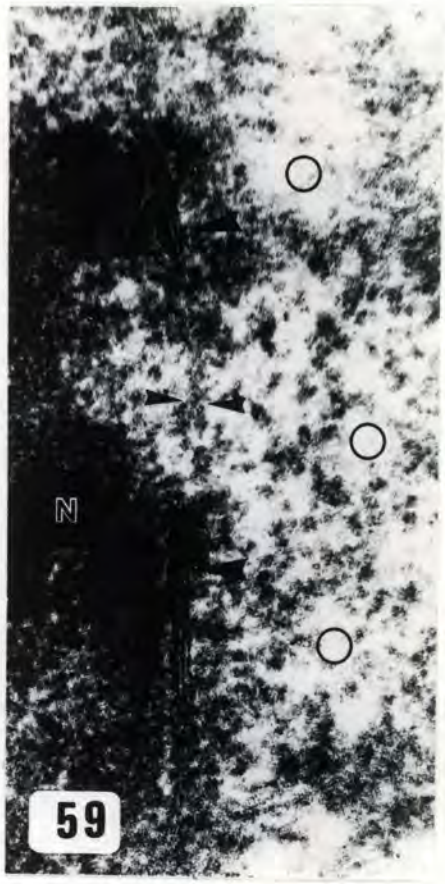
N
59

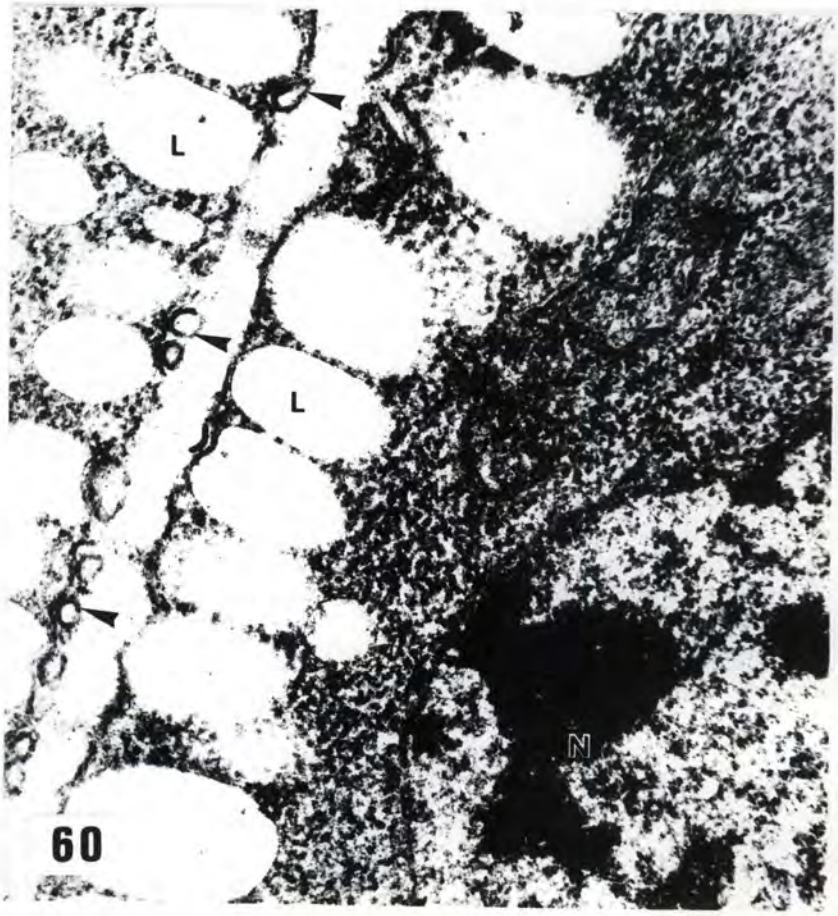
L
L
N
60

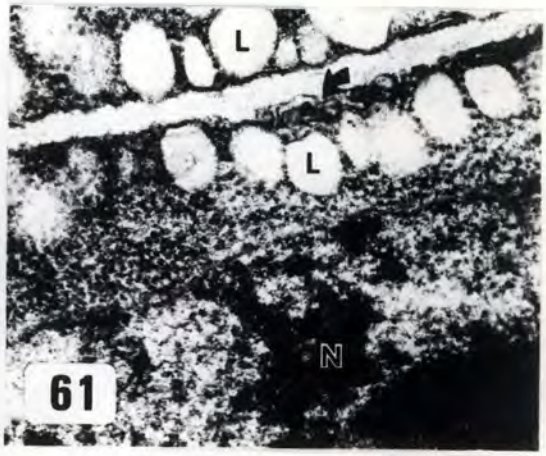
L
L
N
61

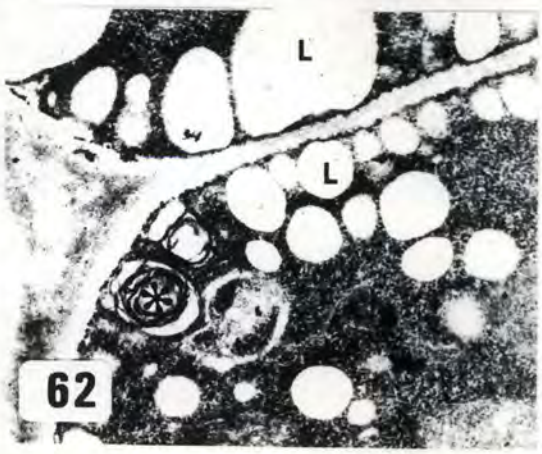
L
L
62

Figure 63 : Appearance of embryo root tip cells after 4 hours imbibition from a seed sample stored for 15 months at 20°C and 100%RH.(88% germination). There is no evidence of plasmalemma-associated vesicles and the membrane appears well-defined and continuous (Curved arrows). The only evident cytoplasmic manifestation of ageing was the coalescence of lipid (L) to form large pools. Plastid (P) is indicated. X 9 660.

Figure 64 : Illustrates membrane whorls seen in the cytoplasm of a root tip cell after 12 hours imbibition. Seeds stored for 2 months at 20°C and 80% RH ; germination 93%. Plasmalemma at wall (W) continuous and electron-dense while ER appears ill-defined in negative relief. X 32 500.

Figure 65 : A myelin-like figure (arrowheads) seen in embryo root tip cell after 12 hours imbibition. Storage conditions as for Figure 64, above. The plasmalemma (curved arrows) is continous in part, although in negative relief. X 81 480.

Figure 66 : Oblique section through a cell from embryo root tip cells after 12 hours imbibition showing how the association of membranes of the plasmalemma may give rise to a stacked membrane array (arrowheads) as seen in Figure 65. Cell wall (W) is indicated. X 81 480.

Figure 67 : Root cap cell of an embryo after 12 hours imbibition drawn from a sample stored for 2 months at 20°C and 100% RH. The plasmalemma appears normal and continuous (arrow) but protein body (PB) vacuolation appears slightly delayed. Amyloplast (A) with starch grains indicated. X 9 660.

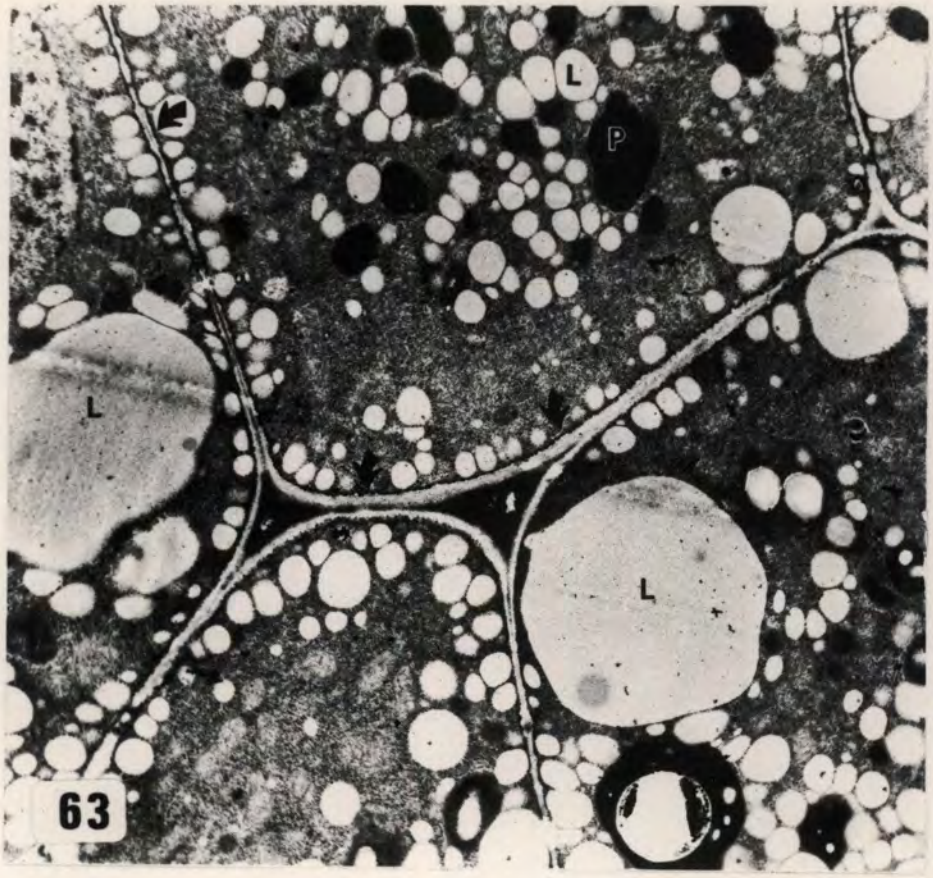
L
P
L
L
63

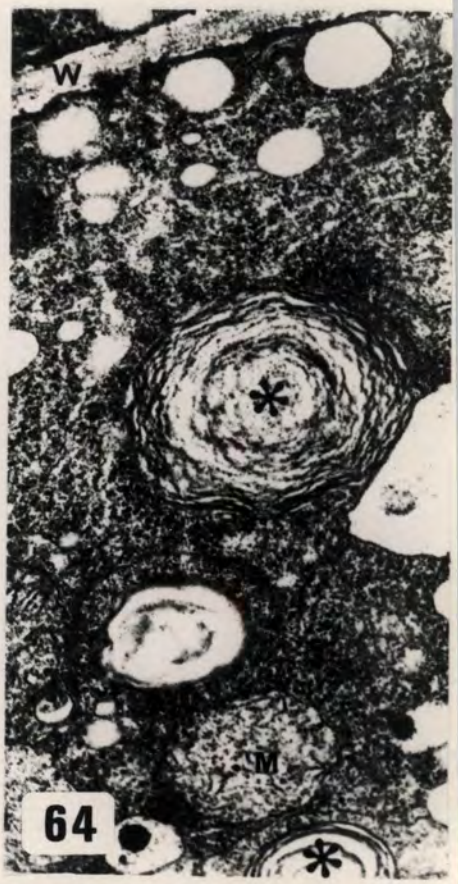
W
M
64

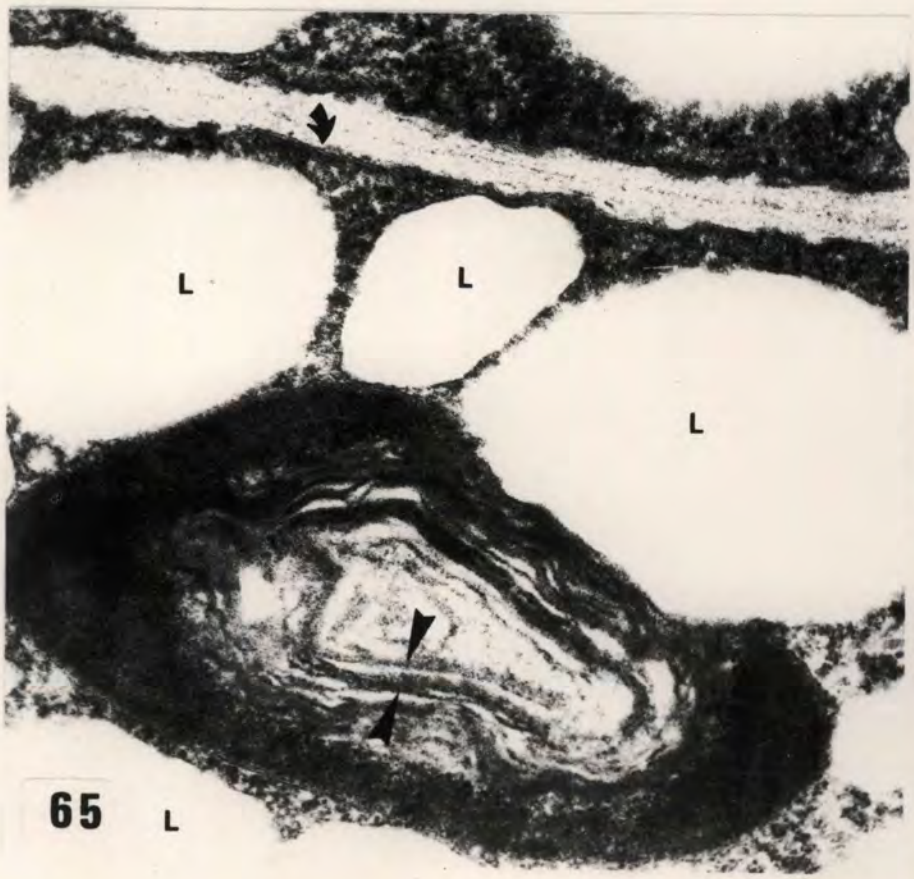
L
L
L
65
L

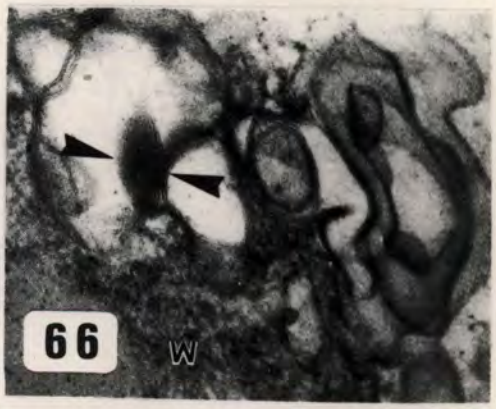
66
W

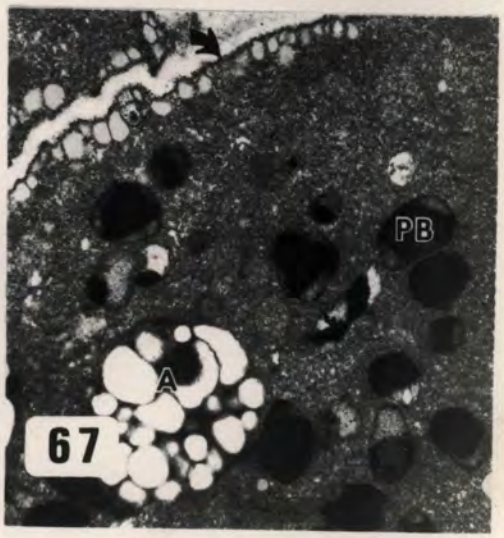
PB
A
67

Figure 68 : Inner root cap cell of a control, high vigour sample (1 month at 10°C and 0% RH) after 12 hours imbibition. Nucleus (N) with well-defined nuclear envelope and continuous plasmalemma at the wall (W). Vacuolar (V) enlargement has begun, numerous polysomes are evident in the cytoplasm. Mitochondria present although membranes poorly stained. X 20 800.

Figure 69 : Cotyledonary vascular cells after 12 hours imbibition from a seed sample stored for 15 months at 20°C and 60% RH. Unlike the localized necrosis reported earlier (Chapter 4, Figure 26) all the cotyledonary cells in the section were necrotic. Note dilation of ER, lipid coalescence, and nuclei with partly clumped heterochromatin. X 7 000.

Figure 70 : Higher magnification of cotyledonary cells from seeds subjected to the above storage regime showing the dilation (asterisk) of the membrane of the nucleus (N) and that of the ER (lower asterisk). Discontinuity of the plasma membrane is evident (arrowheads). X 42 560.

Figure 71 : Root cap cells after 12 hours imbibition from an embryo sampled after 12 hours imbibition. Seeds stored for 15 months at 20°C and 40% RH. Dilation of the ER is evident as is vesiculation of the Golgi vesicles (curved arrows). This situation is directly comparable to that reported earlier (Figures 26 and 29). Plasmalemma is poorly-defined but shows localized withdrawal from the dispersely fibrillar cell wall (W). X 19 500.

Figure 72 : Illustrates the appearance of cells from the meristematic zone of the root tip after 36 hours imbibition from a seed sample stored for 15 months at 20°C and 40% RH. Cell division is evident from the presence of vesicles which give rise to the cell plate (arrowheads). Meristematic activity is also indicated by the small cytoplasmic volume relative to that of the nucleus and numerous proplastids (P). A small degree of plasmolysis is evident in some cells (asterisks) but has assumed major proportions in some cells (top right). Coalesced lipid (L), and numerous mitochondria (M) and nucleolus (NO) with vacuole indicated. X 2 660

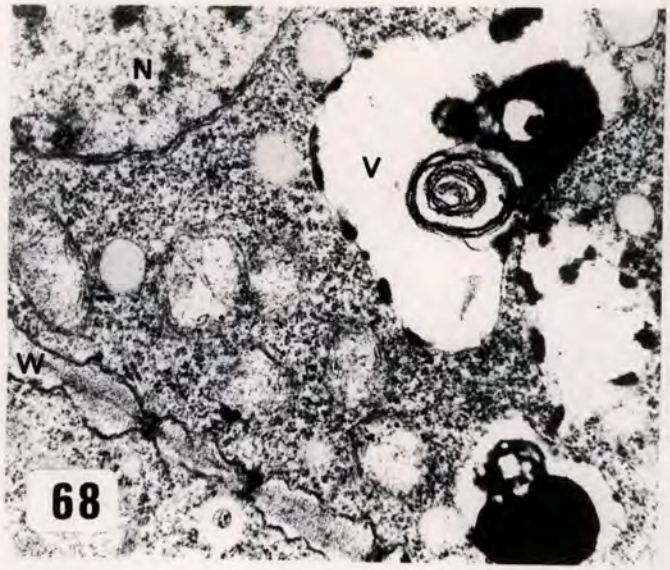
N
V
W
68

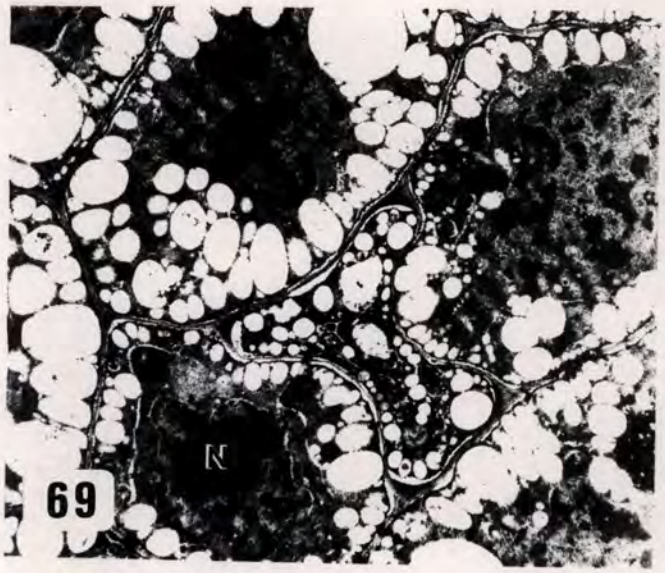
N
69

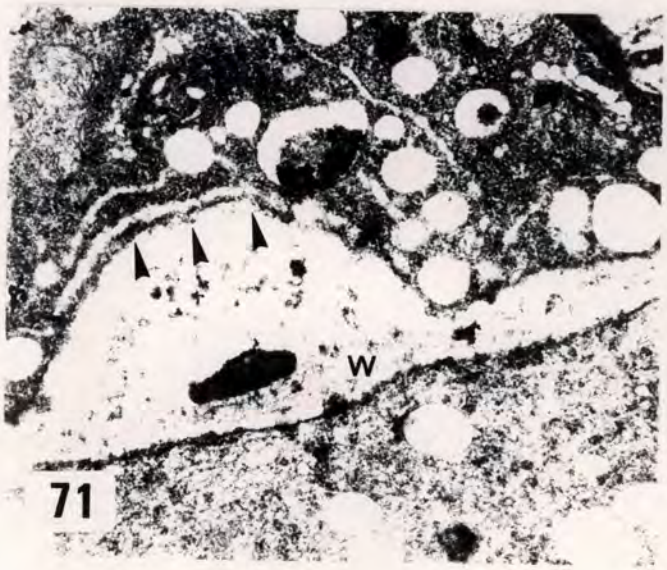
W
71

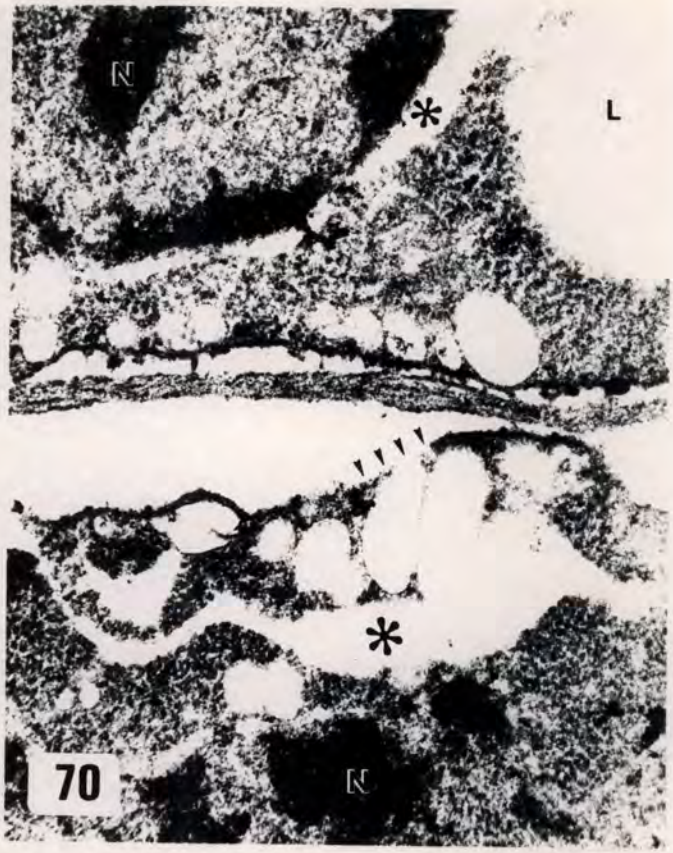
N
L
N
70

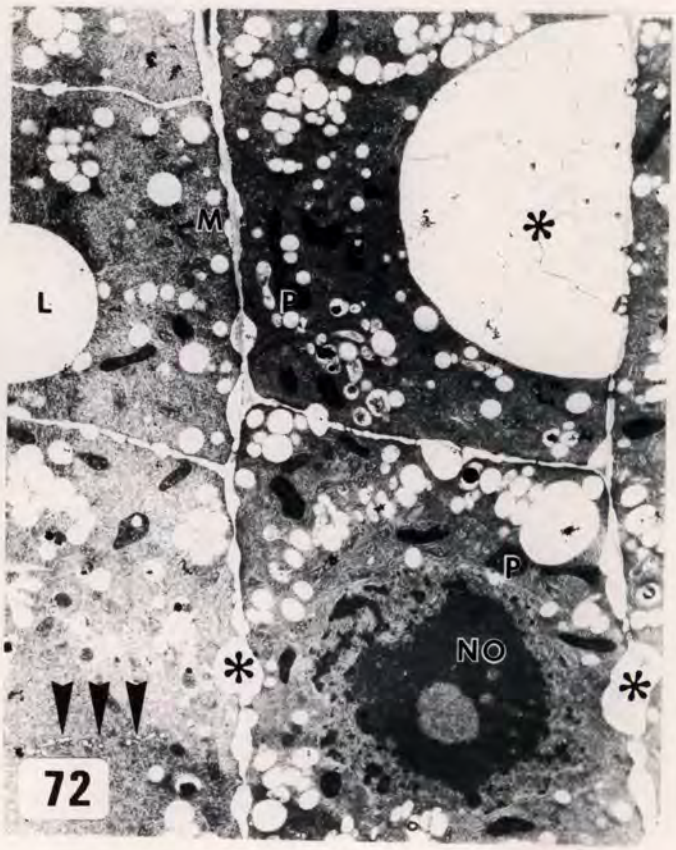
M
L
P
P
NO
72

Figure 73 : Root cap cell of a control, high vigour at 20 hours imbibition) prepared by the Osmium-Zinc Iodide (OZI) metal impregnation method. Section thickness corresponding to purple-green interference colour, and viewed at 100 kV. Numerous amyloplasts (A) and elongate, dumbell-shaped mitochondria (M) are evident. Note nuclear pores seen in face view in the nuclear envelope (arrowheads). Nucleus (N) shows mild lobing typical of a root cap cell and a prominent nucleolus (NO). X 18 400.

Figure 74 : A further view of root cap cells at 20 hours imbibition prepared by the OZI technique, as above. Extensive sheet-like endoplasmic reticulum (ER) is indicated in addition to branched tubular ER (asterisks). Nuclear pores once again evident (arrowheads, upper and lower right). Note absence of wall (W) staining and lighter less intense staining of lipid bodies (L) in comparison to membranes. The plasmalemma is not well stained. Amyloplast (A) with numerous well-resolved starch grains may be seen. X 18 400.

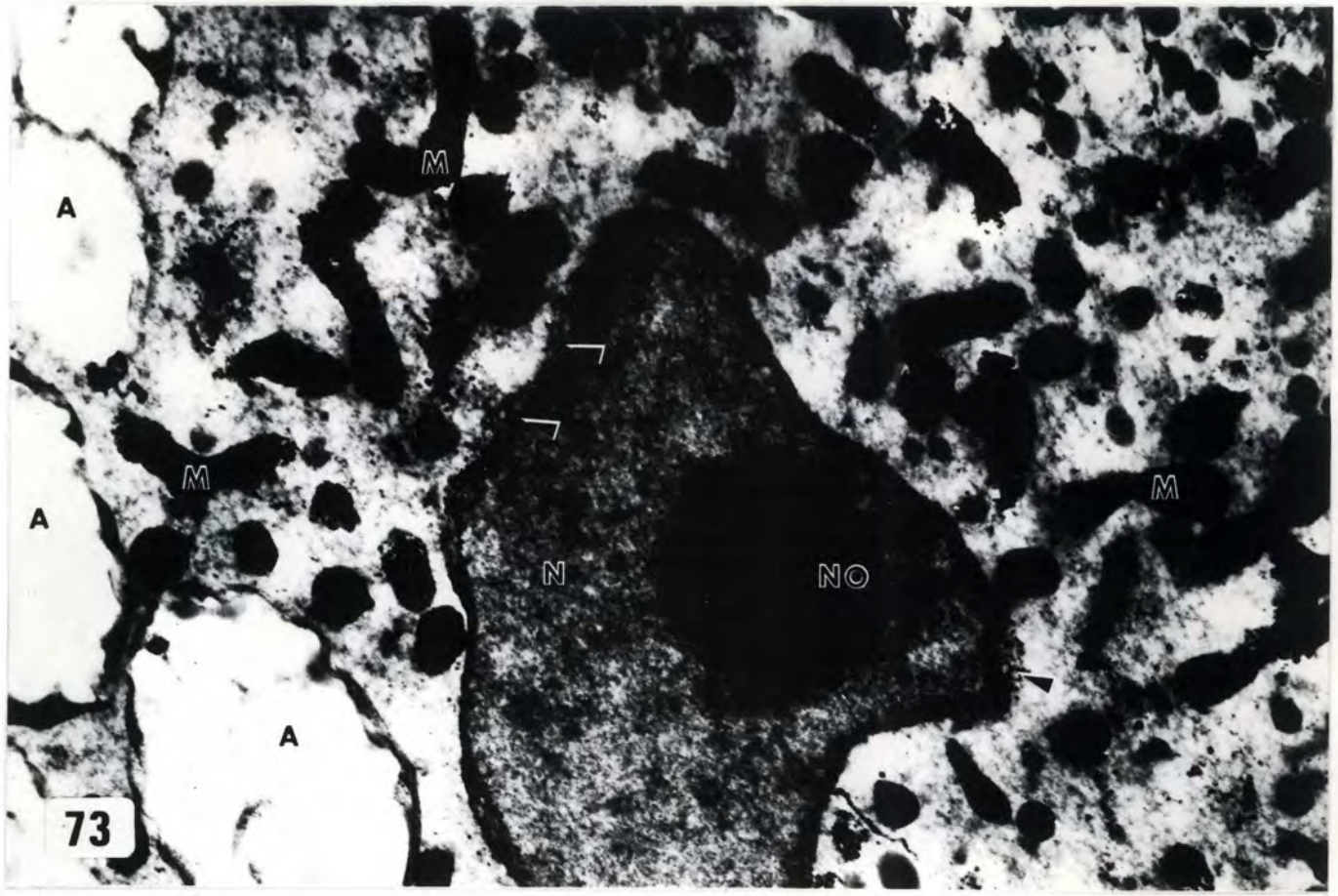
M
A
M
A
N
NO
M
A
73

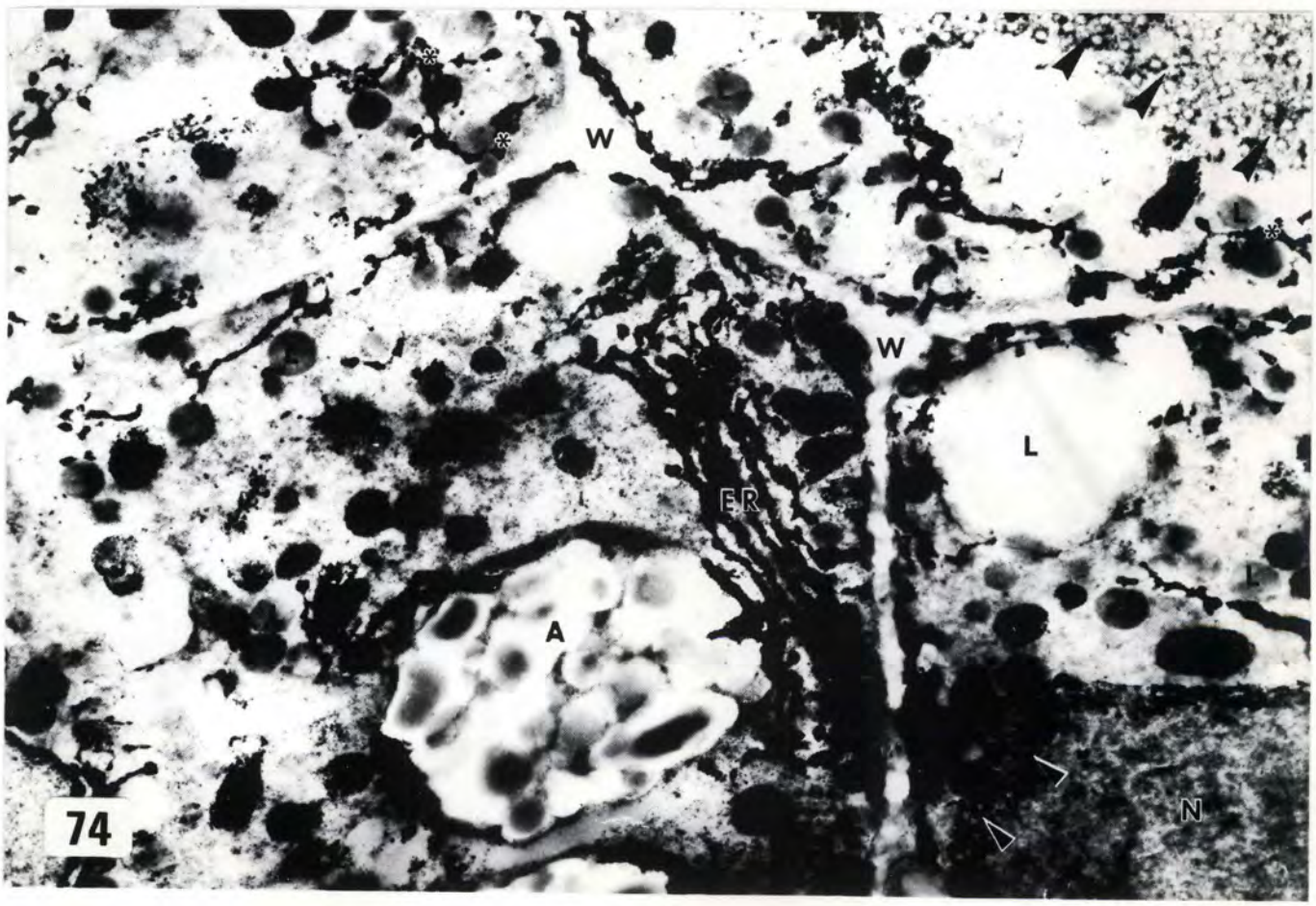
W
W
L
E.R
A
N
74

CHAPTER 5 : (D) ULTRASTRUCTURAL CHANGES DURING IMBIBITION IN SEEDS AFTER γ IRRADIATION

Figure 1 : Illustrates usual ultrastructural appearance of a procortical cell in root tip of an embryo after 12 hours imbibition in seeds which were previously subjected to 12 hours γ irradiation treatment. Nucleolus (NO) with pronounced vacuole and developing amyloplasts (A) suggest normal synthetic activity. Possibly coalesced lipid droplet (L) indicated. X 9 660.

Figure 2 : Shows root cap cells of embryo after 1 day of irradiation, and 12 hours after imbibition. The plasmalemma shows no apparent lack of continuity or abnormalities and, apart from lipid (L) coalescence, cytology is normal. Amyloplasts (A) and protein bodies (PB) are indicated. X 8 740.

Figure 3 : Cytolysome-like structure seen in epidermal cell of root tip after 2 days irradiation treatment and 12 hours post-imbibition. Electron-dense material thought to be protein (P) is contained within portions of the ER which appears to be sequestering cytoplasmic components, including a mitochondrion (M). X 24 700.

Figure 4 : Plasmalemma abnormalities (arrowheads) seen in the epidermal cells of the root of an embryo after 2 days of irradiation. Sample prepared for microscopy after 12 hours imbibition. Note electron transparent regions in the ground cytoplasm. (Compare with Figures 58 and 59, earlier). X 39 200.

Figure 5 : Illustrates apparent engulfment of portions of cytoplasm by the protein bodies (PB) of a cortical cell of an embryo after 2 days irradiation. Coalesced lipid with associated protein body material is evident (upper right). Material fixed after 2 hours imbibition. X 31 360.

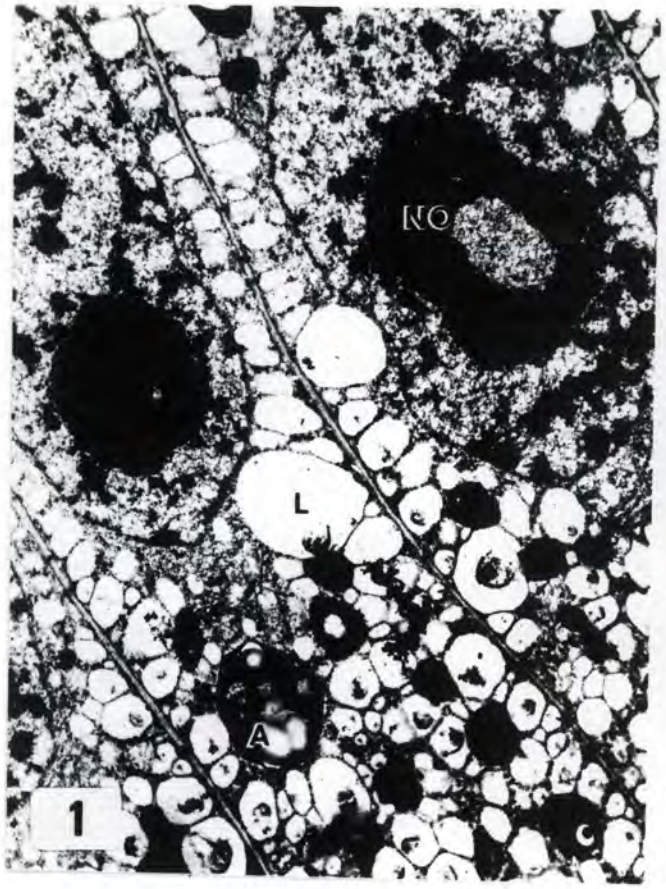

1

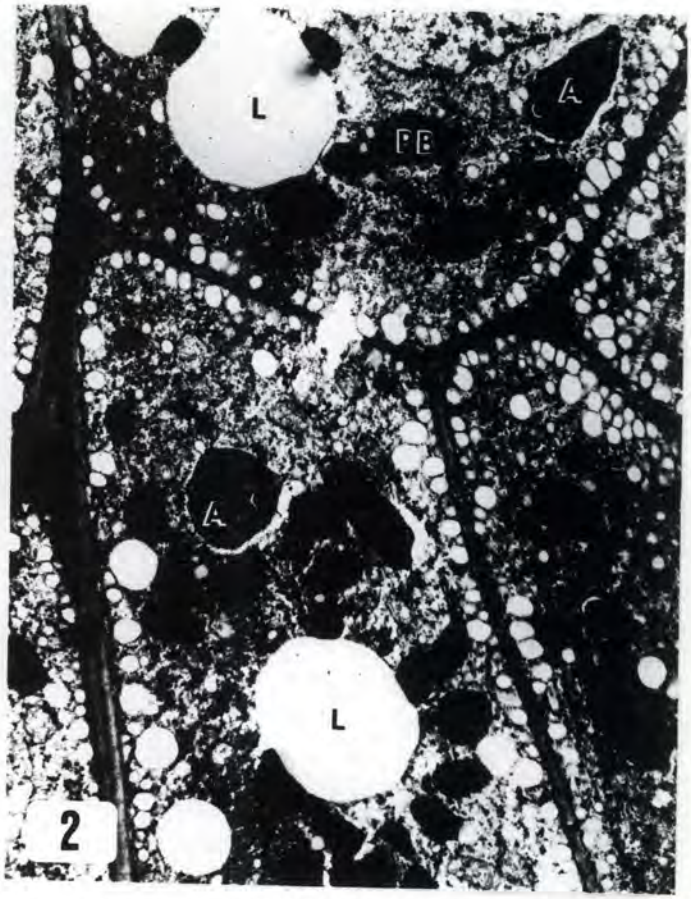

2

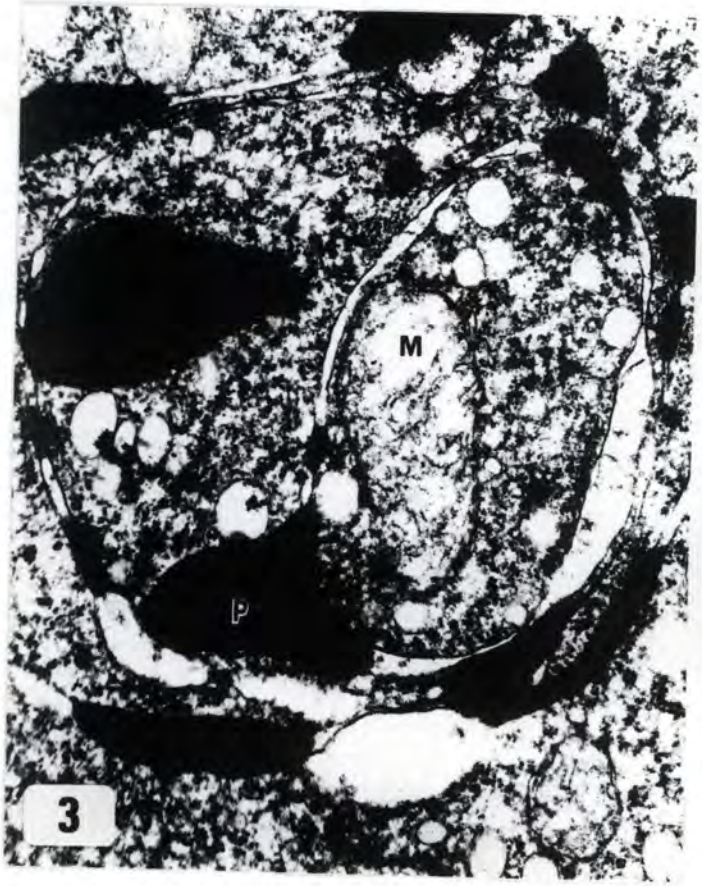

3

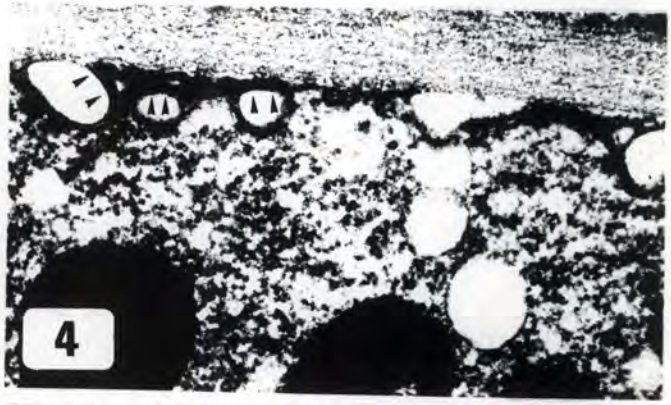

4

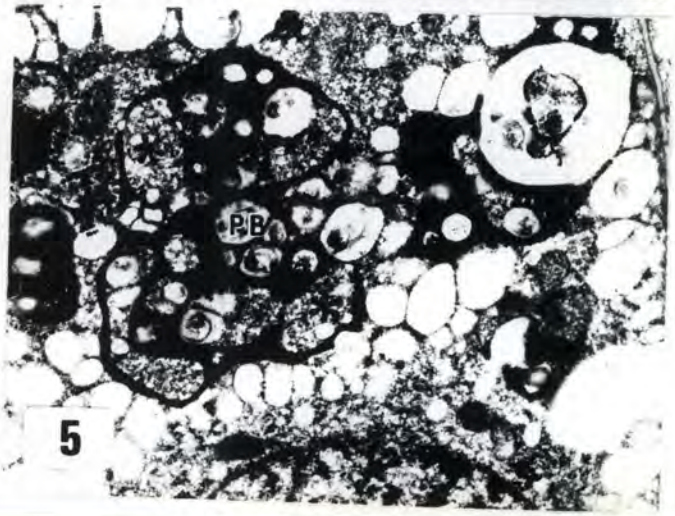

5

Figure 6 : Illustrates apparently normal nuclear and nucleolar (NO) morphology in a pith cell of the root tip of an embryo after 2 days irradiation. Coalesced lipid droplets (L) are shown. Sample prepared for electron microscopy after 12 hours imbibition. X 16 340.

Figure 7 : Root cap cell of embryo after 3 days irradiation treatment. The sample was prepared for electron microscopy after 3 hours imbibition and damage is evident to many subcellular membranes. These include dilation of the mitochondria (M), and ER (arrowheads), and membrane abnormalities at the plasmalemma (curved arrows) and in the amyloplasts. Cytoplasmic disintegration is evident in an adjacent cell (asterisk) in which the plasmalemma has apparently been lost. X 14 440.

Figure 8 : Shows detail of the plasmalemma abnormalities seen above (Figure 7). Numerous vesicles and multiple foldings of the membrane are clearly evident along the cell wall (W). Dilated ER running parallel to the wall is apparent. Lipid (L) indicated. X 50 400.

Figure 9 : Illustrates further cytolysome-like structures seen in epidermal cells of the root tip after 3 days irradiation. Sample fixed after 12 hours imbibition. X 27 300.

Figure 10 : Root cap cell of an embryo from a seed sample subjected to 3 days of irradiation treatment seen after 3 hours imbibition. A large vacuole-like structure (asterisk) is evident within which are membranous components and portions of what appear to be cytoplasmic ground substance. A nucleus (N) typical of the root cap is seen with a compact nucleolus (arrowhead). X 15 580.

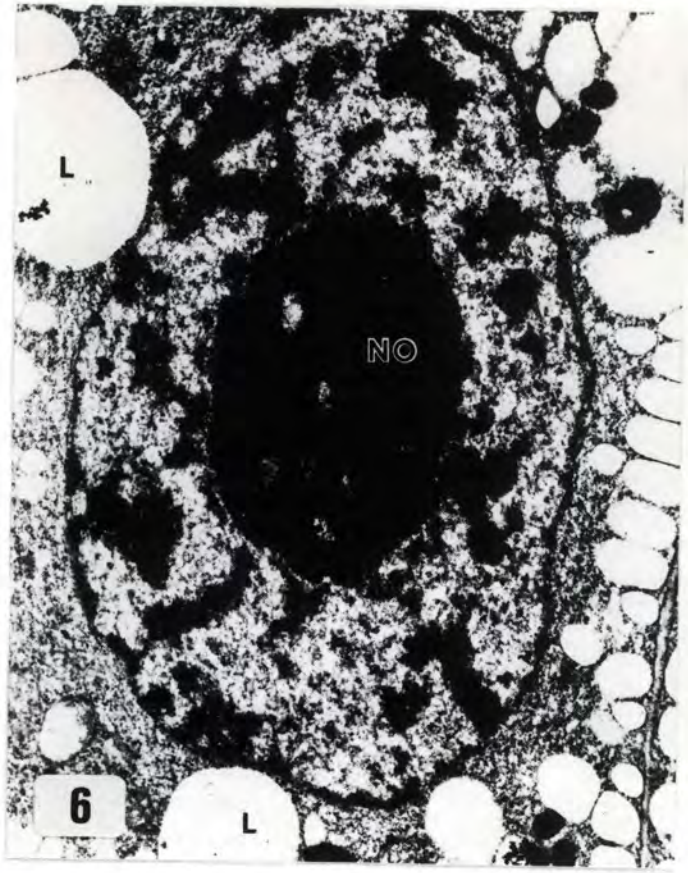
L
NO
L
6

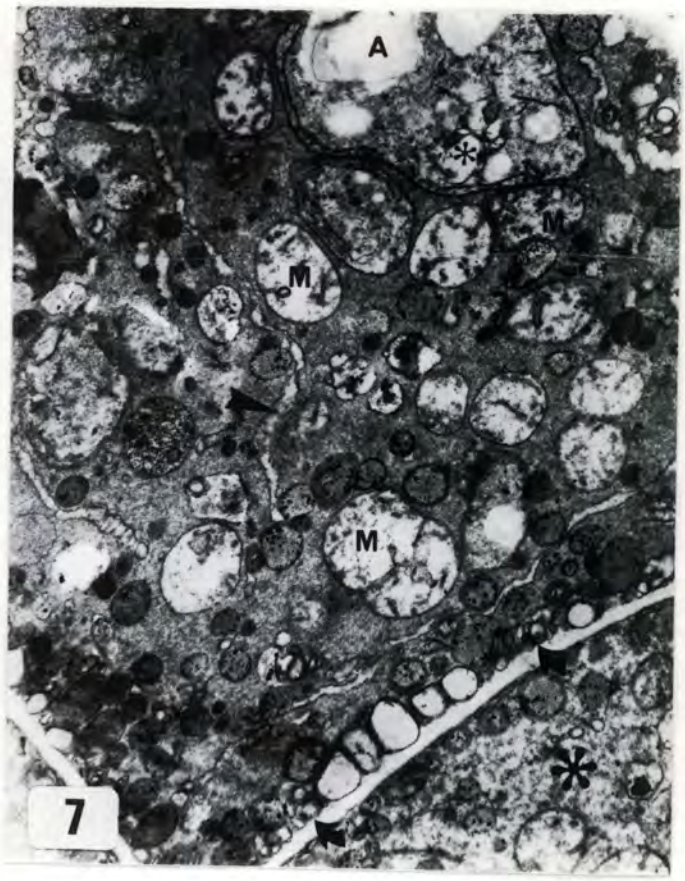
A
M
M
M
7

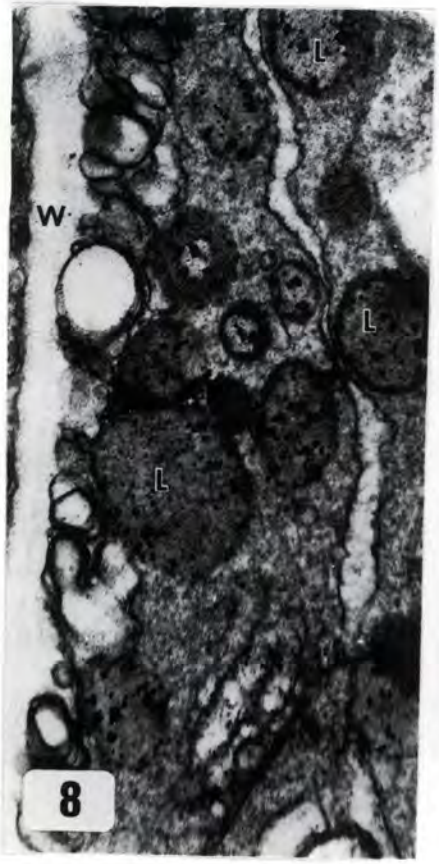
L
W
L
L
8

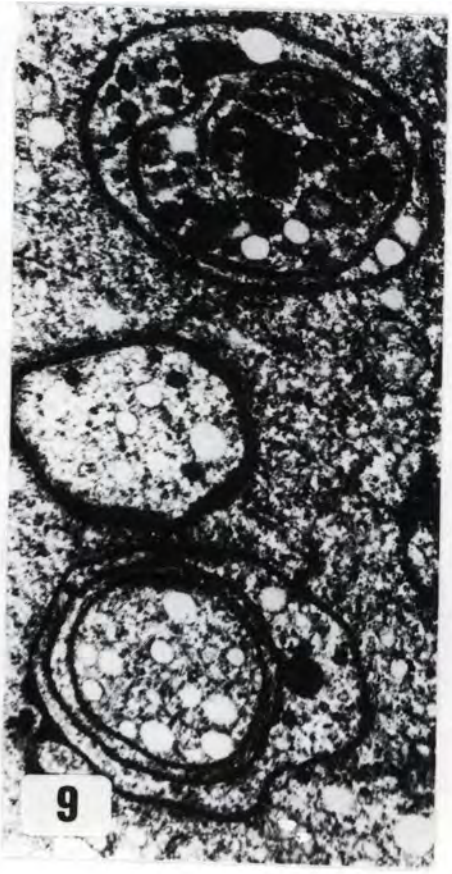
9

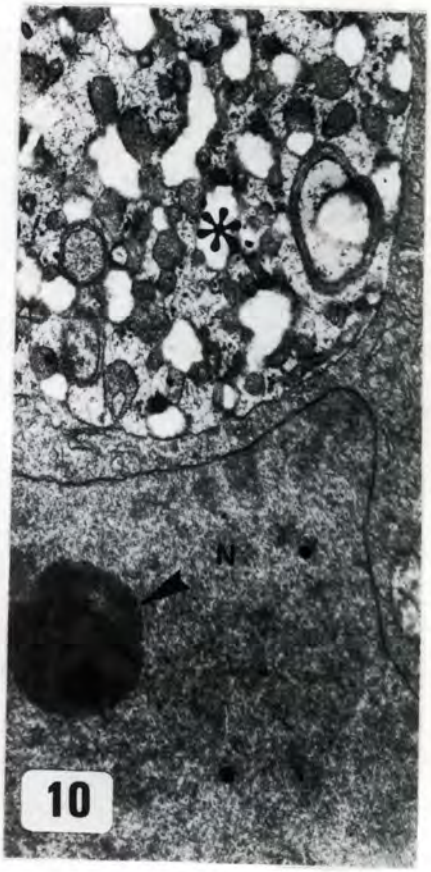
N
10

Figure 11 : Shows a cytolysome-like body in the cortical cell of an embryo root tip after 4 days of irradiation treatment. A portion of engulfed cytoplasm with mitochondria and degenerate amyloplast (A) can be seen. Material prepared for microscopy after 12 hours imbibition. X 42 560.

Figure 12 : A meristematic cell of normal ultrastructure seen in the root tip of an embryo after 4 days irradiation. A compact nucleolus (NO) with karyosome evident and heterochromatin of normal appearance. The nuclear envelope appears intact as does the plasmalemma. Sample fixed after 12 hours imbibition. X 11 400.

Figure 13 : Illustrates the appearance of endosperm cells after 4 days irradiation and 10 days post-imbibition. Little wall hydrolysis is evident and the two structural components of the wall are still evident; the electron dense wall (W) and the lighter-staining fibrillar component (asterisks). Compare with Figures 52 and 56, earlier. Some metabolic interconversions are presumed to have taken place in the endosperm as seen by the marked absence of protein bodies and lipid. X 11 400.

Figure 14 : Cortical cell of embryo after 4 days irradiation and at 12 hours after imbibition. Lipid (L) confluence and a cytolysome-like body (asterisk) are clearly evident. the plasmalemma shows no abnormality, and many mitochondria (arrowheads) of normal appearance are seen. X 6 900.

Figure 15 : Shows dilation of a portion of an otherwise normal mitochondrion (arrowhead) and crista -like vesicle (curved arrow) with the mitochondrial matrix of an epidermal cell from an embryo after 4 days irradiation and 12 hours imbibition. X 35 840.

Figure 16 : Appearance of cortical cells from the radicle of a seedling after 4 days irradiation and at 10 days post-imbibition. The seedling had the appearance of a " γ dwarf". It is evident that extensive vacuole (V) formation had taken place, although reserve mobilization was still incomplete as evidenced by numerous lipid (L) droplets in some cells. Some degenerate (D) cells were seen amongst cells of normal appearance. X 3 920.

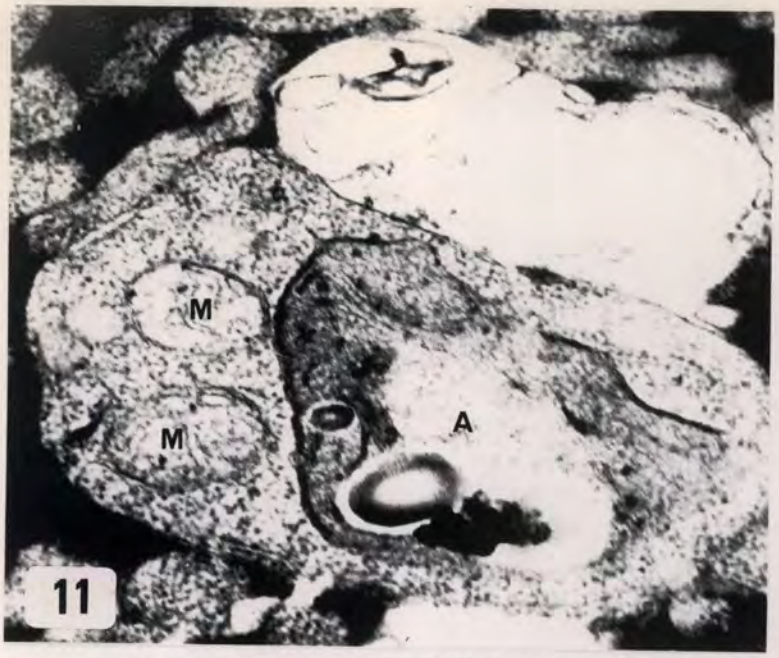
M
M
A
11

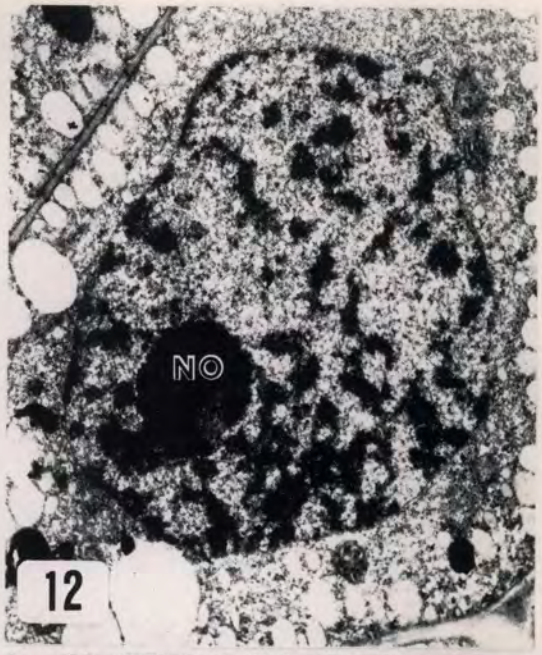
NO
12

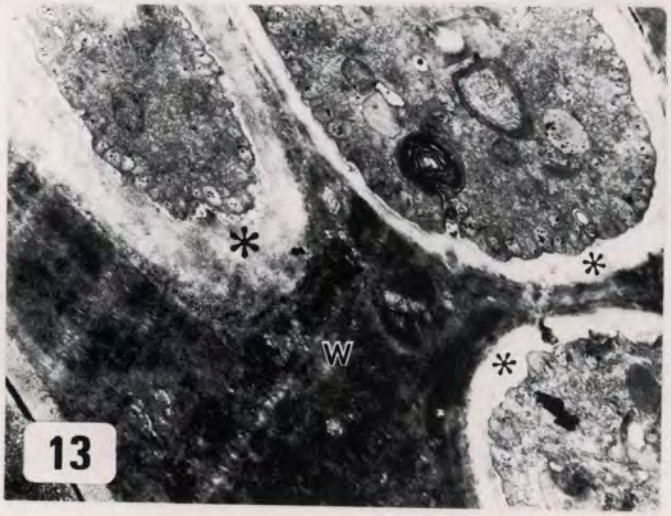
*
*
W
*
13


L
NO
L
*
14

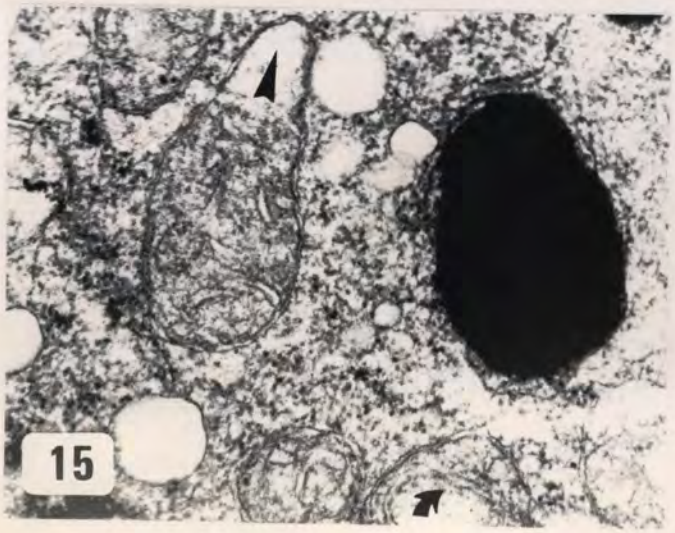
15

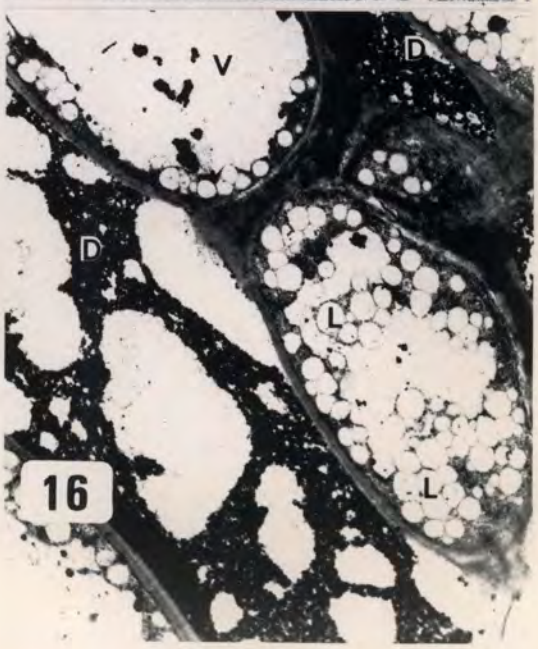
V
D
D
L
L
16